Vehicle-to-Grid Aggregation in Swedish Electricity Markets Under Real-World Availability and Infrastructure Constraints

A Market-Based Optimization Analysis of EV Fleet Flexibility in Electricity Markets

Master's thesis in Sustainable Energy Systems

Julia Cuvier Kåreby & Erik Brissman

DEPARTMENT OF ELECTRICAL ENGINEERING
CHALMERS UNIVERSITY OF TECHNOLOGY
Gothenburg, Sweden 2026
www.chalmers.se

Master's thesis 2026

Vehicle-to-Grid Aggregation in Swedish Electricity Markets Under Real-World Availability and Infrastructure Constraints

A Market-Based Optimization Analysis of EV Fleet Flexibility in Electricity Markets

Julia Cuvier Kåreby & Erik Brissman

Department of Electrical Engineering
Division of Electric Power Engineering
Chalmers University of Technology
Gothenburg, Sweden 2026

Vehicle-to-Grid Aggregation in Swedish Electricity Markets Under Real-World Availability and Infrastructure Constraints
A Market-Based Optimization Analysis of EV Fleet Flexibility in Electricity Markets
Julia Cuvier Kåreby & Erik Brissman

Supervisor: Araavind Sridhar, Department of Electrical Engineering
Examiner: David Steen, Department of Electrical Engineering

Master's Thesis 2026
Department of Electrical Engineering
Division of Electric Power Engineering
Chalmers University of Technology
SE-412 96 Gothenburg
Telephone +46 31 772 1000

Cover: Electric vehicle charging connected to a residential energy system, illustrating the integration of EVs into the electricity system.

Typeset in LaTeX
Printed by Chalmers Reproservice
Gothenburg, Sweden 2026

Vehicle-to-Grid Aggregation in Swedish Electricity Markets Under Real-World Availability and Infrastructure Constraints
A Market-Based Optimization Analysis of EV Fleet Flexibility in Electricity Markets
Julia Cuvier Kåreby & Erik Brissman
Department of Electrical Engineering
Chalmers University of Technology

Abstract

The increasing electrification of the transport sector presents both challenges and opportunities for modern power systems. While uncontrolled electric vehicle (EV) charging may increase peak demand and place additional stress on electricity networks, coordinated EV charging and vehicle-to-grid (V2G) operation offer potential flexibility services that can support grid stability and create economic value. This thesis evaluates the economic potential of aggregated EV-based flexibility in Swedish electricity markets from an aggregator perspective.

A deterministic optimization framework was developed in Python using Pyomo and solved with Gurobi to model individual EV charging and discharging behavior under real-world mobility constraints. The analysis is based on event-level charging and state-of-charge (SOC) data from 152 EVs, of which 149 were successfully optimized, covering approximately 2.5 years of observed operation. Vehicle mobility behavior was converted from event-based data into hourly availability profiles through a preprocessing pipeline including event merging, SOC anchor reconstruction, and validation against the original dataset.

Three market participation strategies were evaluated relative to a smart charging (V1G) reference: spot-market arbitrage, frequency containment reserve (FCR) participation, and co-optimized participation in both markets. Economic performance was assessed under Swedish SE3 day-ahead and FCR market conditions, while accounting for operational constraints including charging power limits, charging efficiency, home availability, grid fees, and simplified battery degradation costs.

The results show that pure spot-market arbitrage generated a limited fleet-level benefit of 125 kSEK relative to the V1G reference case. In contrast, reserve-market participation created substantially higher value, with the FCR-only strategy generating 12.44 MSEK and the co-optimized strategy 12.56 MSEK in fleet value. Sensitivity analyzes demonstrate that spot-market profitability is highly dependent on price volatility and other operational varieties, whereas reserve-driven strategies remain comparatively more robust than pure spot-market arbitrage to changes in grid fees, availability perturbations, and conservative market assumptions for the analyzed time period.

The findings suggest that under the modeled assumptions, the economic value of aggregated EV flexibility in Sweden is primarily driven by ancillary service participation rather than energy arbitrage.

Keywords: electric vehicles, vehicle-to-grid, smart charging, EV aggregation, frequency containment reserve, electricity markets, optimization, energy flexibility, ancillary services, flexibility markets

Acknowledgements

We would like to express our sincere gratitude to our supervisor, Araavind Sridhar, for his invaluable guidance, constructive feedback, and continuous support throughout this thesis. His expertise, encouragement, and willingness to share his knowledge have been essential to the completion of this work. We are especially grateful for his availability and engagement throughout the project, which greatly contributed to both the quality of the research and our learning experience.

We would also like to thank our examiner, David Steen, for his valuable comments, insightful discussions, and critical reflections. His feedback helped strengthen the quality of this thesis and encouraged us to carefully evaluate our assumptions, methodology, and results from multiple perspectives.

Finally, we are deeply grateful to Maria Taljegård and her team for generously providing the dataset used in this study. Their contribution made this project possible and provided the foundation for the analyses presented in this thesis.

Julia Cuvier Kåreby & Erik Brissman, Gothenburg, June 2026

Use of Artificial Intelligence Tools

Artificial intelligence (AI) tools, including large language models, were used as supportive assistants during this thesis. Their use included language refinement, improving the structure and clarity of academic writing, code debugging, code refactoring, and discussion of methodological alternatives during model development.
All AI-generated suggestions were critically assessed, tested, and independently verified before implementation. The authors take full responsibility for the correctness of the developed optimization models, data preprocessing, simulation results, analysis, interpretations, and conclusions presented in this work. AI tools were not used as authoritative scientific sources, and all references, technical statements, and methodological choices were independently validated.
The authors take full responsibility for all methodological choices, optimization models, data processing, analyses, interpretations, and conclusions presented in this thesis.

List of Acronyms

Below is the list of acronyms that have been used throughout this thesis listed in alphabetical order:

AC	Alternating Current
BESS	Battery Storage System
BEV	Battery Electrical Vehicle
DC	Direct Current
DER	Distributed Energy Resource
DSO	Distribution Systems Operator
EV	Electrical Vehicle
FCR	Frequency Containment Reserve
FCR-D	Frequency Containment Reserve - Disturbance
FCR-N	Frequency Containment Reserve - Normal
GHG	Greenhouse Gas
LCOS	Levelized Cost of Storage
LP	Linear Programming
MILP	Mixed-Integer Linear Programming
NPV	Net Present Value
OBD	Onboarding Diagnostic
PHEV	Plug-in Hybrid Electric Vehicle
PV	Photovoltaic
RES	Renewable-based Energy Sources
SOC	State of Charge
TSO	Transmission System Operator
VPP	Virtual Power Plant
V1G	Vehicle Unidirectional Charging/ Smart-Charging
V2G	Vehicle-to-grid

Nomenclature

Below is the nomenclature of indices, sets, parameters, and variables used throughout this thesis.

Indices

v	Index for electric vehicle
t	Index for hourly time step
i	Index for event-based parking or charging event
k	Index for frequency measurement sample
m	Index for month
d	Index for day
s	Index for stochastic scenario

Sets

$\mathcal{V}$	Set of electric vehicles
$\mathcal{T}$	Set of hourly time steps in the optimization horizon
$\mathcal{E}_v$	Set of event-based observations for vehicle v
$\mathcal{S}$	Set of stochastic availability scenarios

Parameters

Δt	Time discretization step
$E_v^{\max}$	Maximum battery energy capacity of vehicle v
$P^{ch,\max}$	Maximum charging power
$P^{dis,\max}$	Maximum discharging power
$P^{FCR,\max}$	Maximum reserve bid power

$P^{bal,dis,\max}$	Maximum balancing discharge power in FCR-only model
η^{ch}	Charging efficiency
η^{dis}	Discharging efficiency
c^{grid}	Grid fee per imported kWh
c^{deg}	Battery degradation cost per kWh throughput
π_t	Spot electricity price at hour t
λ_t^N	FCR-N capacity price at hour t
$\lambda_t^{D,up}$	FCR-D upward capacity price at hour t
$\lambda_t^{D,down}$	FCR-D downward capacity price at hour t
μ_t^{up}	Activation revenue price for upward reserve activation
μ_t^{down}	Activation revenue price for downward reserve activation
$\alpha_t^{N,\uparrow}$	Hourly upward FCR-N activation factor
$\alpha_t^{N,\downarrow}$	Hourly downward FCR-N activation factor
$\alpha_t^{D,\uparrow}$	Hourly upward FCR-D activation factor
$\alpha_t^{D,\downarrow}$	Hourly downward FCR-D activation factor
τ^N	FCR-N activation duration requirement
τ^D	FCR-D activation duration requirement
h_t	Binary home availability parameter
f_t	Binary FCR availability parameter
E_t^{arr}	Observed arrival battery energy anchor
E_t^{dep}	Observed departure battery energy anchor
α	Spot price volatility scaling factor
H	Maximum stochastic availability perturbation horizon
$x_d^{EUR/SEK}$	Daily EUR/SEK exchange rate
γ^{FCR}	FCR bid acceptance factor

Variables

P_t^{ch}	Charging power decision variable
P_t^{dis}	Discharging power decision variable
P_t^N	FCR-N reserve bid power
$P_t^{D,up}$	FCR-D upward reserve bid power
$P_t^{D,down}$	FCR-D downward reserve bid power
E_t	Battery energy at beginning of hour t

E_t^{after}	Battery energy after hourly operation
b_t^{ch}	Binary charging mode variable
b_t^{dis}	Binary discharging mode variable
SOC_i^{start}	Event-based arrival state of charge
SOC_i^{end}	Event-based departure state of charge
ΔSOC_i	State-of-charge change during event i
E_i^{ch}	Charged energy during charging event i
Δt_i	Duration of event i
t_i^{arr}	Hourly arrival anchor time
t_i^{dep}	Hourly departure anchor time
Δt_i^{gap}	Time gap between consecutive parking events
ΔSOC_i^{gap}	SOC gap between consecutive parking events
$\tilde{t}_{i,s}^{arr}$	Stochastically perturbed arrival time
$\tilde{t}_{i,s}^{dep}$	Stochastically perturbed departure time
$\epsilon_{i,s}^{arr}$	Arrival delay perturbation
$\epsilon_{i,s}^{dep}$	Departure advance perturbation
$a_{t,i,s}^{home}$	Stochastic hourly home availability indicator
C^{spot}	Spot-market charging cost
$C^{spot,net}$	Net spot-market cost including discharging revenue
C^{grid}	Total grid fee cost
C^{deg}	Total battery degradation cost
R^{FCR}	Total FCR capacity revenue
R^{act}	Total reserve activation revenue
X_t^{fleet}	Aggregated fleet-level quantity at hour t

Contents

List of Figures

List of Tables

1

Introduction

This chapter introduces the overall context and motivation of the thesis. It presents the background for the study through a brief review of relevant literature, formulates the research questions, and defines the scope and delimitations.

1.1 Introduction

The energy transition towards a low-carbon electricity system is increasing the need for flexibility in the Swedish power system. In 2025, total electricity production in Sweden was approximately 160 TWh, reflecting the scale of the national electricity system [1]. As shown in Figure 1.1, the majority of this production is already low-carbon, dominated by hydropower, nuclear power, and an increasing share of variable renewable energy sources (RES) such as wind and solar power.

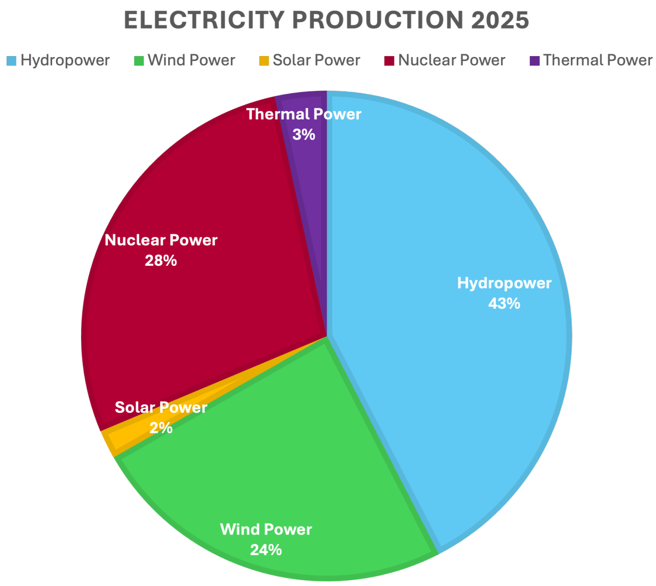

Figure 1.1: Distribution of electricity produced in Sweden 2025 [1]

Unlike conventional dispatchable generation, wind and solar power are weather-dependent and cannot be controlled according to system demand, making it more challenging to maintain the balance between electricity supply and demand. In addition, the growing share of RES also changes the dynamic behavior of the power system, since many renewable technologies are connected to the grid through powerelectronic converters rather than directly through synchronous generators. Consequently, increasing challenges related to frequency stability and real-time system balancing, thereby increasing the need for flexibility resources and ancillary services [2].

At the same time, electricity demand is expected to increase in the coming years. According to the Swedish Energy Agency, electricity production is expected to increase by around 15% by 2028, driven by fast expansion of wind and solar power, while industrial electricity demand is expected to grow substantially due to electrification and hydrogen production [3].

Achieving climate neutrality requires emissions reductions across all major sectors including electricity generation, industry, buildings, and transport. However, the contribution of these sectors differs depending on the structure of the energy system. The transport sector remains the largest source of greenhouse gas (GHG) emissions in Sweden. In 2024, domestic transport accounted for approximately 16.9 million tonnes of CO_2 equivalents, corresponding to slightly more than one-third of Sweden's total GHG emissions. Approximately 94% of these emissions originated from road transport, with passenger cars being the dominant source [4].

The transport sector remains challenging to decarbonize due to its historical dependence on oil-based fuels, especially in road transport. Therefore, the electrification of transport, and particularly the fast deployment of electric vehicles (EVs) has emerged as a central strategy in the energy transition [5]. In Sweden, EV adoption has accelerated rapidly in recent years. In early 2025, rechargeable vehicles accounted for approximately 61% of all new passenger car registrations in Sweden, of which battery electric vehicles (BEVs) represented about 35% [6]. At the same time, Sweden had approximately 45 000 publicly accessible charging points at the end of 2024, corresponding to almost eight EVs per public charging point, indicating both rapid expansion of charging infrastructure and continued growth in EV deployment [7].

The continued adoption of EVs is expected to increase electricity demand in many regions. If EV charging occurs uncontrolled, it could lead to increased peak demand and additional stress on electricity networks. However, EVs also represent a promising source of flexibility due to the storage capacity of their batteries especially since private passenger vehicles are parked the majority of the time, often estimated at around 90% [8]. This allows charging demand to be shifted in time without affecting user mobility needs. When coordinated, EV charging can therefore be scheduled to respond to electricity price signals or system conditions, a concept referred to as unidirectional smart charging (V1G). V1G has been identified as an important strategy for reducing peak loads and improving the integration of renewable electricity in modern power systems [9].

Beyond flexible charging, EVs can also contribute additional system value through vehicle-to-grid (V2G) operation. V2G technology enables bidirectional power exchange between EV batteries and the electricity grid, allowing vehicle to consume electricity but also to supply stored energy back to the grid [10]. Through this bidirectional interaction, EV fleets can function as distributed energy storage resources capable of managing peak demand and supporting grid stability by providing ancillary services such as frequency regulation. Several studies highlight that

V2G-enabled EV fleets can significantly improve grid flexibility and facilitate the integration of renewable energy by utilizing the aggregated storage capacity of EV batteries [10, 11].

A key challenge in evaluating the economic potential of V2G systems is that simplified assumptions may overestimate the practically available flexibility [12]. In practice, V2G operation is constrained by battery capacity, charging and discharging power limits, conversion efficiencies, and vehicle availability. V2G operation is further constrained by practical factors such as when vehicles are connected to chargers, willingness of participation and minimum state of charge (SOC) requirements at departure to satisfy user mobility needs. These constraints play a dominant role in determining how much flexibility can actually be realized and monetized, and neglecting them could lead to optimistic estimates of V2G profitability.

Several pilot projects in Sweden are already exploring the technical and economic feasibility of V2G technology and EV fleet aggregation as flexible grid resources. In Gothenburg, a V2G demonstration project coordinated by Polestar, together with the distribution system operators (DSOs) Göteborg Energi Nät and Vattenfall Eldistribution, the transmission system operator (TSO) Svenska kraftnät, and research partners including Chalmers University of Technology, is evaluating the deployment of bidirectional charging services in Sweden. The project focuses on real-world vehicle availability and charging behaviour to assess operational strategies and business models for commercial V2G aggregation. The initiative is funded by Vinnova and started in 2023 [13, 14]. According to Göteborg Energi, the local DSO in Gothenburg, 20% of future flexibility can be derived from V2G [15].

In parallel, Volvo Cars and Göteborg Energi have conducted a pilot project in which four bidirectional Volvo electric vehicles delivered a total of 111 kWh back to the local grid during a flexibility market demonstration in March 2025. The vehicles exported electricity during peak demand periods, illustrating how EV fleets can provide grid support services in a real distribution network context [16].

These developments highlight the need for optimization-based models that quantify the economic potential of EV aggregation and V2G under realistic operational conditions. By accounting for vehicle availability, SOC requirements, and efficiency losses, such models can identify the key constraints that limit flexibility and determine when EV aggregation becomes economically viable from an aggregator perspective.

To address these challenges, this thesis develops an optimization framework for EV fleet aggregation using real vehicle availability data. The study evaluates the economic potential of EV aggregation under a deterministic perfect-foresight framework, providing a theoretical upper-bound estimate of aggregator value under different market scenarios.

1.1.1 Research Questions

Based on the challenges identified above, this thesis aims to answer the following research questions:

- **RQ1:** What is the economic potential of aggregated EV-based V2G flexibility in Swedish electricity markets from an aggregator perspective?
- **RQ2:** How is the economic potential of aggregated EV-based V2G flexibility influenced by technical, operational, and market-related assumptions?

1.2 Delimitations

Several delimitations were applied in this study to maintain a manageable scope and focus on the main research objectives:

- The analysis is limited to the Swedish electricity market, specifically bidding zone SE3, and considers participation only in the day-ahead spot market and the FCR markets. Other ancillary services, such as aFRR, mFRR, and local flexibility markets, were excluded due to their additional operational complexity and differing market structures.
- Only home-connected EV charging events are considered eligible for flexibility provision. Public charging, workplace charging, and fast-charging infrastructure are outside the scope of the analysis.
- The study evaluates V2G from an aggregator economic perspective. Explicit modeling of customer participation behavior, incentive design, and consumer adoption responses is outside the scope.
- Battery degradation is represented using a simplified economic throughput-based formulation. Detailed electrochemical battery-aging mechanisms are not modeled.
- The study focuses on the technical and economic performance of aggregated EV flexibility rather than wider power-system impacts. Detailed transmission constraints, distribution-grid congestion, and power-flow modeling are therefore excluded.
- Practical deployment aspects, including V2G hardware availability, communication infrastructure, market qualification procedures, and regulatory implementation barriers, are not explicitly evaluated.

1.3 Literature Review

To position the present study, selected representative studies relevant to EV flexibility optimization, V2G aggregation, and electricity market participation are reviewed.

1.3.1 Residential energy system optimization with EV, PV and BESS

Several studies have investigated the integration of electric vehicles (EVs), photovoltaic (PV) systems, and battery energy storage systems (BESS) in residential energy management. Gómez-Quiles et al. [17] developed optimization models for prosumer households equipped with rooftop PV, BESS, and EVs, aiming to balance electricity cost minimization with user convenience. Using real-world data and linear and mixed-integer linear programming formulations, the study demonstrated how coordinated scheduling of EV charging can reduce household electricity costs while maintaining acceptable vehicle availability.

Similarly, Einolander et al. [18] evaluated the economic benefits of vehicle-to-home (V2H) technology for detached households using mixed-integer linear programming (MILP) and real-world EV charging event data. By optimizing bidirectional charging during periods when vehicles would otherwise remain idle, the study showed that V2H operation can significantly reduce household electricity costs regardless of the primary heating technology used in the building.

Recent work by Troyee et al. [19] further expanded residential energy management frameworks by investigating the optimal sizing of PV systems and BESS in households equipped with EVs capable of V2H operation. The study incorporated battery degradation, stochastic EV availability, dynamic electricity pricing, and sensitivity analyses within a rule-based local energy management system. The results indicated that V2H functionality can increase system flexibility and, in some cases, reduce or even eliminate the need for stationary battery storage while maintaining comparable economic performance.

1.3.2 Battery and Vehicle Flexibility Optimization

In contrast to residential prosumer models, Martini et al. [9] develop a MILP framework for optimizing charging and discharging schedules of an electric bus fleet while considering electricity prices, battery degradation, charger constraints, and limited grid capacity. The results show that V1G reduces total energy costs by approximately 35% compared to uncontrolled charging. However, the additional value of bidirectional V2G operation remains relatively limited, providing only 3–8% additional savings under current market conditions. The study further shows that V2G profitability strongly depends on electricity price volatility and battery degradation costs. In scenarios with large price spreads, reaching up to 160 €/MWh, V2G arbitrage becomes significantly more attractive. However, the authors conclude that battery degradation costs and infrastructure complexity substantially reduce the economic benefits of bidirectional operation.

A related fleet-oriented perspective is presented by Leippi et al. [12], where employee EVs are modeled as distributed storage resources within an industrial smart grid. The authors formulate a deterministic multi-objective MILP framework that minimizes both company electricity costs and EV battery degradation costs, using real-time electricity prices, industrial load flexibility, and individual EV characteristics. By explicitly analyzing compensation schemes for EV owners, the study identifies economically beneficial trade-offs between company profitability and battery wear, demonstrating that V2G can create mutually beneficial outcomes for both stakeholders under suitable operational conditions

Another relevant fleet-level contribution is presented by Nespoli et al. [20], who use real operational data from a large Swiss car-sharing fleet to develop a scalable V2G control framework for ancillary service participation. However, the study focuses on fleet flexibility characterization and bidding capability rather than long-term economic profitability across multiple market participation strategies

Recent work by Mirzaei Alavije et al. [21] developed a MILP framework for co-optimizing participation in the Swedish day-ahead and Frequency Containment Response (FCR) markets, including Frequency Containment Response Normal (FCR-N), Frequency Containment Response Disturbance up (FCR-D), and FCR-D down for BESS. The study demonstrates that stacked participation across multiple markets provides the highest potential profitability, particularly through simultaneous participation in FCR-D up and FCR-D down.

A broader system-level perspective is presented by Yuvaraj et al. [22], who develop a multi-objective optimization framework for coordinated scheduling of V2G-enabled EV charging together with renewable distributed generation in an IEEE 85-bus distribution network. The model incorporates stochastic EV arrivals, departures, SOC uncertainty, and user-priority-based charging constraints. The results show significant reductions in peak demand, voltage deviations, power losses, and operational costs compared to uncoordinated charging.

Overall, prior fleet-level studies demonstrate that V2G can create economic value under certain technical and market conditions, but several limitations remain. Vehicle availability is frequently represented using scheduled operations, assumed workplace charging patterns, or probabilistic mobility models rather than observed real-world private EV behavior. In addition, many studies focus on internal fleet optimization, industrial demand response, system operation, or flexibility characterization instead of explicit long-term aggregator profitability in electricity markets. While some studies consider ancillary service participation, explicit benchmarking of V2G against an optimized V1G baseline under combined spot and Swedish FCR market participation remains limited.

1.3.3 Market and aggregator-based V2G optimization

Recent research has increasingly investigated V2G from an aggregator and market perspective. A study performed by Signer et al. [23], an agent-based electricity market model is used to analyze interactions between EV aggregators and the German wholesale electricity market under different tariff structures. The results show that current taxation and grid-fee structures significantly reduce the profitability of V2G arbitrage, requiring large electricity price spreads for profitable operation. The study further demonstrates that reducing taxes and grid fees could substantially increase V2G participation and renewable energy integration. However, as EV penetration increases, competition between flexible resources reduces price volatility and thereby limits long-term arbitrage profitability.

Pradana et al. [24] present a more operational aggregator framework, where an EV aggregator participates in electricity arbitrage using real-time market data from Australia. The study combines probabilistic EV availability modeling with MILP-based charging optimization and reports a daily positive revenue per EV. The results further show that coordinated participation is important, as excessive EV participation can reduce grid benefits and lower system performance.

Another aggregator framework is presented by De Caro et al. [25], who develop a stochastic scheduling framework for EV aggregator participation in day-ahead and ancillary service markets under uncertain EV availability and SOC requirements. The study shows that aggregator profitability depends strongly on EV availability, reserve windows, and imbalance penalties. However, EV behavior is generated from statistical distributions rather than observed real-world mobility data, and the focus is on uncertainty-aware bidding rather than benchmarking V2G against an optimized V1G baseline.

Malik et al. [11] proposed a dynamic-based optimization framework for EV participation in Sweden's day-ahead and FCR-D markets. The study incorporated battery degradation costs, power tariffs, and EV arrival and departure times, while analyzing simultaneous participation in day-ahead, FCR-D up, and FCR-D down markets using historical SE3 market data. The results showed that combined participation in day-ahead and FCR-D markets yielded the highest profitability, while inclusion of battery degradation significantly reduced the achievable economic benefits. However, the study focused on a representative individual EV with assumed mobility behavior rather than aggregated EV fleets based on observed real-world charging and availability patterns.

Geng et al. [26] present a techno-economic assessment of V2G operation from a vehicle-side perspective, evaluating both the costs and profitability under different operational strategies. The study develops a detailed technology-oriented framework including battery degradation, charging/discharging behavior, and economic metrics such as levelized cost of storage (LCOS) and net present value (NPV). The results indicate that V2G can become economically attractive under favorable technological and operational conditions, particularly as battery technologies improve. However, the study focuses primarily on economic assessment rather than optimization of real-world aggregated EV fleets or explicit ancillary-service participation.

1.3.4 Positioning of this study

Table 1.1 summarizes selected studies related to EV smart charging and V2G operation and compares them with the present work. The comparison focuses on several key characteristics relevant to the scope of this thesis, including the use of real EV mobility data, fleet aggregation, participation in ancillary-service markets such as FCR, spot-market optimization, and the consideration of V2G operation. Although previous studies have investigated several of these aspects individually, relatively few studies combine real-world EV mobility data with aggregator-based fleet optimization and co-optimization of spot and reserve markets within a unified V2G framework.

Existing literature has demonstrated the technical and economic potential of EV charging optimization, V2G arbitrage, and ancillary service participation under a variety of system configurations. However, many previous studies rely on scheduled fleet operation, travel-survey-derived mobility profiles, or stationary battery models rather than event-level EV with observed arrival times, departure times, locations, and SOC trajectories. As a result, the practical commercial feasibility of EV flexibility under realistic operational constraints remains to be explored.

Table 1.1: Comparison of existing literature and the present study. ✓indicates that a feature is explicitly considered, while (✓) indicates partial or limited consideration. Similarly, × indicates that a feature is not considered.

Study	Real EV data	Fleet aggregation	FCR/AS	Spot	V2G
Gómez-Quiles et al.	×	×	×	✓	×
Einolander et al.	✓	×	×	✓	×
Troyee et al.	×	×	×	✓	×
Martini et al.	(✓)	✓	×	✓	✓
Leippi et al.	(✓)	✓	×	✓	✓
Nespoli et al.	✓	✓	✓	×	✓
Mirzaei Alavijeh et al.	×	×	✓	✓	×
Yuvaraj et al.	×	✓	×	×	✓
Signer et al.	×	✓	×	✓	✓
Pradana et al.	(✓)	✓	(✓)	✓	✓
De Caro et al.	×	✓	✓	✓	✓
Malik et al.	×	×	✓	✓	✓
Geng et al.	×	✓	×	✓	✓
This study	✓	✓	✓	✓	✓

The present study addresses this gap through an aggregator-oriented optimization framework based on event-level data of real electric vehicles. Each vehicle is optimized individually according to its observed arrival times, departure times, and mobility-related SOC requirements, while economic performance is evaluated at aggregated fleet level. This enables a data-driven representation of EV flexibility grounded in actual vehicle usage behavior rather than assumed availability profiles. A central contribution of the study is the explicit comparison between V1G and V2G, enabling quantification the economic value of bidirectional flexibility under realistic operating constraints. Beyond simple energy arbitrage, the framework further evaluates simultaneous participation in both the day-ahead electricity market and Swedish FCR markets, including FCR-N, FCR-D up, and FCR-D down. This allows both energy market optimization and ancillary service provision to be captured within a unified optimization framework.
The framework incorporates battery degradation costs and realistic operational constraints, including home availability, charging power limitations, departure energy requirements, and grid fees. Robustness is further evaluated through sensitivity analyses across key technical and economic parameters.
Taken together, the study combines real-world event-based EV behavior, explicit V1G-V2G benchmarking, co-optimized multi-market participation, and robustness analysis within a unified fleet-level framework, providing a more realistic assessment of the commercial feasibility of large-scale EV flexibility provision.

2

Theory

This chapter presents the theoretical concepts relevant to the thesis. It introduces EVs and their interaction with the power system, the concept of V2G, electricity market structures such as the day-ahead market and FCR, and the role of EV aggregators.

2.1 Electric Vehicles and Charging Infrastructure

2.1.1 EV Battery Technology and State of Charge

The energy stored in an EV battery is often described using SOC, which represents the current energy level relative to the maximum usable battery capacity. SOC is therefore a dimensionless quantity, typically expressed either as a value between 0 and 1 or as a percentage. The relationship between battery energy and SOC can be expressed as:

$$SOC_t = \frac{E_t}{E_{\max}} \tag{2.1}$$

where E_t [kWh] is the battery energy at time step t, and $E_{\max}$ [kWh] denotes the maximum usable battery capacity.
Modern passenger EVs commonly have battery capacities on the order of tens of kWh, although the capacity varies depending on vehicle type and application. Smaller BEVs typically operate with battery capacities in the range of approximately 40–60 kWh, while larger BEVs commonly exceed 70 kWh. In comparison, plug-in hybrid electrical vehichles (PHEVs) generally use substantially smaller battery systems, commonly below 25 kWh [27]. In practice, however, the full nominal battery capacity is rarely utilized during normal operation. Instead, EV batteries are commonly operated within predefined SOC limits in order to reduce battery degradation, improve battery lifetime, and maintain safe operating conditions [28]. Consequently, the available SOC not only determines the driving capability of the vehicle, but also the flexibility that can be provided to the power system through V2G operation.
In V2G operation, SOC plays a central role in determining the operational flexibility that can be provided to the power system. The available battery energy directly influences the amount of charging or discharging power that can be sustained, while insufficient SOC levels may limit the ability to provide grid-support services or satisfy future mobility requirements. Kempton and Tomić [29] emphasize that the

operational needs of the driver and the grid operator must therefore be balanced in practical V2G operation, where sufficient stored energy must remain available for transportation while enabling power-system support. Consequently, SOC-related constraints are commonly incorporated into optimization-based V2G frameworks in order to maintain physically feasible battery operation and ensure that mobility requirements can be satisfied. Since the available SOC determines the amount of energy that can be exchanged with the power system, it also directly affects the flexibility available for charging optimization, discharging operation, and ancillary-service provision.

Real-world EV charging behavior additionally demonstrates that practical SOC operation is commonly constrained within preferred operating ranges. Kobayashi et al. [30] analyzed GPS-logged charging and driving data from 334 EVs in Sweden and observed that EVs frequently arrive home with relatively high SOC levels, where more than half of the overnight parking events occurred with SOC values above 60%. The study additionally observed charging behavior where some EV owners intentionally stopped charging at SOC levels around 80–90%, particularly for larger-battery EVs, likely in order to reduce degradation-related battery stress. These findings suggest that practical EV operation often avoids both very low and very high SOC levels, while simultaneously maintaining sufficient operational flexibility for smart charging and potential V2G services.

2.1.2 Charging Infrastructure and V2G Operation

EV charging infrastructure is based on the interaction between the alternating current (AC) electricity grid and the direct current (DC) battery system used in EVs. In Sweden, the low-voltage electricity grid typically operates at 230 V for single-phase systems and 400 V for three-phase systems, which influences the available charging power in residential and commercial charging applications [31]. In AC charging systems, the power conversion between AC and DC is handled by the vehicle's onboard charger (OBC), which constrains the charging and discharging capability of the vehicle. Common AC charging power levels for passenger EVs include approximately 3.7 kW for single-phase charging and 11–22 kW for three-phase charging [16]. In practice, the achievable charging power is additionally influenced by the electrical capacity of the household connection and the simultaneous electricity demand of other appliances within the building.

Conventional EV charging is typically unidirectional, where electrical energy is transferred from the grid to the vehicle battery. In V2G operation, however, bidirectional charging enables stored battery energy to be supplied back to the grid when required. This requires bidirectional power electronics capable of converting battery DC power into grid-compatible AC power during discharging. In AC-based V2G systems, this conversion is performed by a bidirectional onboard charger, while DC-based V2G systems instead rely on external power conversion within the charging station [16, 32]. Since DC-based systems bypass the onboard charger limitations, they can generally provide higher charging and discharging power and currently dominate many early commercial V2G implementations [32]. Charging and discharging processes are furthermore associated with conversion losses originating from both the battery system and the power electronics, which reduces the amount of energy that can be exchanged between the vehicle and the grid during V2G operation [33].

2.1.3 Battery Degradation

Battery degradation is an important consideration in V2G operation since repeated charging and discharging could accelerate battery aging and reduce battery lifetime. Battery aging is commonly divided into two main degradation mechanisms: calendar aging and cycling aging.

Calendar aging refers to battery degradation occurring over time regardless of battery usage. This degradation mechanism is strongly influenced by factors such as storage temperature, average SOC, battery chemistry, and the duration for which the battery remains at elevated SOC levels. Even when a battery is not actively cycled, chemical side reactions within the cell gradually reduce the available battery capacity and increase internal resistance over time. Lehtola [34] identifies time, temperature, and SOC as some of the dominant factors influencing calendar aging in lithium-ion batteries.

Cycling aging, in contrast, is associated with active charging and discharging operation and is therefore closely connected to V2G participation. Cycling degradation is primarily affected by factors such as energy throughput, depth of discharge, charging and discharging rates (C-rates), operating temperature, and the total number of charge-discharge cycles. Frequent bidirectional energy transfer during V2G operation may therefore accelerate battery wear compared to conventional charging operation. Lehtola [34] further highlights that intensive charge/discharge cycling, wide SOC variations, and high current rates may significantly increase electrochemical and thermal aging effects within lithium-ion batteries.

In optimization-based V2G studies, degradation modeling is often primarily focused on cycling-related degradation since charging and discharging behaviour can be directly influenced by the optimization framework. Calendar aging is generally more difficult to represent dynamically within operational optimization models because it depends on long-term environmental and storage conditions rather than short-term dispatch decisions.

To account for battery wear within optimization frameworks, degradation costs are commonly incorporated directly into the optimization objective function in order to economically penalize excessive battery cycling and energy throughput. By assigning a degradation-related cost to charging and discharging activity, the optimization can balance short-term market revenues against long-term battery wear, thereby discouraging economically inefficient battery operation.

A common simplified approach is the linear throughput-based degradation formulation:

$$C_{deg} = c_{deg} \sum_{t} (P_{ch,t}\Delta t + P_{dis,t}\Delta t) \tag{2.2}$$

where c_{deg} denotes the assumed degradation cost per transferred energy unit [SEK/kWh]. This formulation should primarily be interpreted as an economic approximation of cycling-related battery wear rather than a physically exact electrochemical degradation model.

Despite its simplified representation, throughput-based degradation modeling is widely used in optimization studies due to its computational manageability to capture the economic trade-off between battery utilization and degradation. Increasing degradation costs within the optimization objective generally causes the optimization framework to adopt more conservative charging and discharging behaviour, thereby reducing unnecessary cycling activity and limiting economically inefficient operation.
Reported degradation-related cost estimates in the literature vary substantially depending on modelling assumptions and system boundaries. Martini et al. [9] evaluate battery wear prices ranging from 0.03–0.31 SEK/kWh.[1] In contrast, studies incorporating broader lifecycle and system-level economic considerations often report substantially larger cost estimates associated with V2G operation. For example, Geng et al. [26] report LCOS values of 0.89–2.55 SEK/kWh.[2] However, these estimates include broader vehicle-side costs and are therefore not directly comparable to pure degradation costs. Similarly, Sagaria et al. [35] estimate V2G compensation requirements of 0.77–1.45 SEK/kWh. These variations shows the uncertainty associated with degradation modelling and highlight the importance of sensitivity analyses when evaluating the economic viability of V2G operation.

2.2 Sweden's electricity infrastructure & electricity markets

2.2.1 Sweden's electricity distribution

The Swedish electricity system consists of electricity generation, transmission, distribution, and consumption operating within the Nordic and European interconnected power market, as seen in Figure 2.1. Electricity is generated from sources such as hydropower, nuclear power, wind power, and solar power, and is transported through three main grid levels: the transmission grid, the regional grid, and the local distribution grid[36].
The transmission grid, also referred to as the national grid, operates at high voltage levels of 400 or 220 kV and is owned and operated by Svenska kraftnät, the Swedish Transmission System Operator (TSO)[37]. The transmission grid transports electricity over long distances, and maintains the real-time balance and frequency stability of the national electricity system. Svenska kraftnät is also responsible for operating ancillary service markets such as FCR, which are used to stabilize the system frequency at 50 Hz[38].
Electricity is then transferred from the transmission grid to regional and local distribution grids operated by Distribution System Operators (DSOs), such as Göteborg Energi Elnät, Vattenfall Eldistribution, and Ellevio [39]. The regional grid typically operates at voltage levels around 130 kV and connects the transmission grid to cities, industries, and larger consumption areas. The local distribution grid operates at voltage levels of 40 kV and below. Through successive voltage transformations,

[1] Converted from 3–28 EUR/MWh using an exchange rate of 1 EUR = 11 SEK.
[2] Converted from 0.085–0.243 USD/kWh using an exchange rate of 1 USD = 10.5 SEK.

electricity is delivered to households, businesses, and electric vehicle charging infrastructure. Before reaching ordinary consumers, the voltage is transformed down to 230–400 V [36].

Like the transmission grid, local distribution grids operate as natural monopolies, meaning that only one DSO is responsible for electricity distribution within a given geographical area. Consumers therefore pay grid tariffs to their local DSO for using the distribution network [36].

In Sweden, electricity consumers typically pay separately for electricity supply and network services. Electricity is purchased from an electricity retailer, while network charges are paid to the local DSO. In addition to fixed subscription fees, DSOs apply variable network tariffs based on the amount of electricity transferred (SEK/kWh). For example, Vattenfall Eldistribution applies a variable network tariff of approximately 44.5 öre/kWh for residential customers under its 2026 simple tariff structure [40].

For bidirectional EV operation, treatment of exported electricity is less straightforward. In some market designs, electricity exported from distributed resources could be subjected to grid-related charges, reduced compensation schemes, or asymmetric import/export tariff structures. Previous V2G literature have therefore suggested different assumptions regarding export network charges, with some explicitly applying grid-related costs to discharged electricity as part of the economic assessment [41].

In the Swedish residential context, no clear and uniformly applicable framework was identified for assigning household-level distribution grid charges to bidirectional V2G exports within the scope of this study. The present analysis therefore applies grid-related charges only to imported charging energy, while exported electricity is treated as compensated through the relevant market mechanisms.

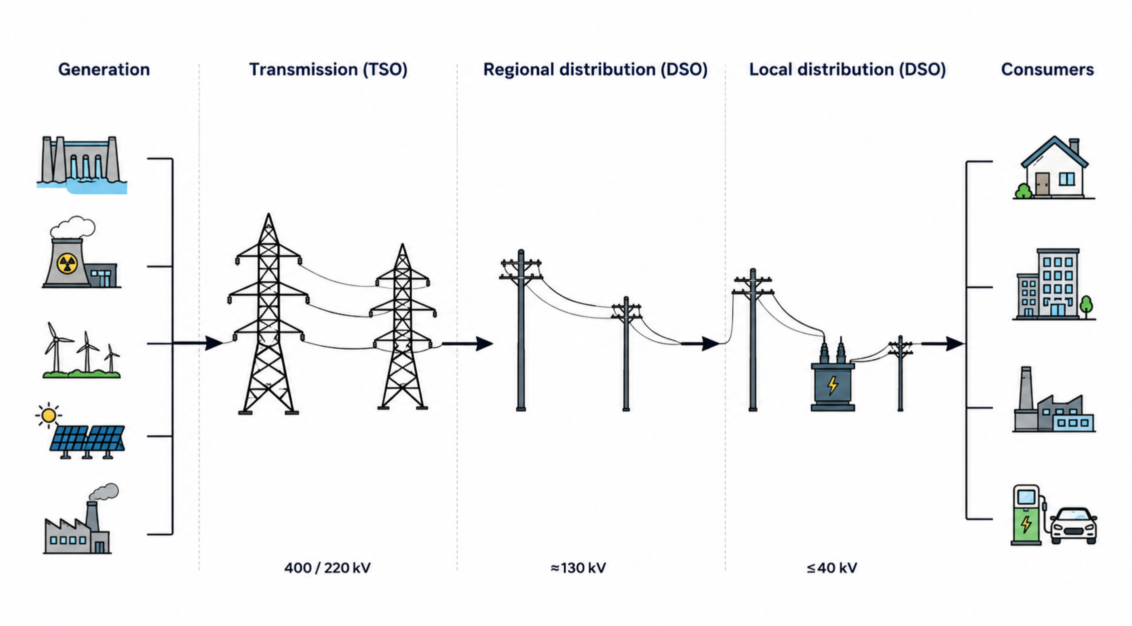

Figure 2.1: Illustration of the Swedish electricity system generated using OpenAI ChatGPT image generation tools.

2.2.2 Peak-demand tariffs

An additional real-world factor relevant to EV flexibility economics is the power-based network tariffs, where customer charges depend partly on peak electricity demand. Such tariff structures may affect both smart charging and V2G operation, since concentrated charging could increase household peak demand, while bidirectional flexibility could potentially reduce it [42, 43].

Peak-demand tariff effects were not explicitly modeled in this study, since the available dataset only captures EV charging behavior and does not include total household load. Although the EV fleet itself can be considered an aggregated flexible load, the interaction between EV charging schedules and household peak demand was not evaluated. Such effects may become increasingly important when assessing the impact of large-scale EV adoption on distribution grid peak loads and demand-based network tariffs, as information on the total household load profile would be required to accurately estimate customer demand charges. In addition, the regulatory implementation of mandatory peak-based tariffs in Sweden remains uncertain. Following the Swedish government's announcement in March 2026 regarding a pause in the rollout requirement, several distribution system operators, including Vattenfall Eldistribution, also paused their implementation plans [43].

2.2.3 The Spot Market

The day-ahead market is one of the largest marketplace for electricity trading in Sweden and across the Nordic and European power system. In the Nordic region, the day-ahead electricity market is operated by NordPool, one of the largest electricity market operators in Europe, where electricity is traded one day in advance using a centralized auction. Historically, market participants submitted hourly supply and demand bids, after which market-clearing prices were determined for each bidding zone and hour of the following day. From 2025, the historical day-ahead price data obtained from ENTSO-E [44] were provided at a 15-minute resolution following the market transition to 15-minute market time units (MTUs). [45].

Electricity prices in the day-ahead market vary depending on factors such as electricity demand, fuel prices, transmission constraints, weather conditions, and the availability of generation resources.

This variability became especially pronounced during the European energy crisis in 2022. Following Russia's invasion of Ukraine, European energy markets experienced severe supply disruptions, particularly in natural gas markets, as Russian gas deliveries were reduced and Europe became increasingly exposed to volatile LNG markets. Since marginal electricity prices in many European electricity markets are strongly influenced by gas-fired generation, these developments led to exceptionally high electricity prices and extreme short-term volatility [46, 47]. The day-ahead price data for SE3 used in this study reflects this clearly, with 2022 showing higher volatility and more extreme price excursions than the comparatively more stable market conditions observed in 2024 Figure 2.2.

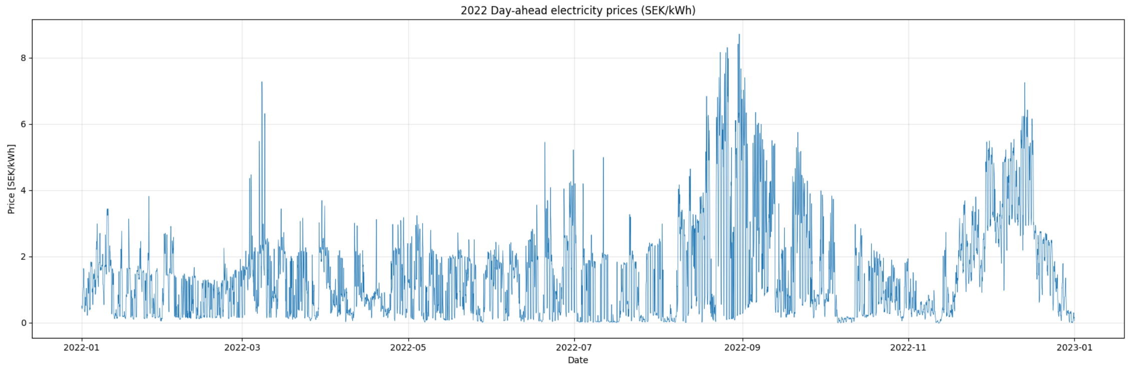

(a) Hourly day-ahead electricity prices in SE3 during 2022.

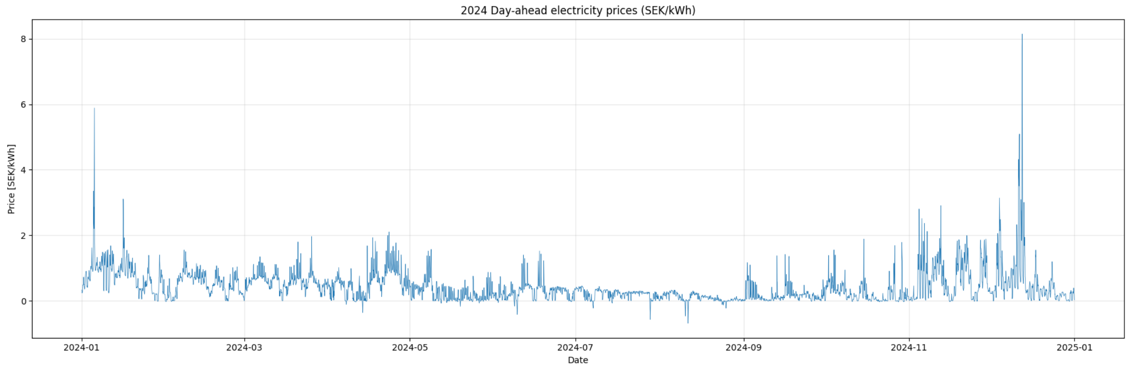

(b) Hourly day-ahead electricity prices in SE3 during 2024.

Figure 2.2: Comparison of hourly day-ahead electricity prices in SE3 for 2022 and 2024.

2.2.4 FCR Market

FCR is an ancillary service used to maintain system frequency at 50 Hz by correcting real-time imbalances between electricity supply and demand. In Sweden, FCR is divided into three products: FCR-N, FCR-D up, and FCR-D down. All three products are automatically activated and provide a linear response within their respective frequency ranges.

As shown in Table 2.1, the three products differ in activation range, symmetry requirements, and activation duration. FCR-N is a symmetric product requiring both upward and downward response capability, while FCR-D up and FCR-D down are asymmetric disturbance reserve products.

Since 1 February 2024, all Swedish FCR markets have applied marginal pricing (pay-as-cleared), meaning that all accepted bids are paid at the market-clearing price determined by the highest accepted bid. Prior to this change, FCR markets used pay-as-bid pricing, where each accepted provider was paid according to its submitted bid price. [48] Only accepted bids receive capacity compensation, while rejected bids receive no compensation. The transition between pay-as-bid and pay-as-cleared was not modelled explicitly, since the optimization does not represent real-time bidding strategies.

FCR-N includes both capacity payment and compensation for activated energy, where net activated energy is settled using mFRR up- and downregulation prices. In contrast, FCR-D up and FCR-D down are only compensated through capacity payments [49, 50, 51].

Table 2.1: Summary of FCR products in Sweden and key participation requirements.

Service	Freq. range (Hz)	Response	Symmetry	Duration	Min bid
FCR-N	49.9–50.1	∼30 s	Symmetric	1 h	0.1 MW
FCR-D Up	49.5–49.9	$\leq$ 7.5 s	Upward	$\geq$ 20 min	0.1 MW
FCR-D Down	50.1–50.5	$\leq$ 7.5 s	Downward	$\geq$ 20 min	0.1 MW

2.2.5 FCR Activation

Figure 2.3 shows the droop-control characteristics used for FCR in the Nordic power system. The horizontal axis represents the system frequency in Hz, while the vertical axis represents the activated reserve power as a percentage of the committed reserve capacity.

The activation follows a proportional droop-control principle, meaning that the activated power increases gradually as the frequency deviation becomes larger. Small frequency deviations therefore result in partial activation, while larger deviations lead to full activation of the offered reserve capacity [21].

For FCR-N, shown in Figure 2.3(a) [21], activation occurs symmetrically around the nominal system frequency of 50 Hz within the normal operating range of approximately 49.9-50.1 Hz. At exactly 50 Hz, no reserve activation occurs because the system is balanced. If the frequency decreases below 50 Hz, the reserve provider gradually injects power into the grid or reduces consumption. The activation increases linearly until full upward activation is reached at 49.9 Hz. If the frequency increases above 50 Hz, the reserve provider gradually absorbs power from the grid by increasing consumption or reducing generation, reaching full downward activation at 50.1 Hz.

Figure 2.3(b) [21] illustrates the activation behavior of FCR-D, which is intended for larger disturbances in the power system. FCR-D up is activated only during under frequency conditions, below 49.9 Hz. As the frequency decreases further, the activated reserve power increases linearly until full activation is reached around 49.5 Hz. Similarly, FCR-D down is activated only during over frequency conditions above approximately 50.1 Hz, with full activation reached around 50.5 Hz.

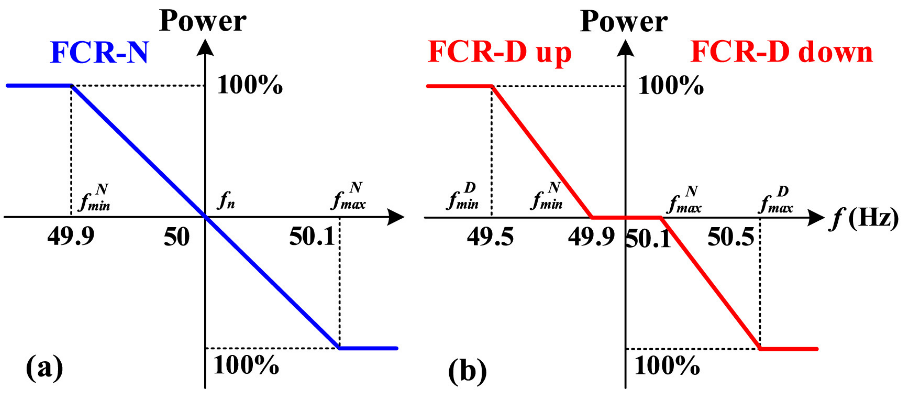

Figure 2.3: Droop-control activation.

2.2.6 Participation of Aggregated EV Fleets in Electricity Markets

Aggregators have emerged as important market actors by coordinating distributed flexibility resources in order to enable participation in electricity markets. Depending on the flexibility resource, aggregators may operate industrial demand-response portfolios, stationary battery storage systems, or distributed energy resource (DER) portfolios. A broader category of aggregators consists of virtual power plant (VPP) operators, which combine multiple distributed assets such as solar generation, battery storage, flexible demand, and electric vehicles into a coordinated market resource capable of participating in energy and ancillary service markets [52].

Aggregators can operate under different organizational models. Fåregård and Miletic [53] describe a distinction between technical aggregators, which primarily provide the technical flexibility resource, market aggregators, which coordinate market participation and balancing responsibilities, and integrated independent aggregators, which combine both technical and commercial functions. Also, ongoing regulatory developments in European electricity markets aim to clarify market access conditions for independent aggregators and facilitate increased participation of distributed flexibility providers [54].

EV aggregators act as intermediaries between distributed EV users and electricity markets, coordinating charging, discharging, and market participation [41]. Compared with stationary battery aggregation, EV aggregation introduces greater complexity due to uncertain vehicle availability, mobility constraints, and user-dependent participation [55]. Consequently, the economic viability of EV aggregation depends not only on technical flexibility, but also on market design and the aggregator's ability to reliably coordinate distributed resources under uncertainty [41, 55]. Accordingly, this study adopts an aggregator-centered perspective to evaluate EV flexibility as a coordinated commercial resource rather than from the perspective of individual vehicle owners.

3

Methods

This chapter presents the methodological framework used to evaluate the economic potential of V2G aggregation from an aggregator perspective. The methodology combines real-world EV data, deterministic optimization, scenario analysis, and uncertainty availiability.

3.1 The methodological framework

The methodological framework consists of six main steps, as illustrated in Figure 3.1. The figure provides an overview of the complete workflow and shows how the individual stages of the analysis are connected, from raw EV event data to the fleet-level economic evaluation.

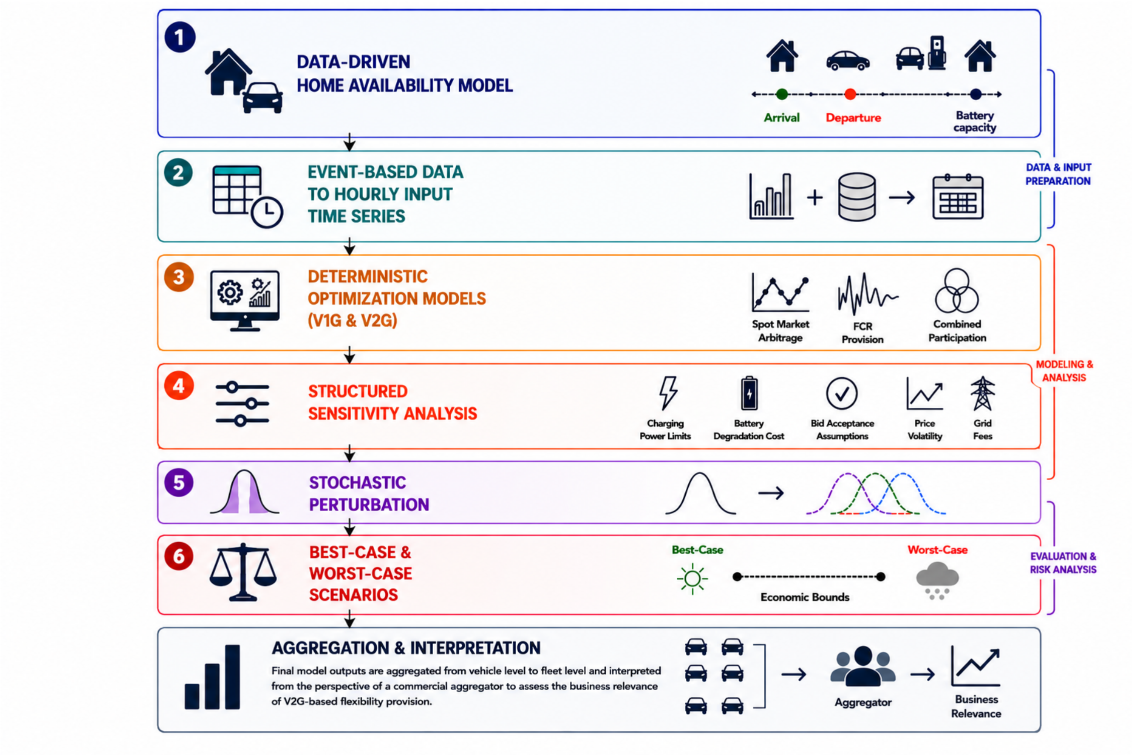

Figure 3.1: Overview of the methodological workflow used to evaluate EV flexibility from an aggregator perspective. Visualization generated using OpenAI ChatGPT image generation tools based on the methodology developed by the authors.

The full methodological workflow, including data preprocessing, availability mod-

elling, scenario generation, and optimization, is implemented in Python. The optimization models are formulated using the Pyomo optimization framework and solved with Gurobi solver.
First, a data-driven availability model is constructed using real-world EV parking and charging behavior. These data are used to infer vehicle availability, home connection status, arrival and departure events, trip energy requirements, and battery capacities.
Second, the event-based data are transformed into hourly input time series suitable for optimization. In this step, historical day-ahead electricity prices and FCR market prices from the Swedish bidding zone SE3 are merged with the vehicle-level data.
Third, deterministic optimization models for V1G and V2G are developed to determine the economically optimal charging, discharging, and reserve bidding strategies for individual vehicles. Separate formulations are used for spot market arbitrage, FCR provision, and combined participation in both markets.
Fourth, structured sensitivity analysis is performed to study how profitability and technical feasibility depend on key assumptions, such as charging power limits, battery degradation cost, bid acceptance assumptions, price volatility, and grid fees.
Fifth, a stochastic perturbation evaluation is conducted to analyze availability uncertainty.
Sixth, best-case and worst-case scenarios are constructed to estimate the upper and lower economic bounds of V2G profitability under optimistic and conservative market and technical assumptions.
The final model outputs are aggregated from vehicle level to fleet level and interpreted from the perspective of a commercial aggregator, making it possible to assess the business relevance of V2G-based flexibility provision.

3.2 Input Data

3.2.1 EV Event Data

The EV driving and charging data used in this thesis are based on the same data-collection campaign described by Kobayashi et al. [30]. However, the dataset employed in this work differs from that analysed in the original study, both in the number of included vehicles and in its temporal coverage. The original dataset consists of real-world EV data collected from 334 privately owned vehicles in Sweden using Geotab devices connected to the onboard diagnostics (OBD) port. The vehicles had battery capacities ranging from 16–100 kWh and were selected using national registry data from Statistics Sweden (SCB) to provide a representative distribution of EV users across different geographic regions, residential categories, and housing types.
The raw data were provided as event-based records, where each event was classified as either a parking event or a charging event. For each event, information such as start time, end time, location (e.g., home, work, or other), state of charge (SOC), and charged energy was available. According to Kobayashi et al. [30], the data were collected from October 2022 to September 2024 using Geotab logging equipment, although the version of the dataset used in this thesis was extended until

March 2025. Some missing values were present due to communication interruptions, software-related issues, temporary loss of connectivity, or the logging device being disconnected.
While the original dataset contains 334 vehicles, the dataset employed in this thesis consists of 152 vehicles. The participating vehicles were not continuously available throughout the entire study period and the duration of the recorded data varied between individual EVs. The resulting temporal variation in fleet participation is illustrated in Figures B.2–B.5.
Before estimating vehicle-specific parameters, the raw event data were standardized and the original column names were renamed according to Table A.1.

3.3 Event-Based Preprocessing

3.3.1 Treatment of Missing and Lower SOC Values

Before constructing the hourly dataset, missing SOC observations were determined to be 3.95%. Missing SOC values were repaired for parking events prior to the hourly transformation. Before the SOC reconstruction procedure, a small number of parking events associated with home charging sessions were removed from the dataset due to physically unrealistic charging behavior. In total, seven parking-event rows associated with five vehicles were excluded, since the corresponding charging and parking observations were considered inconsistent with physically realistic home-charging operation. If both the arrival and departure SOC of a parking event were missing, the event was removed, since no physically grounded reconstruction was possible.
If only one SOC value was missing, the missing value was estimated based on whether overlapping home charging events occurred during the same parking interval, defined as

$$t^{charge,start} < t^{park,end} \qquad \text{and} \qquad t^{charge,end} > t^{park,start}. \tag{3.1}$$

The following equations throughout the model are applied independently for each vehicle v.
If no overlapping charging event existed, the SOC was assumed constant during the parking period:

$$SOC_i^{park,start} = SOC_i^{park,end} \tag{3.2}$$

or

$$SOC_i^{park,end} = SOC_i^{park,start}. \tag{3.3}$$

If overlapping charging events existed, the missing SOC was reconstructed from directly observed charge-event SOC values. Missing arrival SOC was set equal to the start SOC of the first overlapping charging event:

$$SOC_i^{park,start} = SOC_{first}^{charge,start} \tag{3.4}$$

while missing departure SOC was set equal to the end SOC of the last overlapping charging event:

$$SOC_i^{park,end} = SOC_{last}^{charge,end}. \tag{3.5}$$

Finally, for home parking events, cases where the departure SOC was lower than the arrival SOC were corrected by enforcing

$$SOC_i^{park,end} = SOC_i^{park,start} \quad \text{if} \quad SOC_i^{park,end} < SOC_i^{park,start}. \tag{3.6}$$

3.3.2 Fragment Merging

Some parking events appeared as fragmented park events instead of continuous parking period. To avoid treating these as separate independent parking episodes, consecutive park events were merged if they satisfied the following criteria:

1. The time gap between the previous event end and the next event start was non-negative and at most 15 minutes.
2. The absolute SOC difference between the previous end SOC and the next start SOC was at most 0.02.
3. The two events occurred at the same location.

Let event i be followed by event $i + 1$. The time gap was calculated as

$$\Delta t_i^{gap} = t_{i+1}^{start} - t_i^{end}. \tag{3.7}$$

The SOC gap was calculated as

$$\Delta SOC_i^{gap} = \left| SOC_{i+1}^{start} - SOC_i^{end} \right|. \tag{3.8}$$

Two park events were merged if

$$0 \leq \Delta t_i^{gap} \leq 0.25h, \tag{3.9}$$

$$\Delta SOC_i^{gap} \leq 0.02, \tag{3.10}$$

and the location was identical.

When events were merged, the start time and start SOC of the first event were retained, while the end time and end SOC were taken from the final event in the merged sequence. The merged event was then treated as a single continuous parking interval in the hourly mapping, keeping the observed SOC path while avoiding artificial fragmentation of parking behaviour.

The selected thresholds were chosen as conservative heuristics intended to reconnect likely artificially fragmented parking events while minimizing the risk of merging genuinely separate trips. A maximum time gap of 15 minutes was considered sufficiently short to represent a temporary logging interruption rather than actual vehicle movement, while the SOC threshold of 0.02 limited merging to events with only minor state-of-charge deviations consistent with measurement uncertainty, auxiliary battery use, preconditioning, or short charging-related fluctuations.

3.3.3 Hourly Mapping of Parking Availability

For each vehicle v, an hourly time grid was constructed as

$$T_v = \{t_0, t_0 + 1, \ldots, t_N\} \tag{3.11}$$

where the first timestamp was rounded down to the nearest hour and the final timestamp rounded upward.
Each parking event was mapped to the hourly grid through arrival and departure anchors:

$$t_i^{arr} = \left\lfloor t_i^{start} \right\rfloor \tag{3.12}$$

$$t_i^{dep} = \left\lceil t_i^{end} \right\rceil \tag{3.13}$$

Home availability was defined as

$$at\_home_{v,t} = \begin{cases} 1, & t_i^{arr} \le t \le t_i^{dep}, \text{ location} = home \\ 0, & \text{otherwise} \end{cases} \tag{3.14}$$

Frequency reserve availability was restricted to home parking:

$$fcr\_available\_home_{v,t} = at\_home_{v,t} \tag{3.15}$$

3.3.4 Anchor Construction & Consistency Repairs

If a departure anchor overlapped or crossed the next arrival anchor,

$$t_i^{dep} \ge t_{i+1}^{arr} \tag{3.16}$$

the departure anchor was repaired according to

$$t_i^{dep,*} = t_{i+1}^{arr} - 1 \tag{3.17}$$

Segments that remained infeasible after this repair, for example zero-length or inverted intervals,

$$t_i^{dep,*} \le t_i^{arr} \tag{3.18}$$

were removed from the anchor set.
Each valid parking segment generated one arrival anchor and one departure anchor. Arrival anchors were assigned as

$$is\_arrival_{v,t} = 1 \tag{3.19}$$

with associated energy anchor

$$E_{v,t}^{arr} = SOC_{i,v}^{start} E_v^{max}. \tag{3.20}$$

Departure anchors were similarly assigned as

$$is\_departure_{v,t} = 1 \tag{3.21}$$

with

$$E^{dep}_{v,t} = SOC^{end}_{i,v} E^{max}_{v}. \tag{3.22}$$

These anchor values were later used in the optimization model to enforce the observed SOC trajectory.
Diagnostic outputs were retained to quantify merged fragments, repaired boundary conflicts, dropped segments, and post-processing collision checks. No arrival-departure hourly collisions remained in the final dataset.

3.3.5 Validation of Preprocessing Pipeline

To evaluate the impact of the preprocessing pipeline, a validation analysis was conducted to assess both the accuracy of the retained SOC anchors and the information loss associated with dropped segments.
The validation was therefore divided into two components: (i) accuracy of retained anchors and (ii) impact of dropped anchors.
For all retained anchor segments, the SOC values at arrival and departure were compared to the corresponding original SOC values from the event-based dataset. The mean absolute error (MAE) was computed as

$$\mathrm{MAE} = \frac{1}{N} \sum_{i=1}^{N} \left| \mathrm{SOC}_i^{\mathrm{model}} - \mathrm{SOC}_i^{\mathrm{original}} \right|, \tag{3.23}$$

where N denotes the number of matched anchor points. Only retained and successfully matched anchors were included in this calculation. MAE measures the average magnitude of the error without considering its direction.
In addition, the root mean square error (RMSE) is used, defined as:

$$\mathrm{RMSE} = \sqrt{\frac{1}{N} \sum_{i=1}^{N} (x_i - \hat{x}_i)^2} \tag{3.24}$$

RMSE penalizes larger errors more strongly due to the squared term.
Dropped anchor segments were not included in the MAE calculation, since no consistent hourly mapping could be constructed for these segments. Instead, their impact was quantified by comparing their contribution to the total SOC variation in the dataset.
For each anchor segment, the absolute SOC change was computed as

$$\Delta\mathrm{SOC}_i = \left| \mathrm{SOC}_i^{\mathrm{end}} - \mathrm{SOC}_i^{\mathrm{start}} \right|. \tag{3.25}$$

The relative contribution of dropped segments was then defined as

$$\mathrm{Share}_{\mathrm{dropped}} = \frac{\sum_{i \in \mathrm{dropped}} \Delta\mathrm{SOC}_i}{\sum_{i \in \mathrm{all}} \Delta\mathrm{SOC}_i}. \tag{3.26}$$

This metric captures the fraction of total SOC variation that is excluded due to preprocessing.

3.4 Vehicle Parameters Estimation

3.4.1 Battery Capacity Estimation

The battery capacity was not directly available in the dataset. It was therefore estimated from charging events where both charged energy and SOC change were available. For each charging event i, the SOC increase was first calculated as

$$\Delta SOC_i = SOC_i^{\text{end}} - SOC_i^{\text{start}}. \tag{3.27}$$

The event-level battery capacity estimate was then calculated as

$$\hat{E}_i^{\max} = \frac{E_i^{\text{ch}} \eta^{\text{ch}}}{\Delta SOC_i}, \tag{3.28}$$

where $\hat{E}_i^{\max}$ is the estimated battery capacity from event i, E_i^{ch} is the charged energy reported in the dataset, and η^{ch} is the charging efficiency used in the estimation. In this preprocessing step, $\eta^{\text{ch}} = 1$ was used. This means that the reported charged energy was treated as the energy corresponding directly to the observed SOC increase. Operational charging losses were instead handled later in the optimization model.
Not all charging events were considered reliable for capacity estimation. Therefore it was applied a set of filtering criteria. A charging event was only retained if

$$\begin{aligned}
E_i^{\text{ch}} &> 2.0 \text{ kWh}, && (3.29)\\
\Delta t_i &\geq 0.25 \text{ h}, && (3.30)\\
\Delta SOC_i &\geq 0.10, && (3.31)\\
0 \leq SOC_i^{\text{start}} &\leq 1, && (3.32)\\
0 \leq SOC_i^{\text{end}} &\leq 1. && (3.33)
\end{aligned}$$

After the event-level capacity estimate had been calculated, an additional filter was applied:

$$15 \leq \hat{E}_i^{\max} \leq 120 \quad \text{kWh}. \tag{3.34}$$

These thresholds were used to remove events with smaller SOC changes, very short durations, missing or invalid values, or physically unrealistic implied battery capacities.
For each vehicle v, the final battery capacity estimate was calculated as the median of all valid event-level estimates:

$$\hat{E}_v^{\max} = \text{median}\left(\hat{E}_i^{\max}\right), \quad i \in \mathcal{C}_v^{\text{valid}}, \tag{3.35}$$

where $\mathcal{C}_v^{\text{valid}}$ denotes the set of valid charging events for vehicle v. The median was used instead of the mean because it is less sensitive to outliers in the event data.
If no valid charging event was available, the vehicle received a missing capacity estimate at this stage. In the final summary file, a cleaned battery capacity variable was then created as

$$E_{v,\text{clean}}^{\max} = \begin{cases} 50 \text{ kWh}, & \text{if } \hat{E}_v^{\max} \text{ is missing, below 10 kWh, or above 120 kWh,} \\ \hat{E}_v^{\max}, & \text{otherwise.} \end{cases} \tag{3.36}$$

A fallback battery capacity of 50 kWh was used when no reliable vehicle-specific estimate could be obtained. This value was chosen as it was within the range of battery capacities represented in the dataset, avoiding unrealistic assumptions.

3.4.2 Home Charging Power Estimation

In addition to the battery capacity, the observed home charging power from charging events located at home were gathered. Only rows where the event type was classified as `charge` or `charging`, and where the location was equal to `home`, were used for this step.
For each valid home charging event, the average charging power was calculated as

$$\hat{P}_i^{\text{ch}} = \frac{E_i^{\text{ch}}}{\Delta t_i}, \tag{3.37}$$

where $\hat{P}_i^{\text{ch}}$ is the estimated average charging power during event i, E_i^{ch} is the charged energy, and Δt_i is the event duration in hours.
Only data was retained from home charging events satisfying

$$E_i^{\text{ch}} > 0, \tag{3.38}$$

$$\Delta t_i \geq 0.01 \text{ h}. \tag{3.39}$$

To remove invalid or unrealistic power estimates, the following filter was applied:

$$0.1 \leq \hat{P}_i^{\text{ch}} \leq 22 \quad \text{kW}. \tag{3.40}$$

For each vehicle, stored the number of home charging events, the number of valid home charging power observations, and summary statistics of the estimated charging power:

$$\left\{ \text{median}(\hat{P}_i^{\text{ch}}), \text{mean}(\hat{P}_i^{\text{ch}}), \text{std}(\hat{P}_i^{\text{ch}}), \min(\hat{P}_i^{\text{ch}}), \max(\hat{P}_i^{\text{ch}}) \right\}. \tag{3.41}$$

The estimated home charging power was primarily used to characterize observed charging behaviour in the raw data and to inform realistic charging-power assumptions for the optimization model. Rather than directly using observed event-level charging powers, standardized charging and discharging power limits were imposed as explicit model assumptions, with alternative power levels later evaluated through sensitivity analysis.

3.5 Market Data Preprocessing

3.5.1 Market Price Data

Hourly day-ahead spot prices were merged with each vehicle time series. The spot price files were obtained from ENTSO-E [44]. The timestamps were processed and resampled to hourly resolution using the arithmetic mean:

$$\pi_t^{\text{spot,EUR/MWh}} = \frac{1}{n_t} \sum_{q=1}^{n_t} \pi_{t,q}^{\text{spot,EUR/MWh}}, \tag{3.42}$$

where n_t denotes the number of observations within hour t.
Spot prices were converted from EUR/MWh to SEK/kWh using a daily EUR/SEK exchange rate:

$$\pi_t^{\text{spot,SEK/kWh}} = \frac{\pi_t^{\text{spot,EUR/MWh}} \cdot x_d^{\text{EUR/SEK}}}{1000}, \tag{3.43}$$

where $x_d^{\text{EUR/SEK}}$ denotes the EUR/SEK exchange rate for each day d throughout the study period.
Reserve-market price data for FCR-N, FCR-D up, FCR-D down, and mFRR up-/down were obtained from Mimer[56]. FCR and mFRR prices were provided in EUR/MW and converted to SEK/kW using the same daily EUR/SEK exchange-rate methodology.
The daily exchange-rate data were merged with the spot-price and reserve-market price time series by date. The final processed market-price dataframe contained hourly values for spot prices, FCR-N, FCR-D up, FCR-D down, mFRR up, and mFRR down, together with the associated exchange-rate variables. This hourly market dataset was then joined to each vehicle's processed time series using timestamp matching.
Remaining missing market-price values were filled using forward-fill and backward-fill. Missing reserve-market prices were set to zero where no corresponding market data were available.

3.5.2 Frequency Data

To quantify the energy activation associated with FCR, measured frequency data from Fingrid were processed from 3-minute resolution into hourly activation factors [57]. The purpose of this preprocessing step was to construct a time series that could be directly integrated into the hourly optimization model while preserving the relationship between grid frequency deviations and reserve activation.
The preprocessing assumes that the measured frequency at each 3-minute timestamp is representative of the corresponding interval and that reserve activation follows a linear droop relationship within each reserve band. Missing or invalid frequency observations were removed before aggregation.
The measured frequency f_k was translated into normalized activation factors for FCR-N up, FCR-N down, FCR-D up, and FCR-D down. The activation factors

were dimensionless values in the interval $[0, 1]$, where 0 corresponds to no activation and 1 corresponds to full activation.
For FCR-N, upward activation was defined as

$$\alpha_k^{N,\uparrow} = \max\left(\min\left(\frac{50.0 - f_k}{0.1}, 1\right), 0\right) \tag{3.44}$$

and downward activation as

$$\alpha_k^{N,\downarrow} = \max\left(\min\left(\frac{f_k - 50.0}{0.1}, 1\right), 0\right) \tag{3.45}$$

For FCR-D, activation was assumed to occur outside the normal FCR-N band. Upward FCR-D activation was defined as

$$\alpha_k^{D,\uparrow} = \max\left(\min\left(\frac{49.9 - f_k}{0.4}, 1\right), 0\right) \tag{3.46}$$

while downward activation was defined as

$$\alpha_k^{D,\downarrow} = \max\left(\min\left(\frac{f_k - 50.1}{0.4}, 1\right), 0\right) \tag{3.47}$$

where $x \in \{N, up;\ N, down;\ D, up;\ D, down\}$ and N_t denotes the number of 3-minute observations within hour t.
The resulting hourly activation factors represent the average share of reserved reserve capacity activated during the corresponding optimization hour.
If reserve capacity P_t is cleared in hour t, the corresponding activated energy is computed as

$$E_t^{act} = P_t \alpha_t. \tag{3.48}$$

3.6 Model Assumptions

The optimization framework relies on several simplifying assumptions that define the scope of the analysis:

- **Home-only controllability:** EV flexibility is assumed to be controllable only when vehicles are parked at home. Charging behavior outside the home is treated as exogenous.
- **Continuous home connection:** Vehicles are assumed to remain physically connected throughout observed home parking intervals.
- **Hourly discretization:** Vehicle availability, market prices, and reserve activation are represented at hourly resolution.
- **Anchor-based temporal approximation:** Event-based arrival and departure timestamps are mapped to the hourly optimization grid using rounded SOC anchor constraints.
- **Perfect market foresight:** The deterministic baseline assumes full knowledge of future spot prices, reserve prices, and activation outcomes.

- **Fixed technical limits:** Charging/discharging power limits and battery parameters are treated as fixed model inputs.
- **Linear degradation model:** Battery degradation is represented using a constant marginal throughput cost.
- **No local grid constraints:** Household connection limits, transformer congestion, and feeder constraints are not explicitly modeled.
- **Energy-based network tariff assumption:** Charging network costs are represented using volumetric import tariffs only.
- **Uniform market environment:** All vehicles are evaluated under the same electricity market-price assumptions.
- **Minimum reserve-capacity assumption:** Minimum bid size constraints were not explicitly enforced in the optimization model, implying an assumption that the aggregator can participate in the FCR market without bid-size limitations. Practical compliance with 0.1 MW threshold is assessed separately through ex-post analysis.

3.7 Deterministic Optimization Framework for EV Flexibility

This section presents the deterministic optimization framework used to evaluate the economic potential of EV flexibility from an aggregator perspective. Vehicle operation is optimized at the individual vehicle level using preprocessed hourly event-based data, while economic performance is aggregated to fleet level.
To isolate the cost value of different flexibility services, four market configurations are evaluated:

1. V1G reference
2. Spot-market V2G arbitrage
3. FCR-only V2G participation
4. Co-optimized spot and FCR V2G participation

All four configurations rely on the same underlying SOC-constrained vehicle model, while market access, decision variables, and objective functions differ depending on the flexibility strategy.
To enable direct comparison between strategies, the difference in total economic outcome relative to the V1G reference case is used as the primary performance metric:

$$\Delta\Pi = \Pi_{V2G} - \Pi_{V1G} \tag{3.49}$$

where Π_{V2G} represents the total economic outcome of the evaluated V2G strategy and Π_{V1G} the corresponding V1G reference case. where Π_{V2G} and Π_{V1G} denote the total fleet profit under bidirectional and unidirectional operation, respectively.
A complete overview of the input variables and parameters used in the deterministic optimization framework is provided in Appendix A.2. Table A.3 summarizes the baseline parameters used across the four deterministic market optimization models. These parameters define the battery operating limits, charging and discharging

efficiencies, maximum charging and reserve power constraints, degradation cost assumptions, and the variable grid-fee structure applied throughout the optimization.

3.7.1 Decision Variables

For each vehicle and hour, the following decision variables are defined:

$$
\begin{aligned}
P_t^{ch} &\geq 0, && (3.50)\\
P_t^{dis} &\geq 0, && (3.51)\\
P_t^{N} &\geq 0, && (3.52)\\
P_t^{D,up} &\geq 0, && (3.53)\\
P_t^{D,down} &\geq 0, && (3.54)\\
E_t &\geq 0. && (3.55)
\end{aligned}
$$

Here, P_t^{ch} is spot charging power, P_t^{dis} is spot discharging power, P_t^{N} is the FCR-N capacity bid, $P_t^{D,up}$ is the FCR-D up capacity bid, $P_t^{D,down}$ is the FCR-D down capacity bid, and E_t is battery energy at the beginning of hour t.
Binary mode variables are introduced to prevent simultaneous charging and discharging:

$$b_t^{ch}, b_t^{dis} \in \{0, 1\}. \tag{3.56}$$

3.7.2 Battery Energy Dynamics

Battery energy after the hourly decision is defined as

$$
\begin{aligned}
E_t^{after} = E_t &+ \eta^{ch} P_t^{ch} \Delta t - \frac{P_t^{dis} \Delta t}{\eta^{dis}} \\
&+ \eta^{ch} \left(\alpha_t^{N,down} P_t^{N} + \alpha_t^{D,down} P_t^{D,down} \right) \\
&- \frac{\alpha_t^{N,up} P_t^{N} + \alpha_t^{D,up} P_t^{D,up}}{\eta^{dis}}.
\end{aligned} \tag{3.57}
$$

The first term represents the battery energy at the beginning of the time step, while the second and third terms represent charging and discharging. The charging and discharging efficiencies are denoted by η^{ch} and η^{dis}, respectively, both assumed to be 93%. The remaining terms represent activated FCR energy. Downward activation increases battery energy, while upward activation decreases battery energy. Throughout the baseline cases 100% bid acceptance is assumed.
For time steps not followed by an observed arrival event, battery energy is modelled according to

$$E_{t+1} = E_t^{after}, \qquad \forall t : \delta_{t+1}^{arr} = 0. \tag{3.58}$$

If the next time step is an arrival event, this transition is skipped and the battery state is reset to the observed arrival energy.

3.7.3 SOC Anchoring

At arrival events, battery energy is fixed to the observed arrival energy:

$$E_t = E_t^{arr}, \qquad \forall t : \delta_t^{arr} = 1. \tag{3.59}$$

The treatment of departure events differs between the V1G baseline and the V2G models.
In the V1G baseline, departure energy is imposed as a minimum mobility requirement:

$$E_t^{after} \geq E_t^{dep}, \qquad \forall t : \delta_t^{dep} = 1. \tag{3.60}$$

This formulation ensures that the observed mobility requirement is satisfied while avoiding artificial infeasibilities introduced by preprocessing approximations, such as hourly time anchoring and event merging, which may create minor inconsistencies in the reconstructed SOC trajectories. As a result, vehicles are allowed to depart with a slightly higher SOC than observed, while still preserving the required minimum departure energy.
In the V2G models, departure energy is enforced as an exact SOC anchor:

$$E_t^{after} = E_t^{dep}, \qquad \forall t : \delta_t^{dep} = 1. \tag{3.61}$$

This prevents the optimizer from creating artificial value by ending parking intervals with more or less energy than observed in the original event data.
The first modelled time step is fixed to the first observed arrival energy:

$$E_0 = E_0^{arr}. \tag{3.62}$$

3.7.4 Battery Bounds

Battery energy is constrained before and after each hourly decision:

$$0 \leq E_t \leq E^{\max}, \tag{3.63}$$
$$0 \leq E_t^{after} \leq E^{\max}. \tag{3.64}$$

3.7.5 Charging and Discharging Constraints

Charging and discharging are only allowed when the vehicle is connected at home:

$$P_t^{ch} \leq h_t P^{ch,\max}, \tag{3.65}$$
$$P_t^{dis} \leq h_t P^{dis,\max}. \tag{3.66}$$

The binary mode variables enforce mutually exclusive baseline charging and discharging:

$$P_t^{ch} \leq b_t^{ch} P^{ch,\max}, \tag{3.67}$$
$$P_t^{dis} \leq b_t^{dis} P^{dis,\max}, \tag{3.68}$$
$$b_t^{ch} + b_t^{dis} \leq 1. \tag{3.69}$$

When the vehicle is not at home, b_t^{ch} and b_t^{dis} are fixed to zero, thereby forcing P_t^{ch} and P_t^{dis} to zero through the binary power constraints.
In the FCR-only implementation, discharging is restricted to a separate balancing-discharge limit:

$$P_t^{\text{bal,dis}} \leq h_t P^{\text{bal,dis,max}}, \tag{3.70}$$

This variable is introduced to maintain SOC feasibility following reserve activation, which may alter the battery state independently of planned charging decisions. Since the FCR-only formulation does not include explicit spot-market arbitrage, this constrained discharge mechanism is used solely to preserve internal SOC consistency and satisfy mobility requirements.

3.7.6 FCR Availability and Headroom Constraints

FCR bids are only allowed when the vehicle is available for FCR provision at home:

$$P_t^{N} \leq f_t P^{FCR,\max}, \tag{3.71}$$
$$P_t^{D,up} \leq f_t P^{FCR,\max}, \tag{3.72}$$
$$P_t^{D,down} \leq f_t P^{ch,\max}. \tag{3.73}$$

If the vehicle is not available for FCR provision, all FCR bid variables are fixed to zero.
Upward reserve provision and baseline discharging share the upward power limit:

$$P_t^{dis} + P_t^{N} + P_t^{D,up} \leq P^{FCR,\max}. \tag{3.74}$$

Downward reserve provision and baseline charging share the charging power limit:

$$P_t^{ch} + P_t^{N} + P_t^{D,down} \leq P^{ch,\max}. \tag{3.75}$$

FCR-D up cannot be offered while spot charging:

$$P_t^{D,up} \leq (1 - b_t^{ch}) P^{FCR,\max}. \tag{3.76}$$

FCR-D down cannot be offered while spot discharging:

$$P_t^{D,down} \leq (1 - b_t^{dis}) P^{ch,\max}. \tag{3.77}$$

3.7.7 SOC Feasibility for Reserve Provision

The battery must contain enough energy to sustain spot discharging and upward reserve activation:

$$E_t \geq E_{\min} + \frac{P_t^{dis}\Delta t + P_t^N \tau^N + P_t^{D,up}\tau^D}{\eta^{dis}}. \tag{3.78}$$

The battery must also have enough headroom to absorb spot charging and downward reserve activation:

$$E_t \leq E^{\max} - \eta^{ch}\left(P_t^{ch}\Delta t + P_t^N \tau^N + P_t^{D,down}\tau^D\right). \tag{3.79}$$

In the implementation, the reserve duration requirements are defined as

$$\tau^N = 1 \text{ h}, \qquad \tau^D = \frac{1}{3} \text{ h}. \tag{3.80}$$

3.7.8 Cost and Revenue Components

The general objective minimizes net operating cost:

$$\min\left(C^{spot} + C^{grid} + C^{deg} - R^{FCR} - R^{act}\right). \tag{3.81}$$

The spot charging cost is

$$C^{spot} = \sum_{t\in\mathcal{T}} \pi_t P_t^{ch}\Delta t. \tag{3.82}$$

When baseline discharging is remunerated through the spot market, the net spot cost is

$$C^{spot,net} = \sum_{t\in\mathcal{T}} \pi_t \left(P_t^{ch} - P_t^{dis}\right)\Delta t. \tag{3.83}$$

The grid fee is applied only to imported electricity:

$$C^{grid} = \sum_{t\in\mathcal{T}} c^{grid}\left(P_t^{ch}\Delta t + \alpha_t^{N,down}P_t^N + \alpha_t^{D,down}P_t^{D,down}\right). \tag{3.84}$$

Electricity tax is excluded, as the analysis adopts a wholesale-market aggregator perspective rather than that of an individual household end-user. Including electricity tax in both charging and subsequent V2G discharge cycles could also lead to distorted double taxation of the same energy throughput, while electricity tax does not represent a market-based marginal cost that influences aggregator dispatch decisions.

The degradation cost is represented by a linear throughput cost:

$$\begin{aligned} C^{deg} = \sum_{t\in\mathcal{T}} c^{deg}\Bigg(& P_t^{ch}\Delta t + P_t^{dis}\Delta t + \alpha_t^{N,up}P_t^N + \alpha_t^{N,down}P_t^N \\ & + \alpha_t^{D,up}P_t^{D,up} + \alpha_t^{D,down}P_t^{D,down}\Bigg). \end{aligned} \tag{3.85}$$

The degradation cost is included as an internal operational cost to discourage excessive battery cycling and reflect the economic trade-off associated with battery throughput, rather than as a detailed electrochemical aging model.
FCR capacity revenue is given by

$$R^{FCR} = \gamma^{\mathrm{FCR}} \sum_{t \in \mathcal{T}} \left(\lambda_t^N P_t^N + \lambda_t^{D,up} P_t^{D,up} + \lambda_t^{D,down} P_t^{D,down} \right). \tag{3.86}$$

Activation-related revenue from FCR-N is valued using activation prices:

$$R^{act} = \gamma^{\mathrm{FCR}} \sum_{t \in \mathcal{T}} \left(\mu_t^{up} \alpha_t^{N,up} P_t^N + \mu_t^{down} \alpha_t^{N,down} P_t^N \right). \tag{3.87}$$

FCR-D activation affects the SOC trajectory, degradation cost, and grid fee, but is not assigned a separate activation revenue in the implementation.

3.7.9 Model 1: V1G Reference

The V1G reference represents coordinated smart charging without bidirectional export. Only charging flexibility is allowed, while discharging and reserve participation are disabled:

$$P_t^{dis} = 0, \tag{3.88}$$
$$P_t^N = 0, \tag{3.89}$$
$$P_t^{D,up} = 0, \tag{3.90}$$
$$P_t^{D,down} = 0. \tag{3.91}$$

The objective minimizes charging-related operating cost:

$$\min \left(C^{spot} + C^{grid} \right) \tag{3.92}$$

This configuration represents conventional smart charging, where charging is shifted in time to reduce electricity cost while satisfying observed mobility requirements.

3.7.10 Model 2: Spot-Market V2G Arbitrage

The spot-market V2G model extends the V1G baseline by allowing bidirectional energy exchange with the spot market. Reserve participation is disabled:

$$P_t^{dis} \geq 0, \tag{3.93}$$
$$P_t^N = 0, \tag{3.94}$$
$$P_t^{D,up} = 0, \tag{3.95}$$
$$P_t^{D,down} = 0. \tag{3.96}$$

The objective minimizes net spot-market cost:

$$\min\left(C^{spot,net} + C^{grid} + C^{deg}\right) \tag{3.97}$$

This configuration captures pure spot-market energy arbitrage, where the EV battery can charge during low-price hours and discharge during high-price hours, while still following the observed SOC trajectory.

3.7.11 Model 3: FCR-Only V2G Participation

The FCR-only model evaluates reserve-market participation without spot-market arbitrage. In this configuration, reserve provision may alter the battery SOC through activated upward and downward reserve energy. To preserve consistency with the observed empirical SOC trajectory under exact departure constraints, a limited balancing-discharge variable is retained, capped at 0.5 kW:

$$P_t^{dis} \leq h_t \cdot 0.5 \tag{3.98}$$

The objective becomes

$$\min\left(C^{spot} + C^{grid} + C^{deg} - R^{FCR} - R^{act}\right), \tag{3.99}$$

This configuration isolates the economic contribution of reserve-market participation while preserving empirical mobility constraints.

3.7.12 Model 4: Co-Optimized Spot and FCR V2G

The co-optimization model represents the full flexibility case. Charging, discharging, and reserve provision are all simultaneously allowed, subject to shared power, SOC, and availability constraints.
In this configuration, baseline discharging is compensated through the spot market, and the vehicle may dynamically allocate flexibility between spot arbitrage and FCR provision.
The objective becomes

$$\min\left(C^{spot,coopt} + C^{grid,coopt} + C^{deg} - R^{FCR} - R^{act}\right). \tag{3.100}$$

The model represents the most flexible aggregator case, where EV flexibility can be allocated across both energy arbitrage and reserve-market provision.

3.7.13 Fleet aggregation

After solving each individual vehicle, hourly results are aggregated across all successfully optimized vehicles. For any fleet-level quantity X_t, aggregation is performed as

$$X_t^{fleet} = \sum_{i \in \mathcal{V}} X_{i,t}, \tag{3.101}$$

where $\mathcal{V}$ is the set of successfully optimized vehicles.

The aggregated fleet time series includes total charging power, total discharging power, total FCR-N bids, total FCR-D up and down bids, total battery energy, activated FCR energy, costs, revenues, and cumulative profit.

3.7.14 Solver settings and solution procedure

The optimization framework was implemented in Pyomo and solved using Gurobi. Since the study involves a large number of individual vehicle optimization problems across multiple market configurations and sensitivity scenarios, solver settings were adjusted between model runs to balance computational efficiency and solution quality.

Typical solver settings included modifications to parameters such as `Threads`, `Presolve`, `MIPFocus`, `MIPGap`, `Heuristics`, and `DualReductions`, depending on model complexity and scenario requirements.

For the most computationally demanding formulations, particularly the co-optimized spot and FCR models and selected sensitivity analyses, slightly relaxed convergence tolerances were used to ensure manageable runtimes. Across all cases, the accepted optimality gaps remained sufficiently small such that differences were not considered to affect the economic conclusions.

3.8 Scenario & Sensitivity Design

To evaluate the robustness of the deterministic baseline results, a sensitivity and scenario analysis was conducted across key technical and economic assumptions affecting EV flexibility value.

The purpose of this analysis was to assess how the profitability of V1G and V2G operation changes under different market and operational conditions, including variations in electricity price conditions, grid fees, battery degradation costs, and other key model assumptions.

For each scenario, the corresponding optimization model was re-solved using the modified parameter set rather than comparing against a single fixed baseline case. This includes recalculating the V1G baseline dynamically under each scenario. This approach was chosen to ensure a fair comparison between V1G and V2G under identical external conditions.

3.8.1 Charging Power Sensitivity

A charging power sensitivity analysis was conducted to evaluate how different charging and discharging power assumptions influence the economic potential of EV flexibility. To ensure a consistent comparison between charging-power scenarios, the same common fleet of 114 feasible vehicles was used in all cases.

Three different charging-power assumptions were evaluated. In the base case, all vehicles were assigned uniform charging and discharging power limits of

$$P_{\text{ch}}^{\max} = P_{\text{dis}}^{\max} = 11 \text{ kW}, \tag{3.102}$$

representing standard residential AC charging conditions. An additional scenario with

$$P_{\mathrm{ch}}^{\max} = P_{\mathrm{dis}}^{\max} = 22 \text{ kW} \tag{3.103}$$

was included to investigate the impact of increased charging-power availability on V2G operation.
In addition, a realistic charging-power scenario was considered in which each vehicle was assigned an individual maximum charging power estimated from observed home-charging behavior, as described in Section 3.4.2. In this case, the vehicle-specific charging and discharging power limits were defined as

$$P_{\mathrm{ch},v}^{\max} = P_{\mathrm{dis},v}^{\max} = \hat{P}_v^{\max}, \tag{3.104}$$

where $\hat{P}_v^{\max}$ denotes the estimated maximum home-charging power for vehicle v.
The sensitivity analysis was evaluated for the spot-only, FCR-only, and co-optimized market configurations. For each charging-power assumption, the resulting V2G configurations were compared against their corresponding V1G baseline in order to evaluate the economic value of bidirectional charging. The resulting profitability, reserve provision, battery throughput, and fleet-level flexibility were then compared across the different charging-power scenarios.

3.8.2 Battery Degradation Sensitivity

The battery degradation sensitivity evaluates how the assumed degradation cost affects the profitability of V2G-based market participation. Since bidirectional operation increases battery throughput, degradation cost is an important uncertainty when assessing the economic feasibility of V2G. In this thesis, degradation is represented using a simplified throughput-based cost applied to charged and discharged energy. The degradation cost coefficient is varied from 0.00 to 1.00 SEK/kWh in steps of 0.20 SEK/kWh

$$c_{\mathrm{deg}} \in \{0.0,\ 0.2,\ 0.4,\ 0.6,\ 0.8,\ 1.0\} \text{ SEK/kWh}. \tag{3.105}$$

This range is used to represent different assumptions regarding the economic impact of battery wear, from no degradation penalty to a relatively high degradation cost. This sensitivity is applied to the spot-only, FCR-only, and co-optimized market configurations, since these involve different levels of battery utilization and market participation. For each degradation-cost level, the optimization model is solved and the resulting economic value of V2G participation is compared across the different market configurations. This makes it possible to evaluate how strongly the economic value of different V2G participation strategies depends on the assumed cost of battery degradation and to assess the robustness of the results under different degradation-cost assumptions.

3.8.3 Accepted FCR Bid Sensitivity

The accepted FCR bid sensitivity investigates how the economic results are affected by the assumed share of FCR bids that are accepted in the market. In practice, reserve-market revenues depend not only on available reserve capacity and market prices, but also on whether submitted bids are accepted by the market operator. To account for this uncertainty, an accepted-bid factor is introduced to represent different levels of successful market participation. The accepted-bid factor is varied from 0.1 to 0.9 in steps of 0.2, while the base case assumes full bid acceptance:

$$\gamma^{\mathrm{FCR}} \in \{0.1,\ 0.3,\ 0.5,\ 0.7,\ 0.9,\ 1.0\}. \tag{3.106}$$

where γ of 0.1 represents a low level of accepted reserve bids and γ of 1.0 represents full acceptance of all submitted FCR bids. A lower acceptance factor reduces the realized reserve-market revenue, while a higher acceptance factor represents a more favorable market-participation outcome.
This sensitivity is applied to the FCR-only and co-optimized market configurations, since these rely on reserve-market participation for a substantial share of their revenue generation. For each accepted-bid factor, the corresponding reserve-market revenue is scaled according to the assumed acceptance level and the resulting economic value is evaluated. This makes it possible to assess how strongly the obtainable value of EV-based FCR participation depends on successful reserve-market acceptance and to evaluate the robustness of the different market strategies under more conservative bid-acceptance assumptions.

3.8.4 Intra-month spot-price volatility sensitivity

To evaluate the sensitivity of spot arbitrage profitability to electricity price volatility, transformed spot price scenarios were generated by scaling hourly deviations from the corresponding monthly mean while preserving the average price level within each month. For each hourly spot price observation, the transformed price was calculated as:

$$p_t^{\alpha} = \bar{p}_m + \alpha\,(p_t - \bar{p}_m) \tag{3.107}$$

where p_t is the original hourly spot price at time step t, $\bar{p}_m$ is the mean spot price for the corresponding month m, and α is the volatility scaling factor.
A value of $\alpha = 1$ reproduces the original price series. Values $\alpha < 1$ compress hourly price deviations around the monthly mean, reducing the spread between low and high prices, while values $\alpha > 1$ amplify deviations from the monthly mean, increasing price dispersion while preserving the monthly average price. The following values were evaluated:

$$\alpha \in \{0.2,\ 0.4,\ 0.6,\ 0.8,\ 1.0,\ 1.25,\ 1.5,\ 1.75,\ 2.0\} \tag{3.108}$$

.

3.8.5 Grid fee Sensitivity

An additional sensitivity analysis was performed to evaluate the impact of grid fees on the economic performance of the optimized charging strategies. In the base case,

a constant grid fee was added to the electricity purchase price for all charging energy imported from the grid.
To analyse the sensitivity to this assumption, the grid fee level was varied between

$$c_{\text{grid}} \in \{0.0,\ 0.1,\ 0.2,\ 0.3,\ 0.445,\ 0.7,\ 1.0\}\ \text{SEK/kWh}. \tag{3.109}$$

The lower bound represents an idealized case without any grid-related energy fees, while the higher values represent increasingly expensive electricity delivery conditions. The tested range was selected to cover typical Swedish residential electricity transfer fees and related variable network charges.
This sensitivity analysis was conducted to investigate how grid-dependent electricity costs influence the profitability of spot arbitrage, reserve market participation, and combined vehicle-to-grid operation.

3.8.6 Home availability robustness analysis

To assess the sensitivity of the estimated economic value to uncertainty in vehicle home availability, a conservative robustness analysis was performed by perturbing the original event-based home parking data prior to optimization. The purpose of this analysis was to evaluate whether the results were robust to representative reductions in home availability. Fragment merging was performed before the availability perturbation in order to keep the underlying event structure consistent with the deterministic baseline.
For each home parking event i, the observed arrival and departure times were modified as:

$$\tilde{t}_i^{arr} = t_i^{arr} + \epsilon_i^{arr} \tag{3.110}$$

$$\tilde{t}_i^{dep} = t_i^{dep} - \epsilon_i^{dep} \tag{3.111}$$

where t_i^{arr} and t_i^{dep} denote the observed arrival and departure times, while ϵ_i^{arr} and ϵ_i^{dep} represent conservative temporal perturbations that reduce the effective home parking duration.
The perturbations were sampled independently from bounded discrete uniform distributions:

$$\epsilon_i^{arr}, \epsilon_i^{dep} \sim U\{0, 1, \ldots, H\}, \tag{3.112}$$

where H denotes the maximum perturbation magnitude in hours. Two representative robustness cases were evaluated, $H = 1$ and $H = 2$, corresponding to conservative one-hour and two-hour availability uncertainty cases. For each perturbation level, a single randomized realization of the perturbed event dataset was generated and used throughout the analysis.
The resulting perturbed parking duration is given by:

$$\tilde{\Delta t}_i = \tilde{t}_i^{dep} - \tilde{t}_i^{arr}. \tag{3.113}$$

Since arrivals are only delayed and departures are only shifted earlier, the perturbation can only reduce or preserve the original parking duration:

$$\tilde{\Delta} t_i \leq \Delta t_i. \tag{3.114}$$

If the sampled perturbation resulted in an invalid parking interval,

$$\tilde{t}_i^{dep} \leq \tilde{t}_i^{arr}, \tag{3.115}$$

the original unperturbed timing was retained for that specific event. This made sure that the perturbed event dataset did not contain physically impossible parking intervals. The event dataset was then processed using the same preprocessing pipeline as the deterministic baseline. To avoid infeasibility caused by conservative availability reductions, the exact departure SOC constraint was softened using non-negative slack variables. For each departure time step, the departure condition was formulated as

$$E_t^{after} + s_t^+ - s_t^- = E_t^{dep}, \tag{3.116}$$

where s_t^+ represents an energy shortfall relative to the observed departure target and s_t^- represents surplus energy relative to the same target.

Slack was penalized in the objective function using a large penalty coefficient:

$$C^{slack} = \sum_{t \in \mathcal{T}} c^{slack} \left(s_t^+ + s_t^- \right), \tag{3.117}$$

where c^{slack} was set sufficiently high to ensure that slack was used only when the perturbed availability assumptions made exact departure matching infeasible. The slack variables therefore do not represent an economic flexibility mechanism, but only a feasibility-preserving diagnostic used to quantify unmet departure-energy requirements under conservative stochastic perturbations availability assumptions.

3.8.7 Scenario Cases

To complement the one-at-a-time sensitivity analysis, a combined scenario analysis was performed using two bounding cases representing pessimistic and optimistic operating conditions, in addition to the baseline case.

The scenario assumptions are summarized in Table 3.1. The worst-case scenario reflects a conservative operating environment characterized by reduced market participation, low price volatility, high network costs, elevated battery degradation assumptions, and stochastic perturbations home availability pert uncertainty. In contrast, the best-case scenario represents highly favorable conditions with full bid acceptance, increased price volatility, reduced network costs, no degradation penalty, and deterministic vehicle availability.

Table 3.1: Combined assumptions used in the scenario analysis.

Scenario	Strategy	Bid [%]	α [-]	Grid [SEK/kWh]	Deg. [SEK/kWh]	Availability
Worst-case	Spot	–	0.2	1.00	1.00	Stoch. ($H = 2$)
	Co-opt	10	0.2	1.00	1.00	Stoch. ($H = 2$)
Baseline	Spot	–	1.0	0.445	0.50	Determ.
	Co-opt	100	1.0	0.445	0.50	Determ.
Best-case	Spot	–	2.0	0.00	0.00	Determ.
	Co-opt	100	2.0	0.00	0.00	Determ.

4
Results

This section presents the results of the developed EV flexibility optimization framework. It includes validation of the pre-processing methodology, evaluation of the economic performance of the considered market participation strategies, and scenario and sensitivity analyses to assess the robustness of the results.

4.1 Validation of preprocessing and anchor mapping

To assess whether the conversion from event-based vehicle data to an hourly model representation introduced distortions, the preprocessing pipeline was validated in three steps: fragment merging, anchor filtering, and consistency validation against the original event-level data.

4.1.1 Fragment merging of split parking events

Table 4.1 summarizes the effect of this preprocessing step. The procedure reduced the number of fragmented home parking segments while preserving close SOC continuity, indicating that the merging primarily repaired data fragmentation rather than introducing artificial battery-state distortions.

Table 4.1: Summary of fragment merging results for the event preprocessing pipeline.

Metric	Value
Raw home parking segments	77 346
Fragment merge operations	13 358
Post-merge anchor segments	63 988
Reduction through merging [%]	17.3
Median merge gap [min]	1.16
Mean SOC gap [-]	0.0028
Maximum SOC gap [-]	0.02

4.1.2 Anchor filtering and retained segments

Following fragment merging, a small number of anchor segments were excluded because they became too short or temporally inconsistent after preprocessing adjustments. Table 4.2 summarizes the filtering outcome. While some anchor segments were removed, the discarded portion represented only a negligible share of the total SOC signal, indicating that the retained dataset preserved the majority of the underlying behavioral information.

Table 4.2: Summary of anchor filtering results for the preprocessing pipeline.

Metric	Value
Post-merge anchor segments	63 988
Dropped anchor segments	3 430
Retained anchor segments	60 558
Drop share of post-merge anchors [%]	5.36
Retained share of raw segments [%]	78.3
Dropped share of total SOC signal [%]	0.42

4.1.3 Consistency of retained hourly anchors

To validate consistency between the retained hourly anchors and the original event-based vehicle data, original home parking-event anchors were matched to processed hourly anchors using a one-to-one nearest-neighbour matching procedure with a maximum tolerance of two hours.
Table 4.3 summarizes the fleet-wide validation metrics. The very high match rate, low error levels, and strong correlation indicate that the preprocessing pipeline preserved the original SOC signal with minimal distortion. This consistency is further illustrated in Figure 4.1, where most observations lie close to the 1:1 agreement line.

Table 4.3: Fleet-wide validation metrics for consistency between original event-based anchors and processed hourly anchors.

Metric	Value
Unique matched processed anchors	120 747
Match rate of processed anchors [%]	99.7
MAE [percentage points]	0.40
RMSE [percentage points]	2.32
Correlation [-]	0.995
Median absolute error [pp]	0.0
95th percentile error [pp]	2.0
Share of errors > 5 pp [%]	2.58
Share of errors > 10 pp [%]	1.15
Median absolute time shift [h]	0.53
95th percentile time shift [h]	1.16

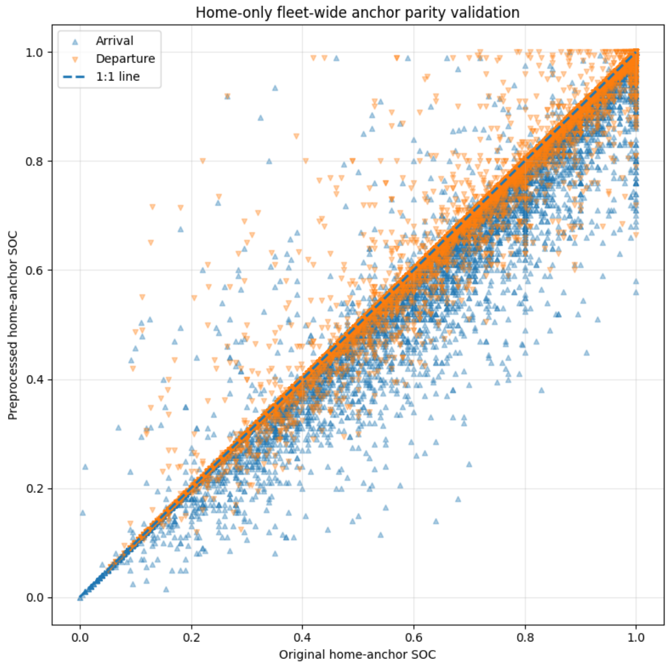

Figure 4.1: Comparison between original and processed home-anchor SOC values. The dashed line indicates perfect agreement (1:1)

4.2 Validation of V1G and V2G operation

To evaluate the validity of the implemented charging-optimization framework, the optimized charging schedules for both V1G smart charging and spot-optimized V2G operation were compared with the observed charging behavior for the same individual vehicle during a representative period with varying spot prices.
Figure 4.2 presents the observed charging behavior extracted from the processed vehicle dataset together with the corresponding spot prices and periods when the vehicle is available at home. The observed charging profile reflects real user charging behavior and already exhibits a tendency to align charging with relatively lower-price periods, indicating partially price-aware charging behavior even without optimization.

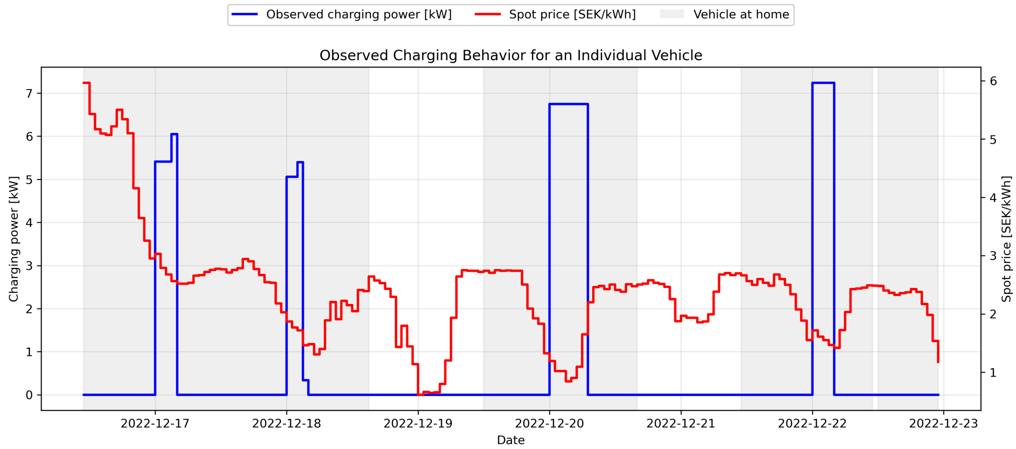

Figure 4.2: Observed charging behavior, spot prices, and vehicle availability at home for an individual vehicle.

Figure 4.3 illustrates the optimized V1G charging schedule for the same vehicle using an individually estimated maximum charging power of 8.4 kW. Compared with the observed charging behavior, the optimization model shifts charging more consistently toward economically favorable periods while simultaneously satisfying the imposed mobility and physical availability constraints. Charging only occurs during periods when the vehicle is connected at home, confirming that the optimization remains physically feasible. Notably, charging is not always deferred to the lowest price hours. For example, the charging event around 17 December occurs despite higher spot prices, reflecting the need to satisfy an upcoming mobility requirement.

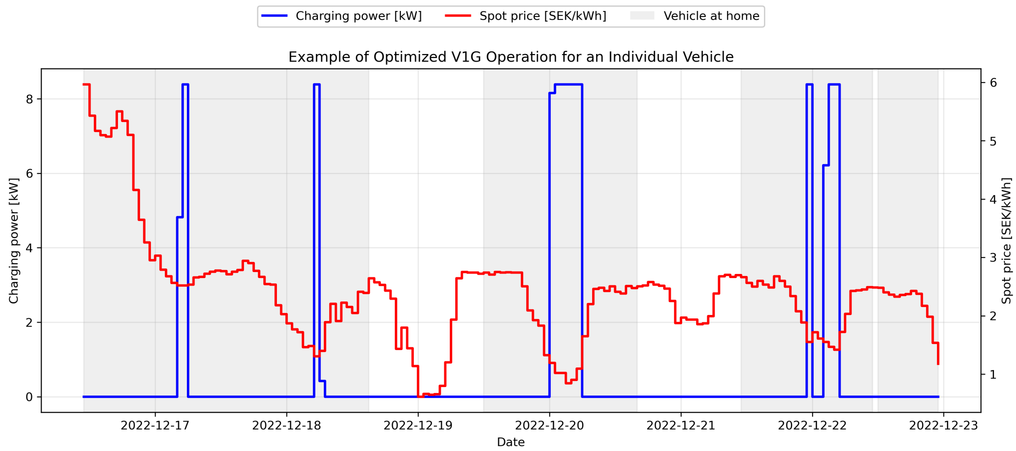

Figure 4.3: Optimized V1G charging behavior, spot prices, and vehicle availability at home for an individual vehicle.

Figure 4.4 presents the spot-optimized V2G charging behavior for the same vehicle. Unlike the V1G framework, the V2G optimization allows bidirectional power flows, enabling the vehicle battery to both charge and discharge in response to market conditions. The resulting schedule exhibits economically motivated arbitrage behavior, where charging is concentrated in relatively low-price periods and discharging occurs during the highest-price hours observed at the beginning of the analysis period. As spot-price variability decreases during the remainder of the week, the economic incentive for discharging is reduced and no further discharge events occur. Both charging and discharging take place exclusively when the vehicle is available at home, demonstrating that the optimization respects the imposed mobility and physical constraints while producing operationally realistic charging schedules.

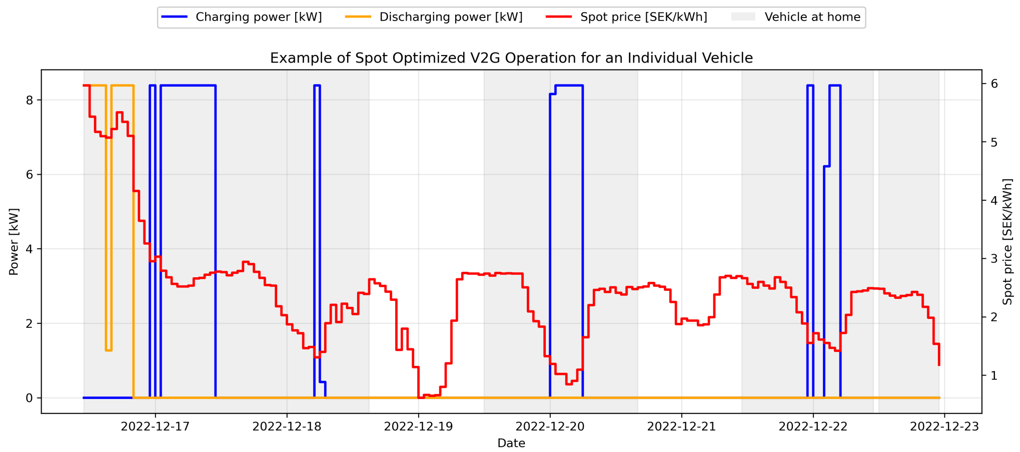

Figure 4.4: Optimized V2G charging and discharging behavior, spot prices, and vehicle availability at home for an individual vehicle.

4.3 Deterministic Market Results

4.3.1 V1G reference case

Over the approximately 2.5-year study period, the V1G reference case establishes the baseline operational charging behavior of the fleet under the observed mobility constraints. The corresponding cost and energy performance metrics are summarized in Table 4.4.

Table 4.4: Operational metrics for the V1G reference case.

Case	V1G
Total charging cost [kSEK]	290.7
Total degradation [kSEK]	190.6
Charging cost [kSEK/kWh]	0.76
Total charged energy[MWh]	381.1
Connected hours [h]	1,094,944
Charging cost per at-home hour[SEK/at-home hour]	0.26

4.3.2 Baseline Cases

Under baseline assumptions, this establishes the reference economic outcome against which the relative performance of alternative flexibility strategies is evaluated through $\Delta\Pi$ and excluding degradation costs.

The analysis treats the available EV population as a single aggregated fleet over the same study period as V1G. Table 4.5 presents the aggregated baseline results.

Table 4.5: Baseline economic performance metrics for the three $\Delta\Pi$.

Case	**Spot**	**FCR**	**Co-opt**
$\Delta\Pi$ [kSEK]	125.0	12,441.7	12,555.6
Degradation cost [kSEK]	267.1	495.7	529.8
Charged energy increase vs. V1G [%]	19.0	85.5	94.2
Fleet value intensity [SEK/at-home hour]	0.11	11.32	11.42

The baseline results show a clear difference between pure spot-market arbitrage and FCR-based V2G strategies. The Spot V2G strategy achieved a modest positive economic improvement relative to the V1G reference case.

This behavior is further illustrated in Figure 4.5. V2G reduced net spot-market costs relative to the V1G baseline, but part of this benefit was offset by higher grid-related and degradation costs associated with increased battery cycling. As a result, the overall economic improvement remained limited, indicating that while available spot-price spreads enabled profitable arbitrage opportunities, the value capture from spot-market participation alone was relatively constrained under the studied conditions.

Figure 4.6 illustrates both the operational cost structure and revenue composition of the reserve-based V2G strategies.

Figure 4.6a shows that reserve-market participation increases total operational costs relative to the V1G reference case. The most clear increase arises from grid-related costs, while baseline charging energy procurement remains of similar magnitude across the cases. This reflects the fact that reserve participation, particularly downward activation, increases total energy throughput and imported electricity even when the primary charging requirement remains comparable.

Figure 4.6b shows that these higher operational costs are more than offset by reserve-market revenues. For both the FCR-only and co-optimized strategies, FCR capacity payments are the dominant revenue stream, while activation revenues provide a smaller contribution. The majority of the reserve-market revenue originates from participation in the FCR-D down and FCR-D up markets, which together account for more than 80% of the total revenue, whereas FCR-N contributes a smaller share. In the co-optimized case, spot arbitrage contributes only a minor fraction of the total revenue, indicating that the economic value is driven almost completely by reserve-market participation rather than spot arbitrage.

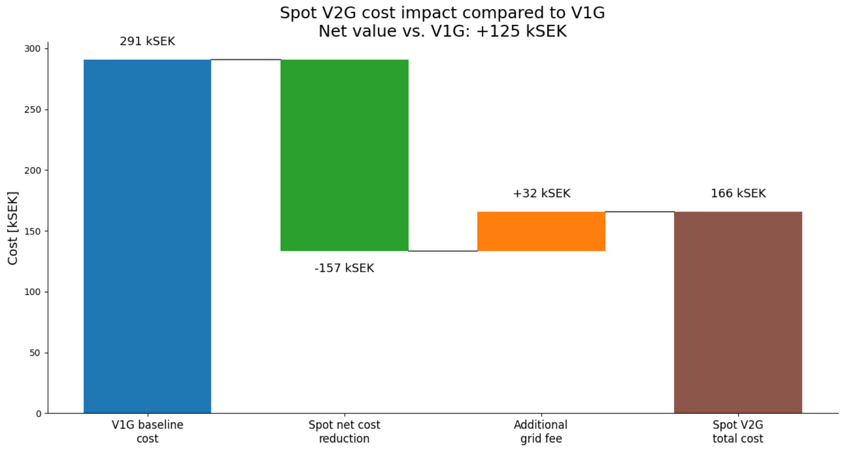

Figure 4.5: Economic breakdown of the Spot V2G strategy relative to the V1G reference case.

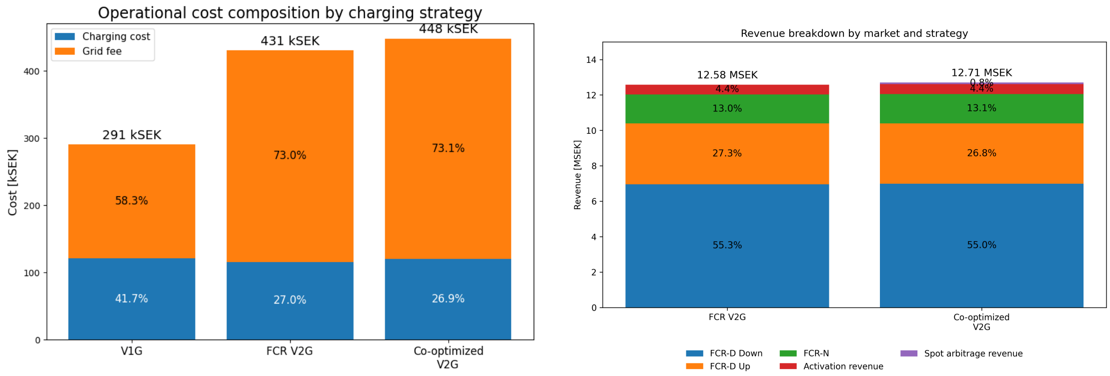

(a) Operational cost components before reserve-market revenues.

(b) Revenue composition for FCR and co-optimized V2G strategies.

Figure 4.6: Comparison of operational cost and revenue composition across the evaluated V2G strategies.

The yearly normalized results in Figure 4.7 show substantial annual variation in $\Delta\Pi$ value density for the different cases. While 2022 and 2025 represent partial observation periods and should therefore be interpreted cautiously, the comparison between 2023 and 2024 indicates a clear decline in normalized profitability.
The normalized $\Delta\Pi$ value decreased substantially between years. This is consistent with the yearly average market prices shown in Figure B.1, where substantial annual variation is observed, particularly in the FCR markets, indicating that the economic value of V2G flexibility is strongly influenced by reserve market conditions.

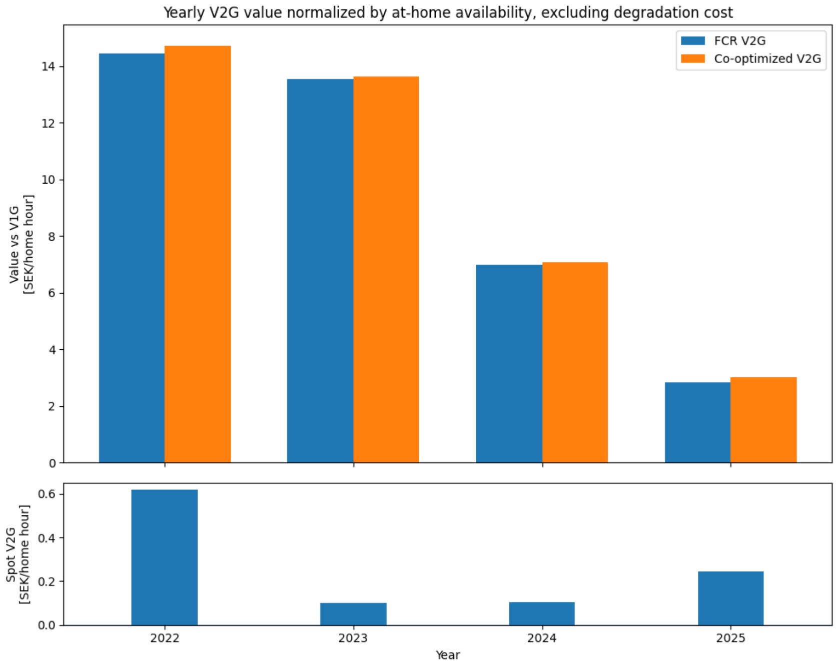

Figure 4.7: $\Delta\Pi$, normalized by at-home availability for each observed year.

Further, to assess the practical market relevance of the optimized reserve bids, the bid trajectories were evaluated ex-post against the representative minimum FCR bid threshold of 0.1 MW, as illustrated in Figures 4.8– 4.10. The aggregated fleet exceeded this threshold for at least one reserve product during 90.7% of all modeled hours. Product-specific threshold exceedance was 39.7% for FCR-N (Figure 4.8), 66.0% for FCR-D up (Figure 4.9), and 64.8% for FCR-D down (Figure 4.10). The maximum optimized reserve bids reached 1.149 MW for FCR-N, 1.188 MW for FCR-D up, and 1.186 MW for FCR-D down.

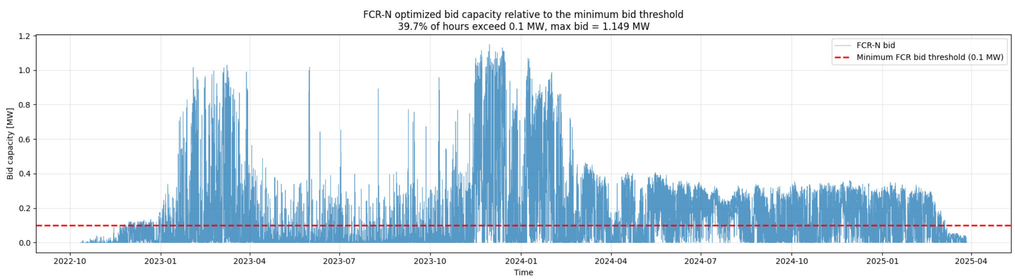

Figure 4.8: Optimized FCR-N bid capacity over the study horizon. The dashed red line indicates the representative minimum FCR bid threshold of 0.1 MW.

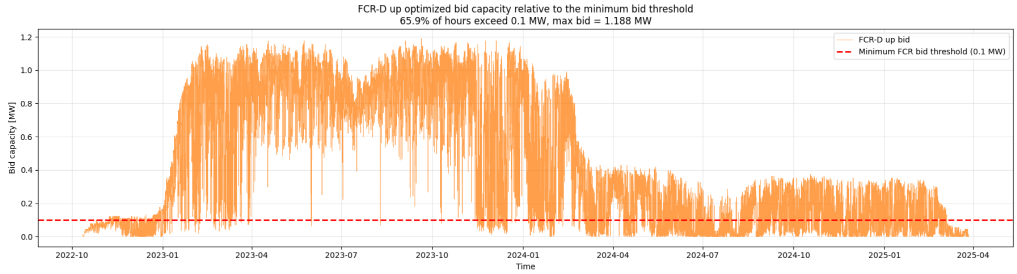

Figure 4.9: Optimized FCR-D up bid capacity over the study horizon. The dashed red line indicates the representative minimum FCR bid threshold of 0.1 MW.

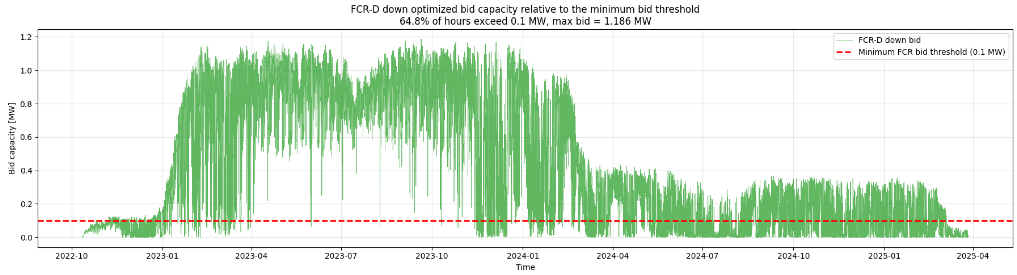

Figure 4.10: Optimized FCR-D down bid capacity over the study horizon. The dashed red line indicates the representative minimum FCR bid threshold of 0.1 MW.

4.4 Sensitivity & Scenario Cases

For the main parameter sensitivities, all three strategies are evaluated for grid fee, degradation cost, and charging/discharging power limit. However, for the bid acceptance, stochastic perturbation availability, spot price volatility and combined scenario analyses, only the spot-only and co-optimized strategies are reported. This is because the FCR-only and co-optimized cases showed nearly identical economic behavior across the main results, indicating that reserve-market revenues dominate the co-optimized value. The co-optimized case is therefore used as the representative reserve-market strategy in these robustness analyses, while the spot-only case is retained to illustrate the different behavior of pure energy arbitrage.

4.4.1 Charger Power Rating

The estimated individual charger capacities for the analyzed EV fleet are illustrated in Figure B.6. Vehicles without observed home-charging events could not be assigned a charger-capacity estimate and are therefore not represented in the figure. This corresponds to seven vehicles in total. The estimated charger capacities exhibit a mean value of 6.6 kW and a median value of 6.8 kW.

The charger power sensitivity analysis evaluates how different charging-power assumptions influence the economic value $\Delta\Pi$. The results are presented for spot-market participation separately from reserve-market participation in order to illustrate how charging power affects the different market configurations.

Figure 4.11 and Table 4.6 present $\Delta\Pi$ for spot market participation only. The results are calculated using the common feasible vehicle set across all charger-rating cases to isolate the influence of charging power from changes in fleet composition. The fleet is therefore composed of 114 cars and the amount of connected hours is reduced from 1,098,944 to 820,368 hours for this sensitivity case.

The results show that higher charger ratings improve the economic potential of spot-market arbitrage, although the overall value remains relatively limited compared to reserve-market participation.

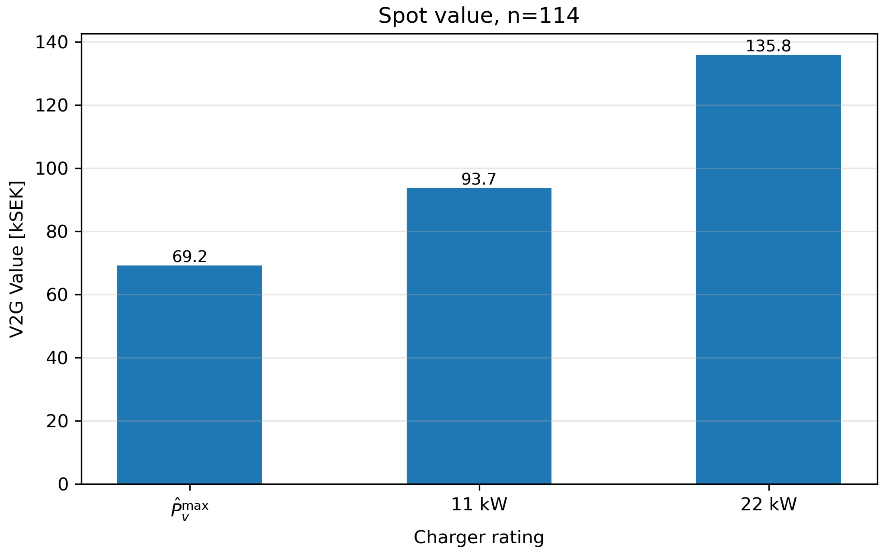

Figure 4.11: $\Delta\Pi$ for spot market participation under different charger ratings.

Table 4.6: $\Delta\Pi$ for spot-market participation under different charger ratings.

Charger rating [kW]	Value [kSEK]	Value/home hour [SEK/h]	Relative change [%]
$\hat{P}_v^{\max}$	69.21	0.084	-26.13
11	93.69	0.114	0.00
22	135.82	0.166	45.02

Figure 4.12 and Table 4.7 present the corresponding results for FCR-only and co-optimized participation. In contrast to the spot-only case, the value increases substantially with higher charging power.

The results indicate that charger power has a considerably larger impact on reserve-market profitability than on spot market arbitrage. This behaviour is physically reasonable since reserve provision is directly constrained by the available charging and discharging power, whereas spot-market arbitrage is more strongly influenced by energy capacity and electricity-price variation. Furthermore, the relatively small difference between the FCR-only and co-optimized cases suggests that most of the economic value originates from FCR participation rather than additional spot-market optimization.

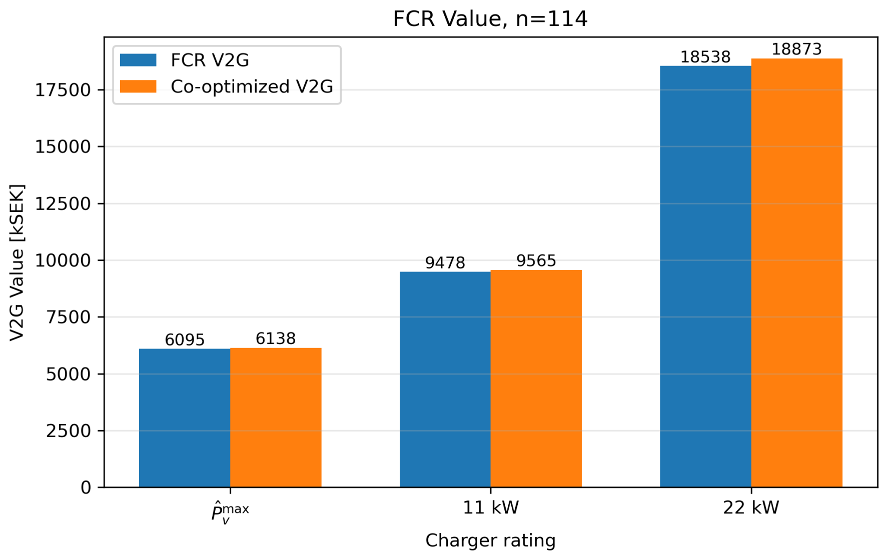

Figure 4.12: $\Delta\Pi$ for FCR and Co-optimized participation under different charger ratings.

Table 4.7: Fleet-level value excluding degradation cost for FCR and Co-optimized V2G participation under different charger ratings.

	FCR V2G			Co-optimized V2G		
Charger rating [kW]	**Value** [MSEK]	**Value/home hour** [SEK/h]	**Relative change** [%]	**Value** [MSEK]	**Value/home hour** [SEK/h]	**Relative change** [%]
$\hat{P}_v^{\max}$	6.10	7.43	-35.69	6.14	7.48	-35.82
11	9.48	11.55	0.00	9.56	11.66	0.00
22	18.54	22.60	95.59	18.87	23.01	97.32

4.4.2 Degradation Cost

The degradation cost sensitivity analysis evaluates how the assumed battery degradation cost influences the economic value of V2G participation. The results are presented for the Spot, FCR, and co-optimized market configurations relative to the baseline degradation cost assumption of 0.5 SEK/kWh used in the main analysis.
Figure 4.13 illustrates the relative change in $\Delta\Pi$ for the different degradation cost assumptions. Lower degradation costs increase the obtainable V2G value relative to the baseline case, while higher costs reduce profitability. The Spot configuration shows the strongest relative sensitivity to degradation assumptions, whereas the FCR and Co-optimized configurations remain comparatively robust due to their substantially higher reserve-market revenues.
Tables 4.8–4.10 summarize the corresponding value metrics and degradation related costs for the three market configurations. As expected, increasing degradation costs lead to reduced profitability and higher total degradation related costs across all strategies.

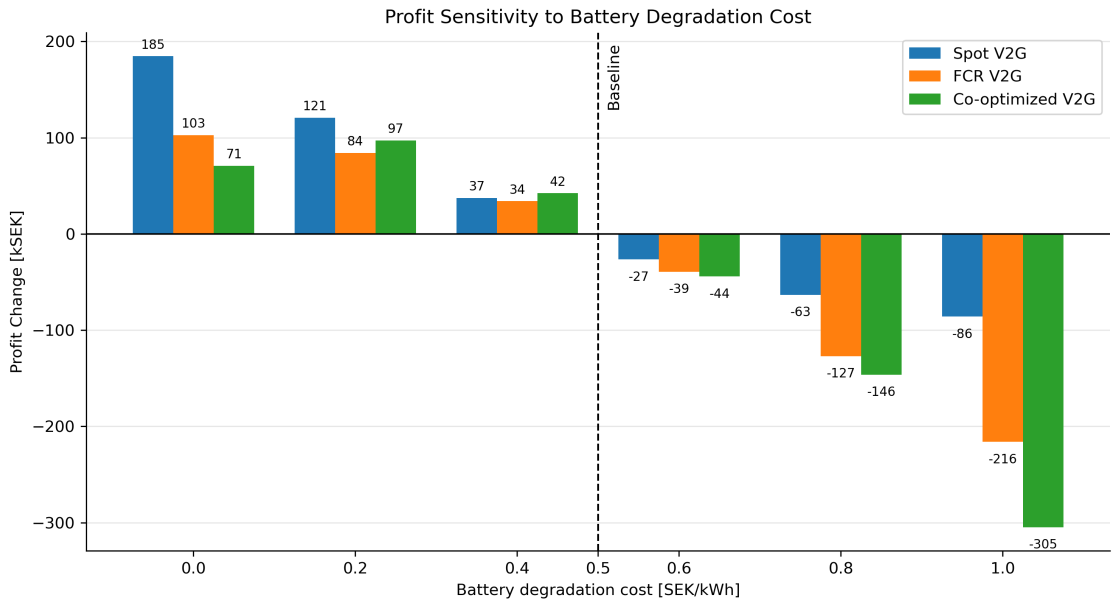

Figure 4.13: Relative change in ΔΠ for different battery degradation costs compared to the baseline degradation cost of 0.5 SEK/kWh.

Table 4.8: Spot arbitrage sensitivity to degradation cost.

c_{deg} [SEK/kWh]	Value [kSEK]	Value/home hour [SEK/h]	Degradation cost [kSEK]
0.00	309.7	0.282	0.0
0.20	245.8	0.224	182.0
0.40	162.3	0.148	246.9
0.50	125.0	0.114	267.1
0.60	98.5	0.090	291.5
0.80	61.7	0.056	346.0
1.00	39.1	0.036	407.2

Table 4.9: FCR-only V2G sensitivity to degradation cost.

c_{deg} [SEK/kWh]	Value [MSEK]	Value/home hour [SEK/h]	Degradation cost [kSEK]
0.00	12.63	11.49	0.0
0.20	12.61	11.47	251.5
0.40	12.55	11.43	433.9
0.50	12.52	11.39	503.6
0.60	12.48	11.36	560.8
0.80	12.39	11.28	644.4
1.00	12.30	11.19	705.0

Table 4.10: Co-optimized V2G sensitivity to degradation cost.

c_{deg} [SEK/kWh]	Value [MSEK]	Value/home hour [SEK/h]	Degradation cost [kSEK]
0.00	12.68	11.54	0.0
0.20	12.71	11.57	273.1
0.40	12.66	11.52	468.4
0.50	12.61	11.48	539.3
0.60	12.57	11.44	597.8
0.80	12.47	11.34	678.4
1.00	12.31	11.20	726.7

4.4.3 FCR bid acceptance

The accepted FCR bid-factor sensitivity analysis evaluates how the profitability of reserve market participation is affected by different assumptions regarding the share of submitted FCR bids that are accepted in the market. The results are presented for both FCR-only and co-optimized market configurations.
Figure 4.14 illustrates $\Delta\Pi$ for different accepted FCR bid factors. The results show that the value increases linearly with increasing accepted bid factor for both market configurations. The highest profitability is obtained for an accepted bid factor of 1.0, corresponding to full acceptance of submitted reserve bids. The co-optimized configuration consistently achieves slightly higher profitability than the FCR-only case, although the difference between the two strategies remains limited across all sensitivity cases.

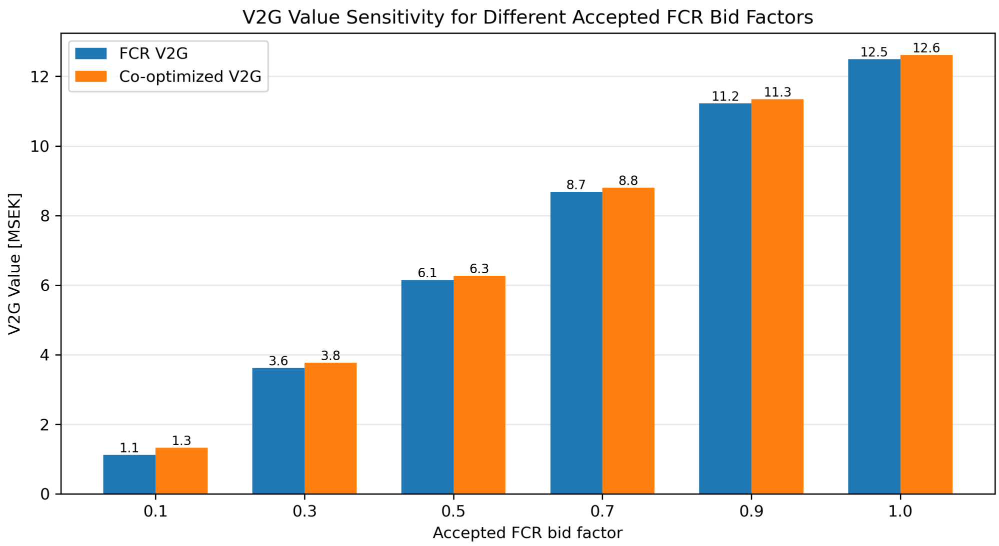

Figure 4.14: V2G value for different accepted FCR bid factors for FCR-only and co-optimized market configurations.

Table 4.11 summarizes the corresponding value metrics for the different accepted FCR bid assumptions. As expected, lower accepted bid factors substantially reduce the obtainable reserve-market value, reflecting the strong dependence of reserve-market profitability on successful bid acceptance.

Table 4.11: Sensitivity to the accepted FCR bid factor for different market participation strategies.

γ^{FCR}	FCR V2G		Co-optimized V2G	
	Value [MSEK]	**Value/home hour [SEK/h]**	**Value [MSEK]**	**Value/home hour [SEK/h]**
0.1	1.12	1.02	1.33	1.21
0.3	3.62	3.29	3.77	3.43
0.5	6.15	5.59	6.27	5.71
0.7	8.68	7.90	8.80	8.01
0.9	11.22	10.21	11.34	10.32
1.0	12.50	11.37	12.61	11.48

4.4.4 Price Volatility

Figure 4.15 illustrates the spot-price volatility scaling methodology used in the sensitivity analysis. The transformation preserves the monthly average price level while compressing or amplifying hourly deviations around the monthly mean according to the volatility factor α.

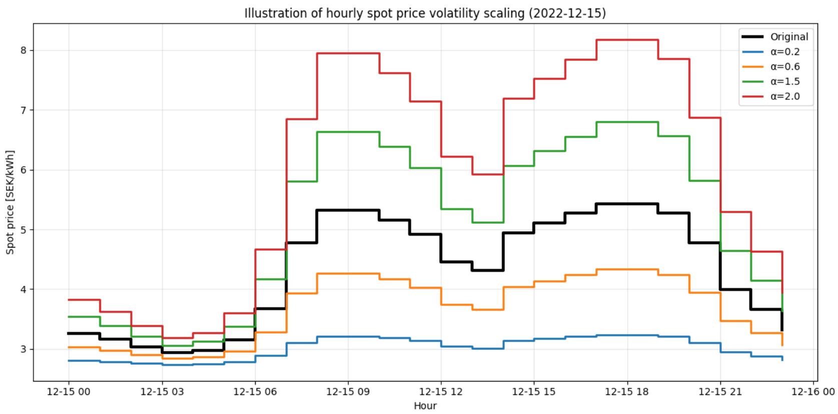

Figure 4.15: Illustration of the hourly spot price volatility scaling methodology for a representative day.

Figure 4.16 and Table 4.12 show the sensitivity of V2G profitability to changes in spot-price volatility. Panel A presents the raw profits of the Spot V2G, co-optimized V2G, and V1G baseline cases. Since the charging cost of the V1G reference is also affected by the volatility scaling, Panel B instead shows the $\Delta\Pi$ value, relative to the volatility-specific V1G reference point. In other words, for each volatility level, the V1G result was re-evaluated and subtracted from the corresponding V2G result. Finally, Panel C shows the change in $\Delta\Pi$ relative to the deterministic baseline case at $\alpha = 1.0$.
The pure Spot V2G strategy shows a clear positive sensitivity to increasing spot-price volatility, consistent with the expected arbitrage mechanism whereby larger

spreads between low- and high-price hours increase the economic potential of charge–discharge shifting. The relationship is nonlinear, with profitability accelerating as volatility increases.
In contrast, the co-optimized strategy remains comparatively stable across the full volatility range, indicating that its overall economic performance is primarily driven by reserve-market revenues rather than spot-market arbitrage.
Although the co-optimized strategy captures increasing spot-market value at higher volatility levels, the limited impact on total profitability indicates that spot arbitrage remains only a minor supplementary value stream relative to reserve-market participation.

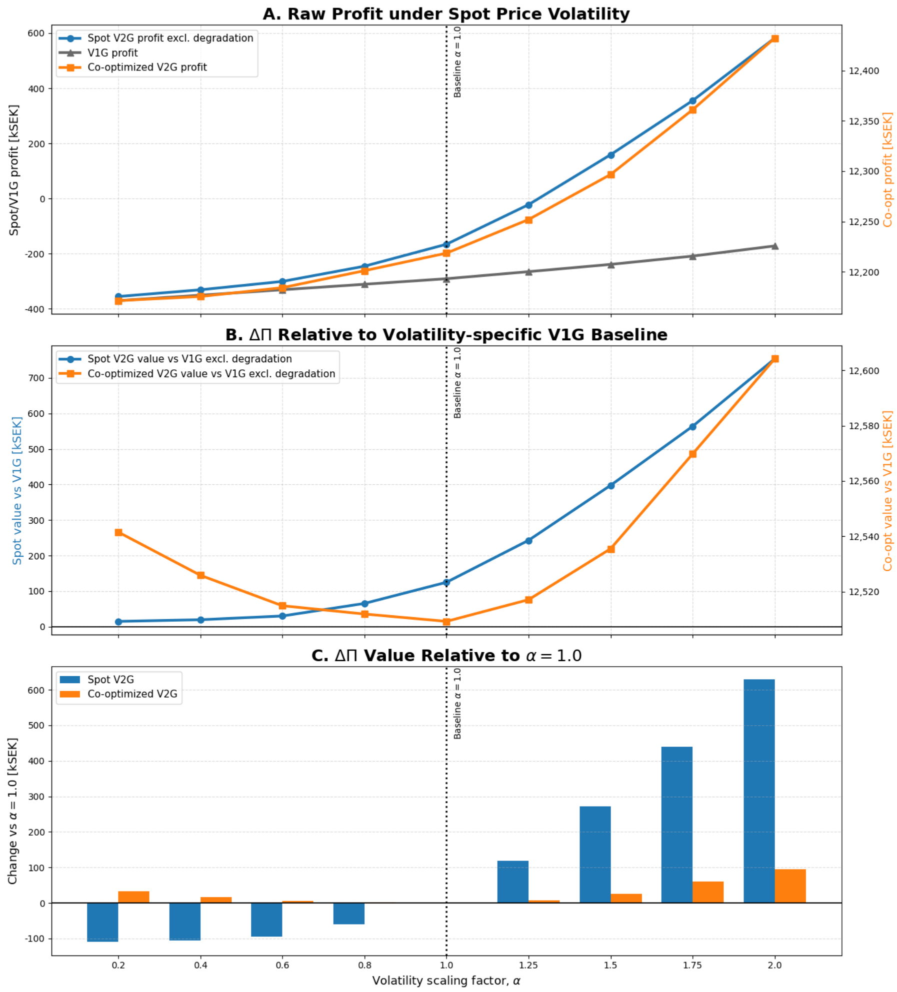

Figure 4.16: Sensitivity of spot-only and co-optimized V2G profitability to spot-price volatility.

Table 4.12: Sensitivity of ΔΠ value metrics to spot-price volatility relative to the corresponding volatility-specific V1G benchmark.

Volatility	**Spot V2G**			**Co-optimized V2G**		
α	**Value** [kSEK]	**Value/discharge** [SEK/kWh]	**Value/home hour** [SEK/h]	**Value** [kSEK]	**Net spot/discharge** [SEK/kWh]	**Value/home hour** [SEK/h]
0.20	15.0	0.77	0.014	12,541.5	-6.84	11.41
0.40	19.6	0.88	0.018	12,525.9	-5.15	11.40
0.60	30.2	1.11	0.027	12,514.9	-3.42	11.39
0.80	65.5	1.36	0.060	12,511.9	-1.90	11.39
1.00	125.0	1.55	0.114	12,509.2	-0.76	11.38
1.25	243.1	1.70	0.221	12,517.0	0.40	11.39
1.50	397.8	1.82	0.362	12,535.5	1.33	11.41
1.75	564.0	1.95	0.513	12,569.8	2.03	11.44
2.00	753.8	2.03	0.686	12,604.2	2.60	11.47

4.4.5 Grid fee sensitivity

Figure 4.17 and Tables 4.13–4.14 show the sensitivity of ΔΠ profitability to increasing volumetric grid fees. Across all three strategies, profitability decreases as grid fees increase, reflecting the direct cost impact of additional imported electricity. The spot-only strategy shows the strongest relative sensitivity, since its comparatively small arbitrage margins are more easily reduced by increasing charging costs.

Although the reserve-driven strategies exhibit larger absolute changes in profitability in kSEK, their relative sensitivity remains comparatively limited because the dominant reserve-market revenues remain substantially larger than the additional grid-related costs across the evaluated grid-fee range.

Normalized profitability per at-home hour follows the same overall trend across all strategies. The value intensity metrics in Table 4.14 further show that spot arbitrage value per discharged kWh remains relatively stable across grid-fee scenarios, while profitability per imported electricity declines as grid costs increase. This reflects the shifting balance between revenue generation and energy-related operating costs under higher grid-fee assumptions.

Table 4.13: Grid fee sensitivity of ΔΠ value metrics relative to the corresponding V1G benchmark.

Grid fee	**Value [kSEK]**			**Value/home hour [SEK/h]**		
[SEK/kWh]	**Spot**	**FCR**	**Co-opt**	**Spot**	**FCR**	**Co-opt**
0.000	307.3	12698.7	12789.0	0.28	11.56	11.64
0.100	248.6	12639.6	12724.5	0.23	11.50	11.58
0.200	203.7	12577.8	12656.4	0.19	11.44	11.52
0.300	167.2	12521.6	12594.7	0.15	11.39	11.46
0.445	125.0	12441.8	12509.2	0.11	11.32	11.38
0.700	80.5	12316.7	12373.6	0.07	11.21	11.26
1.000	53.4	12193.1	12239.1	0.05	11.10	11.14

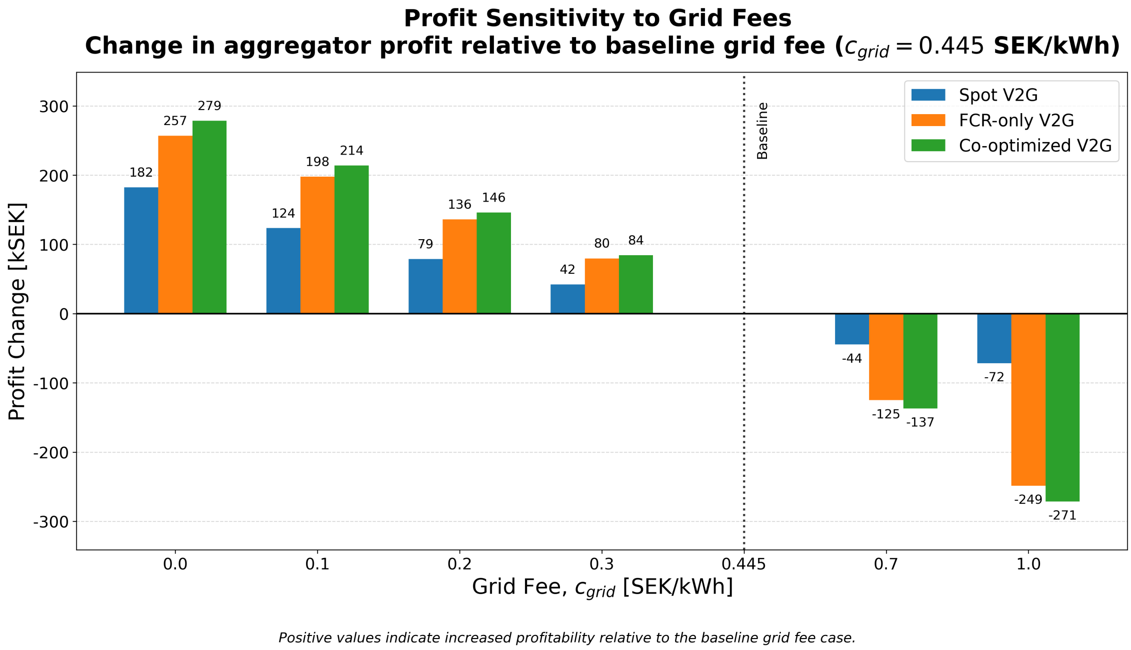

Figure 4.17: Sensitivity of ΔΠ profitability to volumetric grid fee assumptions relative to the baseline grid fee case ($c_{\text{grid}} = 0.445$ SEK/kWh).

Table 4.14: Grid fee sensitivity of ΔΠ intensity metrics.

Grid fee [SEK/kWh]	Spot value/ discharge [SEK/kWh]	Spot value/ grid import [SEK/kWh]	FCR value/ grid import [SEK/kWh]	Co-opt value/ grid import [SEK/kWh]
0.000	1.54	0.52	15.75	15.15
0.100	1.56	0.46	16.14	15.54
0.200	1.55	0.40	16.55	15.98
0.300	1.55	0.34	16.97	16.41
0.445	1.55	0.28	17.60	17.05
0.700	1.53	0.19	18.78	18.25
1.000	1.47	0.13	20.21	19.73

4.4.6 Stochastic perturbations of home availability Uncertainty

Figure 4.18 and Tables 4.15 summarize the impact of stochastic availability assumptions on V2G profitability.
Introducing stochastic perturbations reduces profitability across all strategies, with the strongest relative impact observed for the pure Spot V2G strategy. This reflects the higher dependence of spot arbitrage on precise timing and predictable vehicle availability, making it more vulnerable to uncertainty in arrival and departure behavior.
In contrast, the co-optimized strategy remains comparatively robust under both stochastic assumptions, with only modest reductions in overall economic perfor-

mance. When normalized by total home availability, the impact becomes even smaller, indicating that much of the absolute reduction is explained by reduced aggregate vehicle availability rather than a reduction in value capture efficiency.
The stochastic perturbations also alter the underlying dataset structure by reducing total home availability and increasing the number of arrival-departure anchor pairs, reflecting the fragmentation introduced by random temporal shifts.
Despite these perturbations, service feasibility remains high in both stochastic cases, with only a very small share of departures requiring slack. The corresponding slack distributions are shown in Appendix Figure B.8, indicating that unmet departure energy requirements remain limited even under conservative uncertainty assumptions. This suggests that the optimization framework remains operationally robust under stochastic availability perturbations.

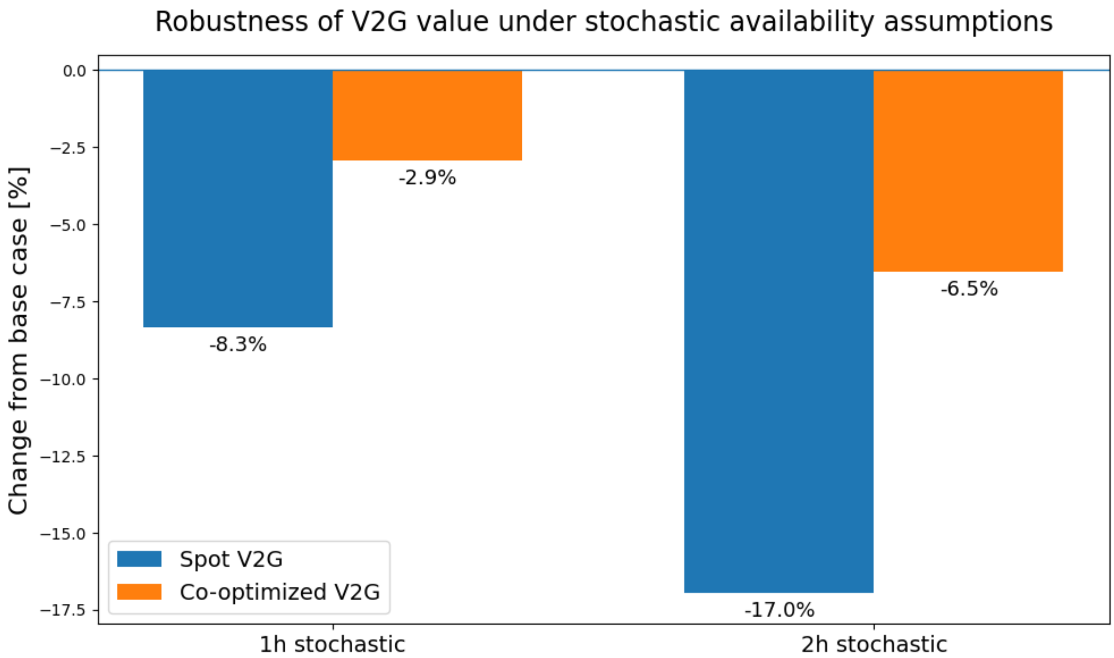

Figure 4.18: Change in $\Delta\Pi$ value under 1h and 2h stochastic perturbation availability assumptions relative to the deterministic base case.

Table 4.15: Robustness analysis under conservative stochastic home availability assumptions.

Case	Base case	1h stochastic	2h stochastic
$\Delta\Pi$ *relative to V1G*			
Spot value [kSEK]	125.0	114.6 (-8.3%)	103.8 (-17.0%)
Co-opt value [kSEK]	12,555.5	12,188.0 (-2.9%)	11,734.2 (-6.5%)
Normalized by home availability			
Home hours [h]	1,098,944	1,062,871 (-3.3%)	1,024,119 (-6.8%)
Spot value/home hour [SEK/h]	0.114	0.108 (-5.2%)	0.101 (-10.9%)
Co-opt value/home hour [SEK/h]	11.43	11.47 (+0.4%)	11.46 (+0.3%)
Dataset and service reliability			
Arrival–departure pairs [-]	59,068	59,893 (+1.4%)	60,307 (+2.1%)
Anchor pair difference [-]	–	+825	+1,239
Departure slack [kWh]	0.0	27.3	166.2
Departures with slack [-]	0	12	26
Departures with slack [%]	0.0	0.02	0.04
Maximum departure slack [kWh]	0.0	7.12	27.58

4.4.7 Worst vs Best Scenario

Figure 4.17 and Tables 4.16–4.17 summarize the combined pessimistic, baseline, and optimistic scenario outcomes for the spot-only and co-optimized V2G strategies.

The spot-only strategy shows substantial sensitivity to the combined scenario assumptions, with profitability varying dramatically across the evaluated cases. Economic performance improves strongly under more favorable assumptions, indicating that pure spot-market arbitrage is highly dependent on market conditions, technical assumptions, and operational constraints. This reflects the relatively thin economic margins of spot arbitrage, where profitability is strongly affected by factors such as price volatility, charging costs, degradation assumptions, and availability uncertainty.

In contrast, the co-optimized strategy remains substantially more profitable across all evaluated scenarios and shows considerably greater robustness to changing assumptions. While profitability improves under more favorable conditions, the relative variation is much smaller than for the spot-only strategy, indicating that reserve-market participation provides a more stable and resilient revenue stream than pure energy arbitrage.

The same overall pattern is observed when normalizing results by total home availability, confirming that the observed differences are not solely driven by variations in aggregate fleet size, but also reflect genuine differences in value capture efficiency.

The scenario assumptions also affect the V1G reference, since changes in market prices, tariff assumptions, and technical constraints directly influence baseline charging costs. Consequently, the reported $\Delta\Pi$ values should be interpreted relative to the corresponding scenario-specific V1G benchmark rather than as absolute standalone profitability measures.

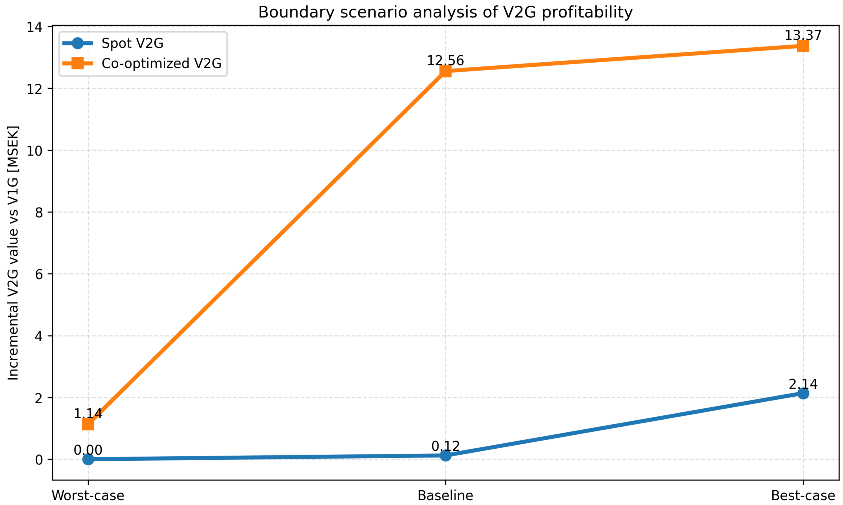

Figure 4.19: Combined pessimistic, baseline, and optimistic scenario outcomes for spot-only and co-optimized V2G strategies, showing $\Delta\Pi$ relative to the corresponding V1G benchmark.

Table 4.16: Scenario analysis for spot-only V2G under pessimistic, baseline, and optimistic assumptions.

Case	**Worst-case**	**Baseline**	**Best-case**
Spot price volatility factor α [-]	0.2	1.0	2.0
Grid fee [SEK/kWh]	1.00	0.445	0.00
Degradation cost [SEK/kWh]	1.00	0.50	0.00
Availability assumption	Stochastic (H = 2h)	Deterministic	Deterministic
Home availability [h]	1,024,119	1,098,944	1,098,944
V1G baseline cost [kSEK]	-581.4	-290.7	-90.9
$\Delta\Pi$ [kSEK]	2.1	125.0	2,139.7
Value per at-home hour [SEK/h]	0.002	0.11	1.95

Table 4.17: Scenario analysis for co-optimized V2G under pessimistic, baseline, and optimistic assumptions.

Case	**Worst-case**	**Baseline**	**Best-case**
Spot price volatility factor α [-]	0.2	1.0	2.0
Grid fee [SEK/kWh]	1.00	0.445	0.00
Degradation cost [SEK/kWh]	1.00	0.50	0.00
Availability assumption	Stochastic (H = 2h)	Deterministic	Deterministic
Home availability [h]	1,024,119	1,098,944	1,098,944
V1G baseline cost [kSEK]	-581.4	-290.7	-90.9
$\Delta\Pi$ [kSEK]	1,136.0	12,555.6	13,371.9
Value per at-home hour [SEK/h]	1.11	11.42	12.17

5

Discussion

This section presents the key findings of the developed EV flexibility optimization framework, including the economic performance of the evaluated market participation strategies and the robustness of the obtained results. It further reflects on methodological limitations, practical implementation considerations, and potential directions for future research

5.1 Preprocessing limitations and assumptions

5.1.1 Excluded infeasible vehicle profiles

Out of 152 processed EV profiles, 149 were successfully solved, corresponding to a model success rate of 98.0%. Three vehicles were excluded due to infeasible optimization conditions.

The infeasibility arose in cases where the required increase in SOC between arrival and departure exceeded what could physically be achieved within the available parking duration under the assumed charging power limit of 11 kW. Since the optimization framework enforces exact departure SOC requirements, these vehicles became infeasible.

This should be interpreted as a modelling limitation rather than a numerical solver failure. In practice, such cases may reflect situations where charging occurred at higher power than assumed, where part of the charging took place outside the modeled home charging window, or where preprocessing compressed the effective charging duration.

Because only three vehicles, corresponding to 2.0% of the fleet, were excluded, the quantitative impact on aggregate fleet-level results is expected to be limited.

5.1.2 Preprocessing assumptions and hourly discretization

A key modeling assumption is the conversion of event-based arrival and departure timestamps into fixed hourly anchors using floor and ceiling operations. This assumption may introduce an optimistic bias in estimated flexibility availability, since vehicles become available immediately at the start of the arrival hour and remain available until the end of the departure hour. This effect is likely most relevant for shorter parking intervals where rounding errors represent a larger share of the parking duration. At fleet level, however, the validation values suggest that the aggregate impact remains relatively limited. The chosen approach was necessary to create operationally feasible hourly optimization framework compatible with hourly market-price and reserve datasets. Alternative formulations based on partial-hour overlap modeling could possibly reduce this approximation but would also increase model complexity. The achieved anchor match rate of 99.7%, together with a mean absolute SOC error of only 0.40 %, suggests that the adopted preprocessing methodology provides a robust representation of the original dataset. Furthermore, the dropped anchor segments represented only 0.42% of total SOC variation, indicating limited information loss. These results support the suitability of the preprocessing methodology for fleet-level techno-economic analysis.

Another limitation to the preprocessing was across 59,068 paired home parking intervals, 2,516 intervals (4.26%) showed a lower departure SOC than arrival SOC. However, the magnitude of these deviations was generally small. Of the affected intervals, 94.8% (2,385 cases) had SOC decreases of 0.02 or less, while only 131 intervals (0.22% of all paired intervals) exceeded 0.02 SOC. Only three intervals (0.005%) exceeded 0.05 SOC, and the maximum observed decrease was 0.07 SOC. The mean SOC decrease among affected intervals was 0.0094, corresponding to approximately 0.53 kWh, while the maximum observed energy difference was 4.18 kWh. These SOC decreases are results from preprocessing the data caused by hourly anchoring and event merging, particularly when multiple short parking events are effectively represented as a longer aggregated interval. However, some cases may also reflect genuine parked energy consumption not explicitly captured in the event structure, such as cabin preconditioning, thermal management, standby consumption, or auxiliary loads. The consequence of this creates two related modelling asymmetries between the V1G baseline and the V2G formulations.

First, the V1G baseline is a charging-only model and cannot reduce battery energy during a parking interval. Therefore, when the processed operational data implies a lower departure SOC than arrival SOC, exact departure SOC matching becomes infeasible unless artificial discharge is introduced. For this reason, the V1G baseline was formulated using a minimum departure SOC constraint rather than exact departure matching. This lead to a small amount of surplus charging relative to the processed departure requirement. However, the quantified impact was negligible: total V1G departure surplus amounted to 2.36 MWh, corresponding to an estimated charging cost of approximately 1.58 kSEK, representing only 0.54% of total V1G charging cost.

Second, the V2G formulations can exactly satisfy lower departure SOC targets through bidirectional discharge. In intervals where departure SOC is lower than arrival SOC, this creates exogenously embedded discharge potential that is not necessarily caused by market-driven arbitrage, but instead originates from the processed operational data itself. This may introduce a slight upward bias in estimated V2G discharge volumes and spot-market value. However, the extent of this effect was also limited. The total energy represented by all departure below-arrival intervals was 1.32 MWh, compared with 80.9 MWh of total Spot V2G discharge. This result in approximately 1.6% of total Spot V2G discharge could theoretically be attributed to this embedded SOC-decrease effect.

Overall, while these preprocessing assumptions introduce minor modelling imperfections, their quantified magnitudes are too small to alter the main fleet-level techno-economic conclusions.

5.2 Interpretation of economic results

The economic outcomes of the three baseline V2G strategies differ substantially because the underlying market mechanisms reward different forms of flexibility.
The spot-only V2G strategy generated a modest $\Delta\Pi$ fleet value of 125.0 kSEK, corresponding to 0.11 SEK per at-home hour. Profitability could be explained by the economic structure of spot-market arbitrage. In the day-ahead market, value is only created when electricity can be purchased at sufficiently low prices and later discharged at sufficiently higher prices to overcome all associated operating costs, including charging losses, grid import costs, and battery degradation. This creates small margins, making profitability highly dependent on repeated access to favorable temporal price spreads. Since arbitrage also requires vehicles to be available at precisely the right charging and discharging hours, the strategy becomes strongly dependent on both user behavior and timing precision. In contrast, FCR participation monetizes availability rather than actual energy throughput. The aggregator is primarily compensated for reserving bidirectional battery capacity that can be called upon for balancing services, rather than depending on repeated profitable energy transactions. This creates a different revenue structure, where profitability depends less on precise temporal price spreads and more on aggregate fleet availability. This difference explains the larger profitability gap between the strategies. FCR-only strategy generated 12.44 MSEK, corresponding to 11.32 SEK per at-home hour, nearly two orders of magnitude higher, suggesting more robust and wider distributed business case across heterogeneous EV usage patterns. The co-optimized strategy generated the highest total profitability, reaching 12.56 MSEK in $\Delta\Pi$ fleet value, corresponding to 11.42 SEK per at-home hour. However, the $\Delta\Pi$ improvement over the FCR-only strategy was only 0.8%, indicating that adding spot-market participation on top of reserve-market participation contributed very limited additional value under the modeled conditions.
It's important to note that the analysis is limited to the Swedish electricity market and specifically uses market data from the SE3 bidding zone. Consequently, the economic results reflect the pricing conditions, reserve market structures, and tariff assumptions relevant to this specific region. Therefore, the quantitative profitability results cannot be directly generalized to other geographical regions without further analysis. Furthermore, the aggregate fleet result shows substantial variation across the study period. As shown in Figure B.1, market conditions differed between years, particularly in the spot and reserve markets, directly affecting the economic potential for flexibility provision. In particular, the declining reserve-market revenues observed in later years likely reflect both increasing market saturation from growing participation of flexibility resources and structural changes to the FCR market design introduced in early 2024. In addition, the number of participating vehicles varied greatly over time, with the largest fleet representation occurring in 2023 and much lower participation in the surrounding years (see Appendix Figures B.2–B.5). These differences in both market conditions and fleet composition should therefore be considered when interpreting aggregate profitability across the full study hori-

zon. Especially the high FCR revenues observed should not be interpreted as stable long-term expectations, but rather as outcomes under a specific market history.

This also implies that the reported strategies profitability represents an upper-bound estimate, since the deterministic perfect foresight framework assumes exact knowledge of future prices and vehicle availability, conditions that would not exist in real-world aggregator operation. Moreover, the historical study period includes elevated market volatility during the 2022 energy crisis and instability, conditions that were favorable for arbitrage. Even under these circumstances, pure spot-market participation generated only limited economic value, suggesting that independent arbitrage is difficult to scale into a robust aggregator business model without highly selective fleet participation or access to additional revenue streams.

Taken together, the baseline results suggest that the economic potential of aggregated EV-based V2G in the modeled Swedish context is driven by ancillary service participation rather than pure energy arbitrage. While exact profitability levels remain dependent on historical market conditions, fleet composition, and optimistic modeling assumptions, the qualitative ranking between strategies appears robust.

5.2.1 Sensitivity to charger power constraints

The charger power sensitivity results demonstrate that charging and discharging power limits have a substantial influence on $\Delta\Pi$, particularly for reserve-market participation. As shown in Table 4.7, increasing the charger rating from the baseline 11 kW case to 22 kW increased the fleet value of the FCR-only configuration from 9.48 MSEK to 18.54 MSEK, corresponding to an increase of approximately 96%. Similarly, the Co-optimized configuration increased from 9.56 MSEK to 18.87 MSEK, representing an increase of approximately 97%. In contrast, the spot-market configuration shown in Table 4.6 showed an increase from 93.7 kSEK to 135.8 kSEK, corresponding to a smaller increase of approximately 45%.

This behaviour is physically reasonable since reserve market participation is fundamentally power constrained. The economic value of FCR participation depends directly on the amount of reserve capacity that can be offered to the market, which in turn is limited by the available charging and discharging power of the connected vehicles. Higher charger ratings therefore allow the EV fleet to provide larger reserve bids and consequently obtain higher reserve market revenues. In contrast, spot-market arbitrage depends more strongly on available battery energy, parking duration, and electricity price than on instantaneous charging power. Since many vehicles remain parked at home for relatively long periods, especially overnight, the baseline 11 kW charging power is already sufficient to shift a substantial portion of charging demand toward low-price hours. Increasing the charger rating therefore provides comparatively smaller additional value for pure spot market arbitrage.

The Individual charging-power case furthermore illustrates the importance of realistic infrastructure assumptions when evaluating V2G profitability. When vehicle-specific charging powers estimated from observed home-charging behaviour were used, the obtainable profitability decreased substantially compared with the uniform 11 kW assumption. For the FCR-only case, the fleet value decreased from 9.48 MSEK to 6.10 MSEK, while the Co-optimized case decreased from 9.56 MSEK to 6.14 MSEK. This corresponds to reductions of approximately 36% relative to the baseline 11 kW case. Similarly, the spot market value decreased from 93.7 kSEK to 69.2 kSEK, corresponding to a reduction of approximately 26%. These results indicate that simplified assumptions regarding uniformly high residential charging power significantly overestimate the practical economic potential of EV aggregation under real-world charging conditions.

The results additionally suggest that investments in higher power bidirectional charging infrastructure may be considerably more important for ancillary service business models than for spot arbitrage. While spot market participation alone appears relatively insensitive to higher charging power, reserve market participation benefits strongly from increased charging and discharging capability. This can partly be explained by the fact that periods with low electricity prices often extend over several consecutive hours. Consequently, the additional value of charging at a higher power during a single hour remains limited, reducing the economic benefit of higher charging power for pure spot-market arbitrage. However, the presented results should still be interpreted as optimistic upper bound estimates, since practical limitations related to residential grid capacity, household fuse constraints, and simultaneous charging behaviour are not explicitly represented in the optimization framework.

5.2.2 Sensitivity to degradation

The degradation cost sensitivity results demonstrate that battery degradation assumptions can substantially influence the economic attractiveness of V2G participation, particularly for spot market arbitrage. Increasing degradation costs consistently reduced obtainable value across all evaluated market configurations, although the magnitude of the effect differed considerably between the market strategies.

The Spot configuration exhibited the strongest relative sensitivity to degradation assumptions. As shown in Table 4.8, the fleet value decreased from approximately 309.7 kSEK at zero degradation cost to only 39.1 kSEK at a degradation cost of 1.0 SEK/kWh, corresponding to a reduction of nearly 87%. Similarly, the value per connected hour decreased from 0.282 SEK/home hour to only 0.036 SEK/home hour across the investigated sensitivity range. Figure 4.13 further illustrates that the spot-market strategy experiences the largest relative changes compared to the base case at 0.5 SEK/kWh, with profitability increasing by approximately 185 kSEK at zero degradation cost and decreasing by approximately 86 kSEK at 1.0 SEK/kWh. These results indicate that pure spot market arbitrage operates with comparatively limited economic margins. Since spot market profitability depends primarily on exploiting temporal electricity price differences, additional degradation related costs rapidly consume a significant share of the obtainable arbitrage value. Furthermore, increasing degradation costs caused the optimizer to adopt more conservative charging and discharging behaviour which reduced battery cycling activity in order to avoid economically inefficient operation.

In contrast, the FCR-only and co-optimized configurations remained comparatively robust to increasing degradation costs. For the FCR-only strategy, the fleet value decreased only from 12.63 MSEK to 12.30 MSEK as degradation costs increased from 0 to 1.0 SEK/kWh, corresponding to a reduction of approximately 2.6%. The value intensity similarly decreased only marginally from 11.49 to 11.19 SEK/home hour. The co-optimized strategy showed similar behaviour, where the fleet value decreased from 12.68 MSEK to 12.31 MSEK over the same degradation-cost interval. Figure 4.13 further demonstrates that the relative profitability changes for the reserve market configurations remained comparatively moderate around the base case. Even at the highest investigated degradation cost, the relative reductions were approximately 216 kSEK for the FCR-only strategy and 305 kSEK for the co-optimized strategy, which are relatively small compared to their total obtainable values exceeding 12 MSEK.

This behaviour is physically reasonable since reserve-market revenues are primarily capacity based rather than directly proportional to discharged energy. Consequently, the obtained reserve revenues remain sufficiently large to offset the simplified degradation related costs included in the optimization model. In addition, the degradation cost tables show that the total degradation costs increased substantially with increasing degradation assumptions, reaching approximately 705 kSEK for the FCR-only configuration and 727 kSEK for the co-optimized configuration at 1.0 SEK/kWh. Despite these considerably larger degradation expenses compared to the spot market model, the reserve market strategies remained highly profitable due to the substantially larger reserve market revenues.

The relatively small difference between the FCR-only and co-optimized strategies further reinforces one of the central findings of this thesis, namely that the majority of the economic value originates from reserve market participation rather than from additional spot market arbitrage. Across the investigated degradation cost range, the co-optimized strategy only increased fleet value by approximately 0.01–0.08 MSEK compared to the FCR-only strategy. Adding spot market optimization therefore only marginally altered the overall degradation sensitivity, indicating that reserve-market revenues dominate the co-optimized profitability.

These findings are generally consistent with previous literature, where battery degradation is often identified as one of the major uncertainties influencing V2G profitability. Several studies have similarly reported that degradation costs can significantly reduce the profitability of electricity arbitrage, while ancillary-service participation tends to remain comparatively more robust due to higher reserve-market revenues and lower net energy throughput requirements. However, the degradation model applied in this thesis is intentionally simplified and should therefore be interpreted primarily as an economic sensitivity parameter rather than a physically exact battery-aging representation.

5.2.3 Sensitivity to FCR bid acceptance

The accepted FCR bid-factor sensitivity results demonstrate that reserve market profitability is highly dependent on the share of submitted reserve bids that are successfully accepted in the market. As shown in Table 4.11, both the FCR-only and co-optimized configurations exhibited an approximately linear increase in profitability with increasing accepted bid factor. For the FCR-only configuration, the obtainable value increased from 1.12 MSEK at an accepted bid factor of 0.1 to 12.50 MSEK at full bid acceptance. Similarly, the co-optimized configuration increased from 1.33 MSEK to 12.61 MSEK across the same range. This linear behaviour indicates that the obtainable economic value scales proportionally with accepted reserve capacity.

This behaviour is physically reasonable since the dominant revenue stream in the reserve market configurations originates from capacity based FCR payments. Increasing the accepted bid factor therefore directly increases the amount of reserve capacity that generates revenue, while the overall operational characteristics of the optimization remain relatively similar. The linear increase in profitability across the investigated sensitivity range additionally suggests that the implemented optimization framework behaves consistently under varying reserve market acceptance assumptions.

The relatively small difference between the FCR-only and co-optimized configurations further reinforces one of the central findings, namely that the majority of the economic value originates from reserve market participation rather than from additional spot market arbitrage. Even at full bid acceptance, the co-optimized configuration only increased the obtainable value from 12.50 MSEK to 12.61 MSEK compared with the FCR-only case. Similarly, at an accepted bid factor of 0.5, the obtainable value increased only from 6.15 MSEK to 6.27 MSEK when spot-market optimization was included. These comparatively small differences indicate that the additional contribution from spot-market arbitrage remains limited relative to the reserve-market revenues.

The results also highlight the importance of realistic market assumptions when evaluating V2G profitability. In practice, reserve markets are characterized by competition, limited procurement volumes, and uncertain bid acceptance. Therefore, assuming full bid acceptance may overestimate the economic value of aggregated EV flexibility.

A further limitation of this analysis is that the FCR activation levels are based on historical observations. Higher activation levels would increase energy throughput, battery degradation, and conversion losses, which could reduce the profitability of V2G operation.

Nevertheless, the results show that reserve market participation can remain profitable even at low bid acceptance levels. For example, both reserve-based configurations remained profitable at an accepted bid factor of 0.1, indicating that reserve-based V2G can still be economically attractive even when only a small share of the submitted bids is accepted.

5.2.4 Sensitivity to price volatility

The volatility sensitivity analysis highlights that spot-arbitrage profitability is strongly dependent on the scale of hourly price spread. For the pure spot strategy, increasing volatility substantially improves profitability, with $\Delta\Pi$ value rising from 15.0 kSEK at $\alpha = 0.2$ to 753.8 kSEK at $\alpha = 2.0$, corresponding to an increase of approximately 4,900%. This confirms that arbitrage value is mainly driven by price spreads rather than average price level alone. However, even under highly amplified volatility assumptions, the normalized value remains modest compared to reserve-driven strategies, reaching only 0.69 SEK per at-home hour at $\alpha = 2.0$, compared to approximately 11.5 SEK/h for the co-optimized case. This suggests that while spot-market profitability is highly sensitive to volatility, pure energy arbitrage alone remains a comparatively weak independent business case.

A limitation of the volatility scaling approach is that it preserves monthly average prices while scaling hourly deviations around the monthly mean. While this isolates the effect of price spread, it does not fully capture structural changes in market behavior, such as changed frequency of extreme hourly events, negative-price episodes, prolonged scarcity periods, or shifts in intraday temporal price structure. Real electricity markets could therefore exhibit a more complex volatility dynamics than represented by this simplified transformation.

The elevated volatility observed in European electricity markets during the 2022 energy crisis provides a real-world example of how extreme external events can alter V2G economics. Geopolitical disruptions, fuel supply constraints, and broader energy-system stress led to unusually large hourly price spreads, creating temporary arbitrage opportunities beyond typical market conditions. Looking forward, increasing electrification and higher shares of variable renewable generation may also contribute to greater price variability, although the exact market impact remains uncertain and depends on system flexibility, storage deployment and market design evolution.

For the co-optimized strategy, the limited variation across volatility scenarios does not suggest that spot-market profitability is insensitive to volatility. The modest increase from 12.54 MSEK to 12.60 MSEK across the full volatility range should not be interpreted as evidence that low volatility benefits spot-market participation. Since $\Delta\Pi$ is calculated relative to a volatility-specific V1G reference, changes in the reference case also influence the avalue of co-optimization, making performance appear relatively stronger under lower-volatility conditions. The underlying contribution from spot-market arbitrage is still limited.

5.2.5 Sensitivity to grid fees

The grid fee sensitivity analysis confirms the expected economic trend that increasing volumetric grid fees directly reduce V2G profitability across all strategies. Since all modeled strategies rely on grid imports for charging, higher import tariffs increase operating costs and thereby reduce net profitability.

Relative to the baseline grid fee of 0.445 SEK/kWh, reducing the grid fee to zero increases profitability by approximately 146% for the spot-only strategy, 2.1% for the FCR-only strategy, and 2.2% for the co-optimized strategy. Conversely, increasing the grid fee to 1.0 SEK/kWh reduces profitability by approximately 57% for the spot-only strategy, 2.0% for the FCR-only strategy, and 2.2% for the co-optimized strategy.

The stronger absolute sensitivity observed for the reserve-driven strategies is directly linked to their substantially higher electricity import volumes. Both the FCR-only and co-optimized cases intentionally import significantly more electricity to maintain reserve availability and restore battery SOC following activations. This increases exposure to volumetric grid tariffs. However, despite this operational dependence, the relative profitability impact remains surprisingly small. Even under the highest modeled grid fee, the reserve-driven strategies retain over 12 MSEK of $\Delta\Pi$, indicating that reserve-market revenues remain highly lucrative under the assumed market conditions. However, this result should be interpreted in light of the deterministic perfect-foresight formulation. Since the model has full knowledge of realized reserve activations, it can use downward FCR activation energy to restore battery SOC instead of relying entirely on conventional grid charging. This may reduce explicit charging needs and avoid degradation costs that would otherwise arise from additional active charging and cycling. As a result, the reserve-driven strategies may appear less sensitive to volumetric grid fees than they would be under real operational uncertainty, where future activation energy is not known in advance. This highlights that the grid-fee sensitivity results depend not only on tariff assumptions, but also on the deterministic treatment of reserve activation.

Another important limitation is that the grid-fee sensitivity analysis excludes electricity energy taxes, since the modelling framework adopts an aggregator market perspective focused on wholesale market participation rather than end-user electricity pricing. In practice, such taxes would further increase the effective cost of imported electricity and could reduce V2G profitability, particularly for import-intensive reserve-driven strategies.

Additionally, the present study assumes a volumetric grid fee structure, where costs depend only on imported energy. In practice, electricity network tariffs may also include capacity-based or peak-demand charges rather than relying only on energy consumption. Under such tariff structures, the economic impact on V2G could differ significantly. Reserve-driven strategies, which could require high charging power during shorter periods, could become less attractive if tariffs penalize high peak electricity demand.

Another relevant uncertainty concerns future treatment of bidirectional power flows. The present framework assumes that exported V2G electricity does not use network charges. However, future tariff reforms may introduce fees for electricity fed back into the grid as distributed flexibility participation increases. Such changes would most likley affect discharge-intensive V2G business models and could weaken pure arbitrage profitability.

Taken together, these findings suggest that V2G economics are not determined only by electricity market revenues, but are also highly dependent on regulatory tariff design. While reserve-market participation appears economically robust under the present assumptions, future network pricing reforms could alter aggregator business case attractiveness.

5.2.6 Sensitivity to home availability uncertainties

The stochastic perturbation for availability analysis shows that V2G profitability decreases when arrival and departure times are perturbed, but the effect differs between the spot-only and co-optimized strategies. The effective reduction in total home availability was 3.3% and 6.8% for the 1h and 2h stochastic cases, respectively. For the spot-only case, $\Delta\Pi$ value decreases by 8.3% under the 1h stochastic assumption and by 17.0% under the 2h assumption. This larger reduction reflects the fact that spot arbitrage is highly time-sensitive which means that the vehicle must be connected during specific low-price and high-price hours in order to exploit price spreads. If arrivals are delayed or departures occur earlier, the optimizer loses access to some of the most valuable arbitrage windows.

The co-optimized strategy is more robust to stochastic availability. Its $\Delta\Pi$ value decreases by only 2.9% in the 1h case and 6.5% in the 2h case. This indicates that reserve-market participation is less dependent on individual high-value spot hours and can instead extract value across a wider set of available hours. The normalized value per home hour remains almost unchanged, increasing slightly from 11.43 to 11.47 SEK/h in the 1h case and to 11.46 SEK/h in the 2h case. This suggests that most of the reduction in total co-optimized value is explained by fewer available home hours rather than a substantial decline in value intensity.

Within the tested perturbation realizations, service reliability remained high. In the 1h case, only 12 departures require slack, corresponding to 0.02% of departures, while the 2h case increases this to 26 departures, or 0.04%. This indicates that most vehicles remain available to meet departure energy requirements even when arrival and departure times are perturbed.

A limitation of this robustness test is that only one randomized realization was evaluated for each stochastic case. Therefore, the results should not be interpreted as a full probabilistic assessment of mobility uncertainty. Other combinations of delayed arrivals and early departures could lead to different economic outcomes, particularly if they remove availability during high-value market periods. Furthermore, only 1h and 2h perturbations were tested. Larger deviations would likely reduce profitability more strongly, especially for spot arbitrage, and could increase departure slack. Still, the results provide evidence that the co-optimized strategy remains relatively robust under moderate availability uncertainty, while spot-only V2G is more sensitive to timing errors.

5.2.7 Sensitivity to worst vs best case scenario

The combined worst-case and best-case scenario analysis provides practical economic boundaries for the modeled V2G business cases rather than probabilistic forecasts of future market outcomes. By simultaneously combining pessimistic and optimistic assumptions across the most influential parameters, the analysis illustrates the approximate lower and upper bounds of economic performance under the present modeling framework.

For the spot-only strategy, profitability remains sensitive to the combined assumptions. Under the pessimistic case, value relative to V1G is effectively eliminated, falling to only 2.1 kSEK, corresponding to 0.002 SEK per at-home hour. This indicates that pure arbitrage profitability can be almost entirely reduced when low price volatility, high charging costs, battery degradation, and reduced vehicle availability occur simultaneously. In contrast, the optimistic case increases spot-only profitability to 2.14 MSEK, corresponding to 1.95 SEK per at-home hour. This represents an increase of over 1,700% relative to the baseline case, highlighting the extreme sensitivity of pure arbitrage to market conditions.

The co-optimized strategy shows substantially greater robustness. Even under the pessimistic combined scenario, the strategy retains 1.37 MSEK of value relative to V1G, corresponding to 1.33 SEK per at-home hour. While this represents an approximately 89% reduction relative to the baseline case, the business case remains economically positive. Under optimistic assumptions, profitability increases more modestly to 13.37 MSEK, corresponding to 12.17 SEK per at-home hour, an increase of approximately 6.5% relative to baseline.

This asymmetry reinforces a key finding of the study: reserve-driven V2G value appears significantly more resilient to unfavorable operating conditions than pure spot-market arbitrage. Whereas spot profitability can collapse almost entirely under adverse assumptions, co-optimized participation remains economically attractive due to the dominant contribution from reserve-market revenues.

However, these scenarios should be interpreted carefully. The constructed combinations represent deliberately conservative and optimistic parameter bundles rather than realistic market conditions. Some combinations may be unlikely to occur simultaneously in practice, while other relevant uncertainties were not explicitly included. The purpose of the analysis is therefore not prediction, but boundary testing of the economic robustness of the modeled strategies.

The scenario analysis also highlights the importance of external market conditions. The optimistic case resembles environments characterized by unusually high volatility, low network costs, and strong flexibility revenues, conditions partially observed during periods such as the European energy crisis in 2022. Conversely, the pessimistic case illustrates how regulatory changes, reduced volatility, or tighter operational constraints could materially weaken V2G economics. As electricity markets evolve with higher shares of renewable generation, increased electrification, and changing tariff structures, the true operating environment may shift between these extremes.

5.3 General Limitations

5.3.1 Solver tolerance and numerical consistency

Both the FCR-only and co-optimized models were computationally demanding in this study, with substantially longer solution times than the V1G and spot-only formulations due to the increased complexity associated with reserve market participation and co-optimization.

To keep the sensitivity analysis computationally feasible, selected sensitivity runs were solved using slightly adjusted solver settings to reduce computational time, including, for example, a relaxed relative optimality tolerance (MIPGap). In these cases, the corresponding baseline case was also re-solved using the same solver settings to ensure consistency and comparability between results.

As an example, the baseline point in the grid fee sensitivity analysis was re-solved using the same relaxed solver settings as the corresponding sensitivity runs. This resulted in a small numerical variation between the reported baseline co-optimized value of 12,555.6 kSEK and the corresponding baseline point in the sensitivity analysis of 12,509.2 kSEK under the same grid fee assumption (0.445 SEK/kWh). The difference equals to 46.4 kSEK, or approximately 0.37%.

This deviation is small relative to the magnitude of the economic effects analyzed in the sensitivity studies, where profitability changes typically range from hundreds of thousands to several million SEK. The minor numerical variation is therefore not expected to affect the qualitative conclusions of the study.

In particular, the main findings remain unchanged: co-optimized participation remains highly profitable under the modeled assumptions, reserve-market revenues dominate the value stack, and the contribution from spot-market arbitrage within the co-optimized strategy remains comparatively limited.

5.3.2 Centralized fleet control & market participation assumptions

The optimization assumes full participation of all modeled EV users and perfect centralized control of the aggregated fleet. This implies that all participating vehicles follow the optimized dispatch schedule exactly, without behavioural deviations, communication delays, user overrides, or technical failures. Real-world EV aggregation systems would inevitably face uncertainty related to user behaviour, participation rates, charger compatibility, communication, and other operational constraints.

A related practical implementation consideration concerns access to reserve markets. The present framework assumes that the aggregated EV fleet can participate in the modeled ancillary service markets under the modeled technical conditions. In reality, participation require sufficient bid size, reliable communication, and technical control of the connected vehicles, which could limit practical implementation.

As an indicative ex-post feasibility check, the optimized aggregate reserve bids were compared against the representative 0.1 MW minimum FCR bid threshold. The fleet exceeded this threshold for at least one reserve product during 90.7% of modeled hours, suggesting that the aggregated fleet would often be sufficiently large from a bid-volume perspective. However, since the minimum bid threshold was not enforced within the optimization framework, the model could assign economically optimal reserve capacities below practical participation limits. The ex-post threshold comparison should therefore be interpreted as an indicative feasibility assessment rather than proof of full real-world market eligibility.

Furthermore, the vehicles are geographically distributed across Sweden rather than concentrated within a single local distribution network. As a result, the aggregated fleet behavior modeled in this study does not correspond to a physically co-located fleet sharing common grid infrastructure constraints. This has two important implications. First, the absence of local grid congestion could make aggregated power peaks appear less problematic than they would be for a geographically concentrated fleet. Second, the charging patterns and operational characteristics of the sample may not fully represent general EV populations or future commercial aggregation customers.

Another important consideration is fleet scale. While the present study analyzes 149 successfully optimized EVs, real commercial aggregators may operate substantially larger fleets, particularly in a country such as Sweden with a rapidly growing EV population. A larger aggregated fleet would likely improve reserve-market participation robustness by increasing available bid capacity, reducing sensitivity to individual vehicle behavior, and smoothing uncertain availability fluctuations. The analyzed fleet is relatively small compared with the scale of possible future commercial EV aggregation, which may limit the direct generalizability of fleet-level reserve-market behavior.

5.3.3 SOC operating bounds and practical user constraints

The optimization framework was constrained by the observed arrival and departure SOC requirements derived from the processed dataset. However, additional conservative user-protection constraints, such as restricting battery operation to intermediate SOC ranges (e.g. 20–80%), were intentionally not included.
This choice was made to estimate the theoretical upper economic bound of V2G flexibility from an aggregator perspective, while remaining consistent with the observed operational dataset, which included realized SOC trajectories extending both above 80% and below 20% SOC.
Introducing narrower user-protection SOC windows would likely reduce accessible flexibility, lower reserve capacity availability, and decrease arbitrage potential, resulting in a more conservative estimate closer to practical commercial deployment.

5.4 Future Work

Several extensions could improve both the realism and applicability of the developed optimization framework.
A natural next step would be to move beyond the deterministic perfect-foresight formulation and incorporate stochastic uncertainty. While the present robustness analysis perturbs vehicle home availability, the optimization itself still assumes perfect knowledge of future prices, reserve activations, and vehicle availability. Future work could instead adopt stochastic or robust optimization approaches that account for uncertainty in user plug-in behaviour, departure times, participation rates, market prices, reserve activations, and bid acceptance outcomes. This would provide a more realistic representation of operational decision-making, where aggregators must submit bids and schedule charging under incomplete information.
Another important extension would be to include more detailed electricity network constraints and tariff structures. While the present model includes volumetric grid fees, it does not consider peak power limitations, demand-based tariffs, export tariffs, or local distribution grid capacity restrictions. Incorporating such constraints would improve the realism of dispatch decisions and provide a more operationally relevant estimate of economic performance.
The temporal resolution of the framework could also be refined. Since ancillary service activation occurs on much shorter timescales than one hour, future work could explore higher-resolution optimization models to better capture short-term operational dynamics, particularly for frequency containment reserve participation.
Battery degradation modelling represents another area for further development. The current linear throughput-based approximation provides computational simplicity but neglects important degradation drivers such as charging rates, temperature,

depth of discharge, battery chemistry, and calendar ageing. More advanced battery ageing models could improve the accuracy of long-term economic assessments.

Future work could also expand the system boundary beyond EV aggregation alone. In practice, aggregators may coordinate EV flexibility alongside other distributed energy resources such as residential demand response, BESS, heat pumps, or behind-the-meter solar PV generation. Modeling integrated distributed flexibility portfolios could provide a more realistic representation of aggregator operations and reveal synergies between multiple flexibility resources for peak management, self-consumption optimization, and reserve-market participation.

Future research could also expand the market modeling framework. The present study focuses on historical Swedish market conditions, primarily within the SE3 bidding zone. Extending the analysis to multiple bidding zones, alternative market designs, or international electricity systems would improve the generalizability of the results.

In addition, the market participation assumptions could be refined by incorporating dynamic bid acceptance probabilities, changing reserve market competition, and market-driven price impacts from increasing EV flexibility participation.

The vehicle fleet representation could also be expanded. A larger and more diverse dataset with greater variation in vehicle models, battery capacities, charging infrastructure, and geographical concentration would improve representativeness and allow investigation of how fleet composition affects flexibility potential.

Finally, future work could extend the framework toward a full business case assessment by incorporating investment costs, aggregator platform costs, charging infrastructure requirements, customer compensation mechanisms, and regulatory market access conditions. This would enable evaluation not only of technical flexibility potential, but also of commercial viability for real-world EV aggregation business models.

6
Conclusion

This section concludes the study by summarizing the main findings of the developed EV flexibility optimization framework in relation to the research questions. It highlights the key economic insights regarding the evaluated market participation strategies and outlines the overall contributions of the work

This study evaluated the economic potential of aggregated EV-based (V2G) flexibility in Swedish electricity markets from an aggregator perspective under perfect foresight, using real-world vehicle availability data from 149 successfully optimized EVs across approximately 2.5 years of operation.
The results show that the economic potential of V2G depends strongly on the selected market participation strategy. Pure spot-market arbitrage generated only modest economic value, suggesting that profitability was highly dependent on favorable charging behavior, timing, and sufficiently large electricity price spreads. This indicates that pure arbitrage can provide limited and unevenly distributed value across heterogeneous EV usage patterns.
In contrast, reserve-market participation fundamentally transformed the business case. The FCR-only strategy generated approximately 9,850% higher economic value than pure spot-market arbitrage, demonstrating that reserve capacity compensation rather than energy arbitrage was the dominant value driver under the modeled assumptions. The co-optimized strategy delivered a similarly large improvement of approximately 9,950% relative to pure spot arbitrage. However, the additional benefit of combining spot-market participation with reserve-market participation remained below 1%, indicating that co-optimization provided only marginal $\Delta\Pi$ value beyond the reserve-market strategy alone.
Several technical and operational constraints were found to shape this economic potential. Spot-market arbitrage was constrained by narrow price spreads, charging losses, battery degradation, grid import costs, and the requirement for precise temporal vehicle availability. In contrast, reserve-driven strategies proved significantly more robust due to their reduced dependence on exact timing of energy dispatch. Power constraints also influenced flexibility, with higher charging/discharging power limits increasing economic potential, particularly for reserve participation.
The scenario analysis showed that V2G economics remain highly dependent on market and operational assumptions, but with important differences between strategies. Spot-market profitability showed strong sensitivity to electricity price volatility, grid fees, degradation costs, and stochastic availability perturbations, with profitability ranging from near-zero under pessimistic assumptions to over 2.1 MSEK in optimistic conditions. In contrast, reserve-driven strategies remained comparatively

robust, with only modest sensitivity to grid fee increases, stochastic availability perturbations, and other conservative assumptions. Even under the pessimistic combined scenario, the co-optimized strategy remained economically positive at 1.37 MSEK.

Taken together, the results suggest that aggregated EV-based V2G can represent a highly profitable aggregator business model in Sweden under the modeled assumptions, but primarily through ancillary service participation rather than pure spot-market arbitrage. The findings also demonstrate that while reserve-driven V2G appears robust across a wide range of tested conditions, the economic viability of V2G remains closely linked to market design, tariff structures, battery degradation assumptions, and future regulatory conditions.

Bibliography

[1] S. kraftnät, "Elstatistik," 2025.

[2] A. Fernández-Guillamón, E. Gómez-Lázaro, E. Muljadi, and Molina-García, "Power systems with high renewable energy sources: A review of inertia and frequency control strategies over time," *Renewable and Sustainable Energy Reviews*, vol. 115, p. 109369, Nov. 2019.

[3] Energimyndigheten, "Energimyndighetens nya prognos visar: Industrins omställning tar fart 2026," 2025.

[4] Naturvårdsverket, "Inrikes transporter, utsläpp av växthusgaser," 2025. Reviewed 16 December 2025.

[5] International Energy Agency, "Europe – co_2 emissions by sector," 2024.

[6] T. A. Sweden, "Sweden's electric vehicle momentum continues - 35% bev," Apr. 2025.

[7] International Energy Agency (IEA), "Ev adoption in sweden," 2025. Accessed: 2026-05-05.

[8] Naturvårdsverket, "Smart och hållbar mobilitet," 2023. Granskad: 19 december 2023,.

[9] D. Martini, M. Longo, and L. Daniel, "Milp framework for v2g optimization with battery degradation and price arbitrage in scheduled fleets," *IEEE Open Journal of the Industrial Electronics Society*, vol. PP, no. 99, pp. 1–10, 2025.

[10] M. S. Eltohamy, M. H. Tawfiq, M. Ahmed, Z. Alaas, B. Mohammed, I. Ahmed, H. Youssef, and A. Raouf, "A comprehensive review of vehicle-to-grid v2g technology: Technical, economic, regulatory, and social perspectives," *Energy Conversion and Management: X*, vol. 27, p. 101138, 2025.

[11] S. M. Malik, D. Jung, C. Sundström, and J. Hellgren, "An optimal v2g charging and discharging schedule for electric vehicles in sweden's day-ahead and fcr-d markets," in *2025 IEEE PES Innovative Smart Grid Technologies Conference Europe (ISGT Europe)*, pp. 1–5, 2025.

[12] A. Leippi, M. Fleschutz, K. Davis, A.-L. Klingler, and M. D. Murphy, "Optimizing electric vehicle fleet integration in industrial demand response: Maximizing vehicle-to-grid benefits while compensating vehicle owners for battery degradation," *Applied Energy*, vol. 374, p. 123995, 2024.

[13] Polestar, "Polestar initierar v2g-projekt och utvecklar virtuellt kraftverk för att stödja storskalig energiomställning," 11 2023.

[14] Vinnova, "Implementation of vehicle-to-grid services in sweden," 2023. Accessed: 2026-06-24.

[15] Göteborg Energi, "Så kan elbilar stärka elnätet," Nov. 2023.

[16] V. Cars, "What is the difference between ac and dc charging?," 2023.

[17] C. Gómez-Quiles, P. Paramo-Balsa, J. Riquelme-Santos, and A. Gómez-Expósito, "Minimum-time milp-based ev charging scheduling for prosumers," *International Journal of Electrical Power & Energy Systems*, vol. 172, p. 111293, November 2025.

[18] J. Einolander, A. Kiviaho, and R. Lahdelma, "Household electricity cost optimization with vehicle-to-home technology and mixed-integer linear programming," in *2023 International Conference on Future Energy Solutions (FES)*, pp. 1–5, 2023.

[19] A. D. Troyee, N. Das, and A. J. Datta, "Unlocking grid-independent local network: Optimized pv and ev-based storage with v2h for local energy management in western australia," *IEEE Access*, vol. 14, pp. 79757–79780, 2026.

[20] L. Nespoli, N. Wiedemann, E. Suel, Y. Xin, M. Raubal, and V. Medici, "National-scale bi-directional ev fleet control for ancillary service provision," *Energy Informatics*, vol. 6, no. Suppl 1, p. 40, 2023.

[21] N. Mirzaei Alavijeh, R. Khezri, M. Mazidi, D. Steen, and A. T. Le, "Profit benchmarking and degradation analysis for revenue stacking of batteries in sweden's day-ahead electricity and frequency containment reserve markets," *Applied Energy*, vol. 381, p. 125151, 2025.

[22] T. Yuvaraj, R. Krishnamoorthy, S. Arun, M. Bajaj, V. Blazek, and L. Prokop, "Smart energy strategies for dynamic ev charging and renewable integration in distribution systems: A multi-objective optimization framework," *Energy Strategy Reviews*, vol. 63, p. 102051, 2026.

[23] T. Signer, N. Baumgartner, M. Ruppert, T. Sandmeier, and W. Fichtner, "Modeling v2g spot market trading: The impact of charging tariffs on economic viability," *Energy Policy*, vol. 189, p. 114109, June 2024.

[24] A. Pradana, M. Nadarajah, and M. M. Haque, "Optimising grid support and ev owner profit: The dual role of aggregators in v2g energy management," in *Proceedings of the 2025 IEEE Power Electronics Specialists Conference*, IEEE, 2025.

[25] F. De Caro, G. Graber, V. Calderaro, A. Vaccaro, and V. Galdi, "Exploring economic profit of ev aggregators in supplying flexibility services through v2g," *Sustainable Energy, Grids and Networks*, vol. 43, p. 101851, 2025.

[26] J. Geng, B. Bai, H. Hao, X. Sun, M. Liu, Z. Liu, and F. Zhao, "Assessment of vehicle-side costs and profits of providing vehicle-to-grid services," *eTransportation*, vol. 19, p. 100303, 2024.

[27] International Energy Agency, "Global ev outlook 2023," 2023.

[28] S.-J. Park *et al.*, "Depth of discharge characteristics and control strategy to optimize electric vehicle battery life," *Journal of Energy Storage*, vol. 59, p. 106477, 2023.

[29] W. Kempton and J. Tomić, "Vehicle-to-grid power implementation: From stabilizing the grid to supporting large-scale renewable energy," *Journal of Power Sources*, vol. 144, no. 1, pp. 280–294, 2005.

[30] Y. Kobayashi, M. Taljegard, and F. Johnsson, "Assessment of real-world driving patterns for electric vehicles: an on-board measurements study from sweden," *Applied Energy*, vol. 401, p. 126608, 2025.

[31] G. Energi, "Så funkar det svenska elnätet," 2026. Accessed: 2026-04-20.

[32] omEV, "Forskningsstudie: Marknadsmognad för vehicle-to-grid (v2g) i europa," 2023. Accessed: 2026-04-20.

[33] W. Schram, N. Brinkel, W. van Sark, and G. Smink, "Empirical evaluation of v2g round-trip efficiency," in *Proceedings of the International Conference on Smart Energy Systems and Technologies (SEST)*, 2020.

[34] T. Lehtola, "Vehicle-to-grid applications and battery cycle aging: A review," *Renewable and Sustainable Energy Reviews*, vol. 208, p. 115013, 2025.

[35] S. Sagaria, M. van der Kam, and T. Boström, "Vehicle-to-grid impact on battery degradation and estimation of v2g economic compensation," *Applied Energy*, vol. 377, p. 124546, 2025.

[36] Energimarknadsinspektionen, "Elnätet i sverige," 2025.

[37] Svenska kraftnät, "Technology in the transmission grid," 2025.

[38] Svenska kraftnät, "Information on different ancillary services," 2025.

[39] Vattenfall Eldistribution, "Elnätets uppbyggnad," 2025.

[40] Vattenfall Eldistribution, "Säkringsabonnemang (16–63a)," 2026.

[41] N. et al., "Vehicle-to-grid: A sociotechnical transition beyond electric mobility," *Energy Policy*, 2019.

[42] Göteborg Energi, "Vad är skillnaden mellan energi och effekt?," 2026. Accessed 2026-05-16.

[43] Vattenfall Eldistribution, "Effektguiden," 2026. Accessed 2026-05-16.

[44] ENTSO-E, "Entso-e transparency platform," 2025.

[45] Nord Pool, "Day-ahead market," 2025.

[46] Council of the European Union, "Energy price rise since 2021," 2026.

[47] European Commission, "A more secure and stable energy system," 2026.

[48] Svenska kraftnät, "Introduction of marginal pricing on fcr markets," Feb. 2024.

[49] Svenska kraftnät, "Frekvenshållningsreserv störning nedreglering (fcr-d ned)," 2026.

[50] Svenska kraftnät, "Frekvenshållningsreserv störning uppreglering (fcr-d upp)," 2025.

[51] Svenska kraftnät, "Frekvenshållningsreserv normaldrift (fcr-n)," 2025.

[52] Boston Consulting Group, "Renewable energy's value trap and the need for systemic flexibility," 2025.

[53] S. Färegård and M. Miletic, "A swedish perspective on aggregators and local flexibility markets: Considerations and barriers for aggregators and sthlmflex together with their potential to manage grid congestions in stockholm," degree project in energy and environment, second cycle, 60 credits, KTH Royal Institute of Technology, Stockholm, Sweden, 2021.

[54] Energimarknadsinspektionen, "Tjänster för efterfrågeflexibilitet: Sammanställning av tekniska krav och andra villkor för tillhandahållandet av tjänster i form av ändrad elanvändning," Tech. Rep. Ei R2021:13, Energimarknadsinspektionen, Sweden, 2021.

[55] B. K. Sovacool, J. Kester, L. Noel, and G. Z. de Rubens, "Actors, business models, and innovation activity systems for vehicle-to-grid (v2g) technology: A comprehensive review," *Renewable and Sustainable Energy Reviews*, vol. 131, p. 109963, 2020.

[56] Svenska kraftnät, “Primary regulation market data (mimer).” https://mimer.svk.se/primaryregulation/primaryregulationindex, 2025.
[57] Fingrid, “Frequency - historical data.” https://data.fingrid.fi/en/datasets/339, 2025.

A

Appendix 1

Table A.1: Standardisation of raw event-data column names.

Original column	**Standardised column**
Event Type	event_type
Start Time	start_time
End Time	end_time
Location	location
Start SOC	start_soc
End SOC	end_soc
Charged Energy	charged_energy

Table A.2: Main input variables used in the deterministic optimization framework.

Category	Variable	Description
Vehicle state	h_t	Home connection indicator
	f_t	FCR availability indicator at home
	δ_t^{arr}	Arrival indicator
	δ_t^{dep}	Departure indicator
Energy	E_t^{arr}	Observed arrival energy
	E_t^{dep}	Observed departure energy
	$E^{\max}$	Battery capacity
Market prices and costs	π_t	Spot electricity price
	c^{grid}	Grid fee applied to imported electricity
	λ_t^N	FCR-N capacity price
	$\lambda_t^{D,up}$	FCR-D up capacity price
	$\lambda_t^{D,down}$	FCR-D down capacity price
	μ_t^{up}	mFRR up activation price
	μ_t^{down}	mFRR down activation price
Activation factors	$\alpha_t^{N,up}$	FCR-N upward activation factor
	$\alpha_t^{N,down}$	FCR-N downward activation factor
	$\alpha_t^{D,up}$	FCR-D upward activation factor
	$\alpha_t^{D,down}$	FCR-D downward activation factor

Table A.3: Baseline parameters used in the deterministic optimization models.

Parameter	Value	Description
Δt	1 h	Time-step duration
$SOC^{\min}$	0.0	Minimum state-of-charge limit
$SOC^{\max}$	1.0	Maximum state-of-charge limit
$P_{\mathrm{ch}}^{\max}$	11.0 kW	Maximum charging power
$P_{\mathrm{dis}}^{\max}$	11.0 kW	Maximum discharging power
η_{ch}	0.93	Charging efficiency
η_{dis}	0.93	Discharging efficiency
c_{deg}	0.5 SEK/kWh	Battery degradation cost coefficient
c_{grid}	0.445 SEK/kWh	Grid fee applied to charging
γ^{FCR}	1.0	Accepted FCR bid fraction
τ^{N}	1 h	FCR-N activation duration
$\tau^{\mathrm{D,up}}$	1 h	FCR-D up activation duration
$\tau^{\mathrm{D,down}}$	$\frac{1}{3}$ h	FCR-D down activation duration

B

Appendix 2

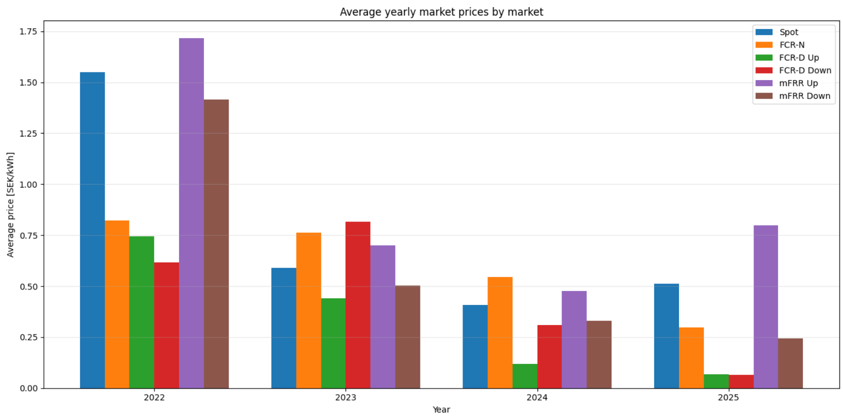

Figure B.1: Average yearly market prices for the electricity markets considered in this study, including the day-ahead spot market, FCR-N, FCR-D up/down, and mFRR up/down

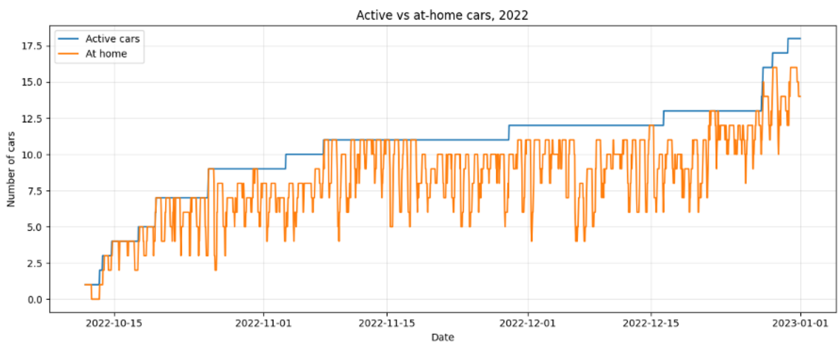

Figure B.2: Number of EVs participating throughout 2022.

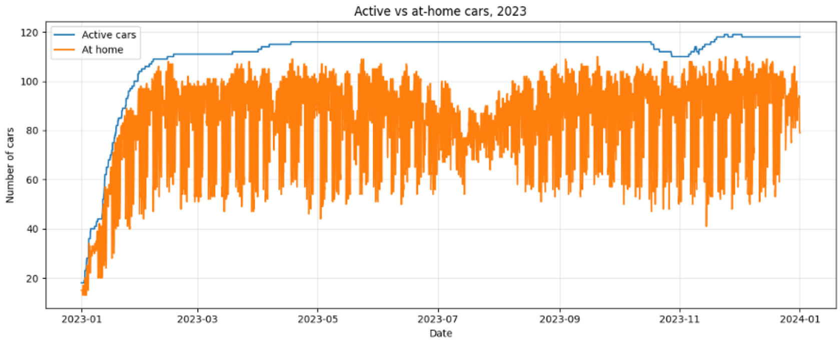

Figure B.3: Number of EVs participating throughout 2023.

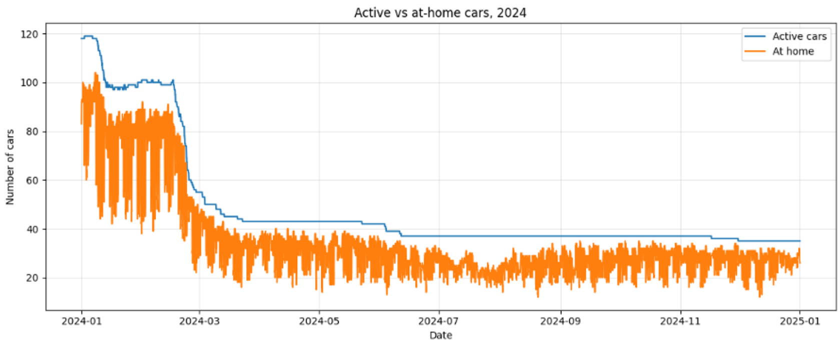

Figure B.4: Number of EVs participating throughout 2024.

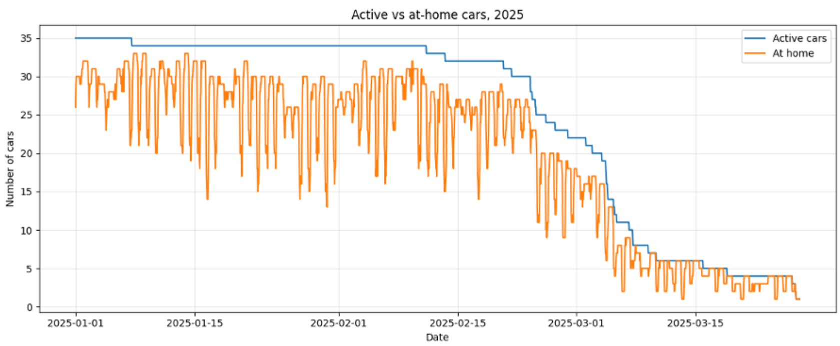

Figure B.5: Number of EVs participating throughout 2025.

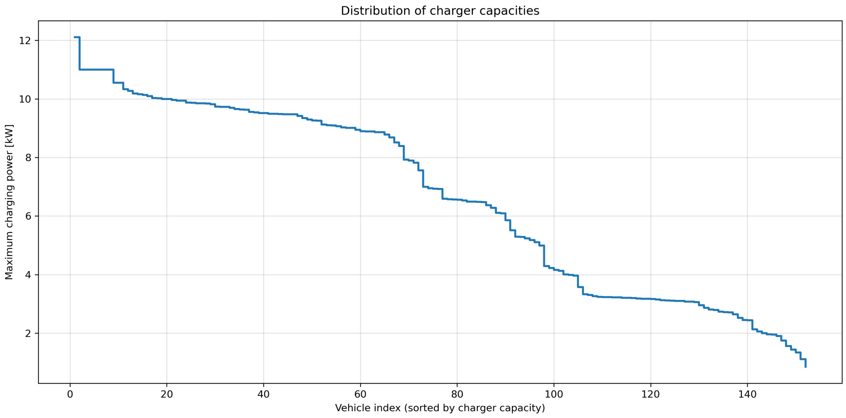

Figure B.6: Distribution of estimated maximum charging power, $\hat{P}_v^{\max}$, for the analyzed EV fleet.

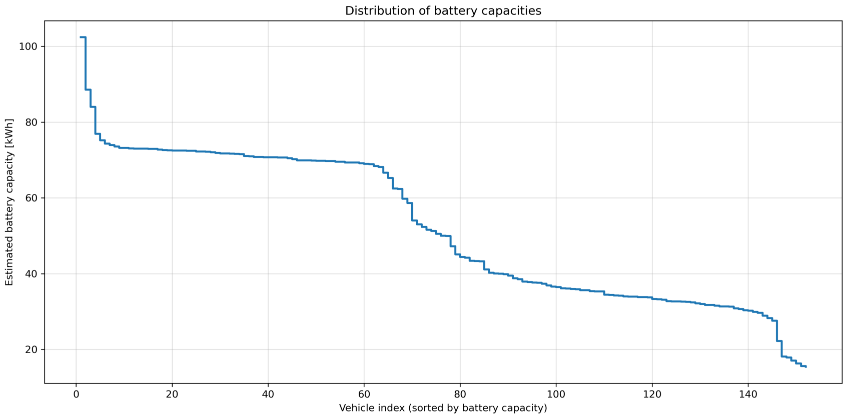

Figure B.7: Distribution of estimated battery capacities for the modeled EV fleet.

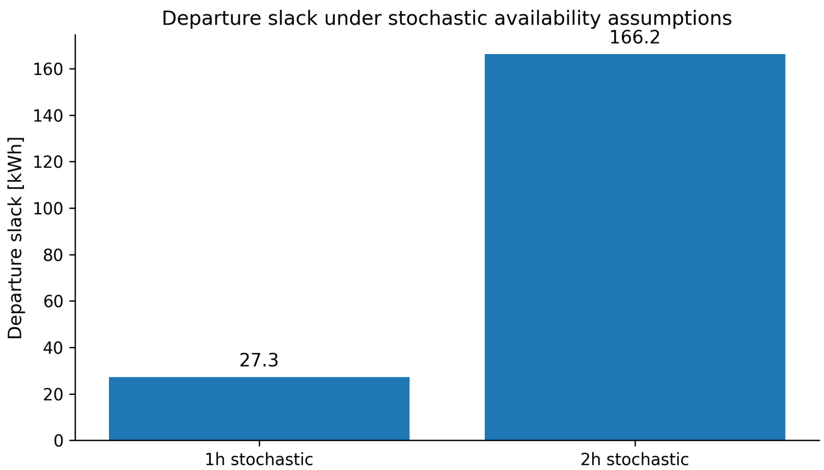

Figure B.8: Departures with slack during stochastic perturbations.

DEPARTMENT OF ELECTRICAL ENGINEERING
CHALMERS UNIVERSITY OF TECHNOLOGY
Gothenburg, Sweden
www.chalmers.se

CHALMERS
UNIVERSITY OF TECHNOLOGY